

# Interactions and Reactions Within Synthetic Self - Assembling Molecular Capsules

by

Jongmin Kang

B.S., Chemistry, Yonsei University, Seoul, Korea

M.S., Chemistry, Yonsei University, Seoul, Korea

submitted to the Department of Chemistry in partial fulfillment of the  
requirements for the degree of  
Doctor of Philosophy

at the

Massachusetts Institute of Technology

June, 1997

© 1997 Massachusetts Institute of Technology

All rights reserved

Signature of Author \_\_\_\_\_

\_\_\_\_\_  
Department of Chemistry  
May 5, 1997

Certified by \_\_\_\_\_

\_\_\_\_\_  
Professor Julius Rebek, Jr.  
Thesis Supervisor

Accepted by \_\_\_\_\_

\_\_\_\_\_  
Professor Dietmar Seyferth  
Chairman, Departmental Committee on Graduate Students

MASSACHUSETTS INSTITUTE  
OF TECHNOLOGY

JUL 14 1997 Science



This doctoral thesis has been examined by a Committee of the Department of Chemistry as follows :

Professor Daniel S. Kemp \_\_\_\_\_ Chairman

Professor Julius Rebek, Jr. \_\_\_\_\_ Thesis Supervisor

Professor Rick L. Danheiser \_\_\_\_\_





# Interactions and Reactions Within Synthetic Self - Assembling Molecular Capsules

by  
Jongmin Kang

Submitted to the Department of Chemistry on May 5, 1997 in partial fulfillment of the requirements for the degree of Doctor of Philosophy

## Abstract

Experimental details are given for the preparation of large self-complementary molecules capable of assembly into pseudo-spherical capsules. These structures exist as hydrogen bonded dimers in organic solvents, and they form and dissipate on a time scale that permits direct NMR observation of the reversible encapsulation of smaller molecules. The cavity is roomy enough to accommodate more than one molecule and two solvent molecules such as benzene appear to occupy the resting state of the capsules. Liberation of these solvents is responsible for the unexpected thermodynamic parameters of the encapsulation process. Accordingly, a bimolecular reaction - the Diels-Alder reaction - is shown to be accelerated by the capsule. Although product inhibition prevents the first system showing true catalytic behavior, size selectivity, saturation kinetics, and product inhibition studies point to a reaction that takes place within the capsule. A new system was designed to make the reaction turnover and it showed turnover behavior although original idea was not born out. The results augur well for the use of reversibly formed capsules as reaction chambers.

Thesis Supervisor : Dr. Julius Rebek, Jr.

Title : Director of The Skaggs Institute for Chemical Biology



*to  
my God*



## **Acknowledgments**

First, I wish to thank my advisor, Dr. Julius Rebek, Jr. for accepting me into his group, and giving me chance to explore and develop as a researcher. His scientific vision has inspired a lot of people and will always be a source of inspiration for me.

Furthermore, I wish to thank my former advisor at Yonsei University, Professor KwanSoo Kim for supporting my start as a researcher and application to M.I.T.

The members of the Rebek Group, past and present are to thank for scientific advice, tips, and tricks, and good times in the lab and outside. I would like to express special thanks to Dr. Rene Wyler and Dr. Robert S. Meissner for their support during the research. It has been a long journey to make the "Softball" with them.

I would like to thank Jean Harrington and Michelle Bateman for lifting many a bureaucratic burden from my shoulder.

I am grateful to my parents and I cannot forget their prayer for me for the last 5 years. I also cannot forget prayers from pastor Sejin Kim and many church members in Kungok Evangelical Church in Inchon and New England Korean Evangelical Church in Stoneham Massachusetts.

Above all, I do thank my wife Mikyung for making me happy and encouraging me while I am in despair. Also, I cannot apologize enough to my son Jungwook for the time we could not spend together to write this thesis.



## Chapter 1

<b>Three-Dimensional Self-Assembled Structures</b> .....	17
1.1 Introduction .....	17
1.2 Self-Assembly in Biological System .....	18
1.3 Self-Assembly in Chemical Systems .....	21
1.3.1 Metal-Ligand Interaction .....	21
1.3.2 Self-Assembling Systems Based on $\Pi$ -donors and $\Pi$ -acceptors .....	26
1.3.3 Cyclodextrins .....	28
1.3.4 The Hydrogen Bond .....	33
1.4 Self-Assembling Dimeric Molecule .....	39
1.5 References .....	46

## Chapter 2

<b>Self-Assembling Dimeric Molecule - The First Designed Flexible System</b> ..	51
2.1 Design .....	51
2.2 Retrosynthesis of Molecule 21 .....	53
2.3 Synthesis .....	54
2.3.1 Glycoluril and Central diimide .....	54
2.3.2 The synthesis of 4,7-dimethoxy-2-indanol .....	55
2.3.3 Coupling reactions of glycoluril, Central diimide and 2- benzyloxy-4,7-dimethoxyindane 33 .....	56
2.4 Characterization .....	59
2.4.1 The polar isomer .....	61





2.4.2 Nonpolar Isomer	62
2.5 Conclusion	65
2.6 Experimental	68
2.7 References	81

### Chapter 3

#### The Second Generation Self-Assembling Dimeric Molecule - The Rigid

<b>System</b>	82
3.1 Design	82
3.2 Retrosynthesis of molecule <b>42</b>	84
3.3 Synthesis	85
3.3.1 The synthesis of di-(4-n-heptylphenyl)glycoluril	85
3.3.2 The synthesis of 1,4-dimethoxy-5,6-di-bromomethyl-2,3-(di-t-butyl-1,2,3,4-tetrahydrophthalazine-2,3-dicarboxylate)	86
3.3.3 The synthesis of Bicyclo[2,2,2]-octa-2,5-diene-2,3,5,6-tetracarbonyl chloride <b>59</b>	87
3.3.4 Coupling reactions of <b>43</b> , <b>50</b> , and <b>59</b>	88
3.4 Characterization	88
3.5 Encapsulation	91
3.6 Some comparison of molecules <b>41</b> and <b>42</b>	100
3.7 Experimental	103
3.8 References	114



## Chapter 4

<b>Artificial Receptors Capable of Enzyme-like Recognition</b> .....	115
4.1 Introduction .....	115
4.2 Macrocyclic Polyether .....	115
4.3 Cyclophane .....	118
4.4 Cyclodextrins .....	121
4.5 Micelles .....	123
4.6 Template effect by metal-ligand interaction .....	124
4.7 Hydrogen bonding .....	126
4.8 Cavity .....	128
4.9 References .....	131

## Chapter 5

<b>Acceleration of a Diels-Alder Reaction by a Self-Assembled Capsule 42</b> ..	133
5.1 Introduction .....	133
5.2 Diels - Alder reaction inside the dimeric capsule 42 .....	134
5.3 Kinetic studies .....	140
5.4 Turnover in the Catalysis of the Diels-Alder Reaction by Encapsulation .....	145
5.5 References .....	152



## Chapter 1. Three-Dimensional Self-Assembled Structures

### 1.1 Introduction

Molecular self-assembly is the spontaneous association of molecules under equilibrium conditions into stable, structurally well-defined aggregates joined by noncovalent bonds <sup>1</sup>.

For molecular self-assemblies, the appearance of identical subunits in many biological examples suggests that *self-complementarity* is both useful and advantageous. Complementarity of shape, size and surface drives molecular recognition and self-complementarity is the singular feature of biological molecules capable of assembly. The result of this complementarity is a structure stabilized by many, relatively weak, noncovalent bonding interactions. These may be shape-dependent (van der Waals/hydrophobic), or directed (hydrogen bonds/dipole interactions), distributed over the whole molecular volume, rather than limited to a few strong, localized covalent bonds. The common feature of all biological self-assembly process is the ability to take advantage of many of these weak noncovalent interactions between preformed subunits or well-defined subassemblies to guide the formation of a superstructure. Since self-assembly involves the intermediacy of many weak and reversible interactions, the final structures formed represent a thermodynamic energy minimum for the system. In addition, owing to the dynamic nature of the assembly process, defective or incorrectly attached subunits are eliminated from the growing structure, *ensuring high*

*overall fidelity in the assembly of the final structure.* The modular nature of self-assembly process, involving the construction of stable subassemblies, which are then carried forward into the final structure, permits great synthetic efficiency; in chemical terms, the synthesis of the final structure is highly convergent <sup>2-4</sup>. The use of several identical subunits within a structure also requires that only a limited set of binding interactions is necessary to form the structure correctly, *minimizing the amount of information* needed to describe the structure fully.

## **1.2 Self-Assembly in Biological System**

Molecular self-assembly is ubiquitous in biological systems and underlies the formation of a wide variety of complex biological structures <sup>5,6</sup>. Biological self-assembly provides striking illustration of these kind of architectures including tobacco mosaic virus (TMV) <sup>7</sup>, DNA <sup>8</sup>, numerous multimeric proteins <sup>9,10</sup> and viral capsids <sup>11</sup> all of which reveal an economy of information. Held together by weak intermolecular forces, these structures consist of interlocking, identical subunits. The instructions for assembly are written within the shapes of the subunits and the orientation of their recognition surfaces. Tobacco mosaic virus is one of the best known example.

The tobacco mosaic virus (TMV) <sup>7</sup> is a helical virus particle, 300 nm in length and 18 nm in diameter, whose self-assembly serves to illustrate many of the features present in self-assembling biological systems <sup>12</sup>. The

viral particle is composed of 2130 identical subunits, each comprising 158 amino acids, which form a helical sheath around a single strand of RNA, 6390 base pairs (bp) in length. This information illustrates the first point about self-assembling systems-the amount of genetic information required by such structures is remarkably small. If the protein coat of TMV were coded by a single, contiguous gene, then the structure would require a section of RNA approximately  $1 \times 10^6$  bp long. As 2130 identical subunits capable of self-assembling are utilized to form the protein coat, the complete structure maybe coded for in a gene of around 500 bp in length - less than 8 % of the total genome. TMV particles maybe dissociated readily into their component parts and then subsequently reassembled accurately in vitro to give totally functional viral particles. In this way, The mechanism of TMV self-assembly has been investigated extensively <sup>12-15</sup>. Under physiological conditions the protein subunits form a disk-shaped subassembly, which is transformed into a helical form by insertion of a loop of RNA into the central hole of the protein disk. Additional protein disks, each corresponding to two turns of the final helix, associate with the growing viral particle until assembly is complete. The association of individual subunits into the disk subassembly through noncovalent interactions permits the overall construction process to be dynamic, that is, at or close to equilibrium. As a result, assembly and disassembly of protein subunits is a facile event and the overall self-assembly process is intrinsically error-checking and self-correcting.

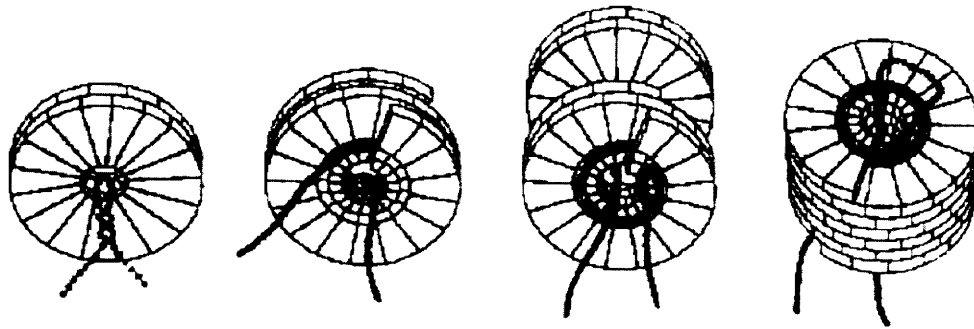
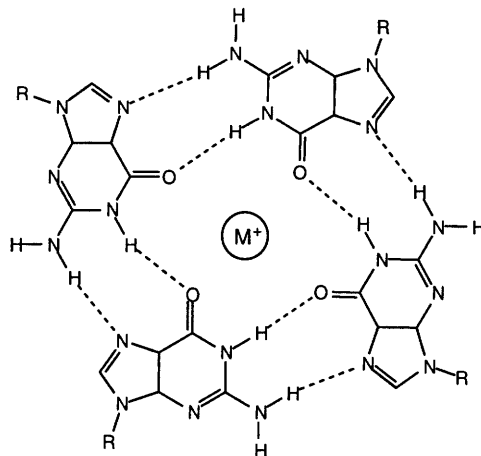


Fig. 1 Schematic model for the assembly of the tobacco mosaic virus.

The assembly of TMV demonstrates the ability of biological systems to construct large, ordered molecular and supramolecular arrays from small, relatively simple subunits by a mechanism of self-assembly. Such processes are responsible for the wide diversity of structure and function observed at both the cellular and subcellular levels in Nature. The evolution of self-assembly pathways in natural systems can be rationalized in terms of the selective advantages conferred upon organisms that utilize such synthetic routes.

Another example is given by guanine tetramers <sup>16</sup>. The cyclic array of four guanosine around the metal is ultimately due to the readout of hydrogen-bonding information provided by the purine's edges at 90° from one another.





**Fig. 2** Guanine tetramer.

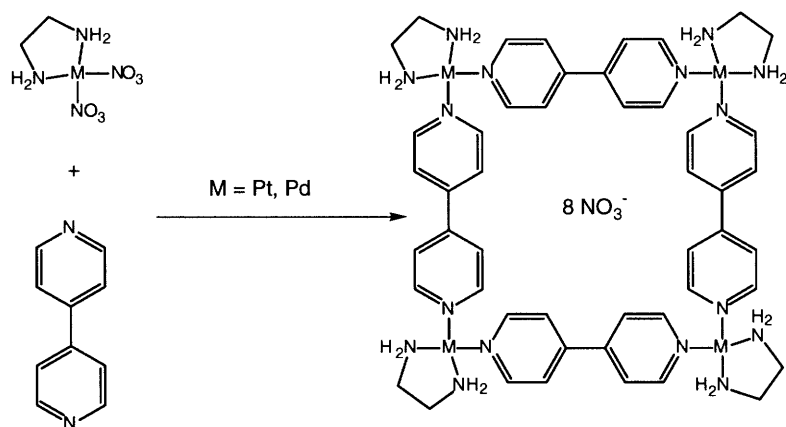
### 1.3 Self-Assembly in Chemical Systems

#### 1.3.1 Metal-Ligand Interaction

Metal coordination chemistry has many useful features that can be applied to the field of self-assembly. Metal-ligand bonds can be strong, lending stability to a structure, yet kinetically labile, allowing reorganization to occur. Additionally, metal-ligand interactions provide the chemist with a lexicon of well-defined geometries for the design of a wide range of structural forms.

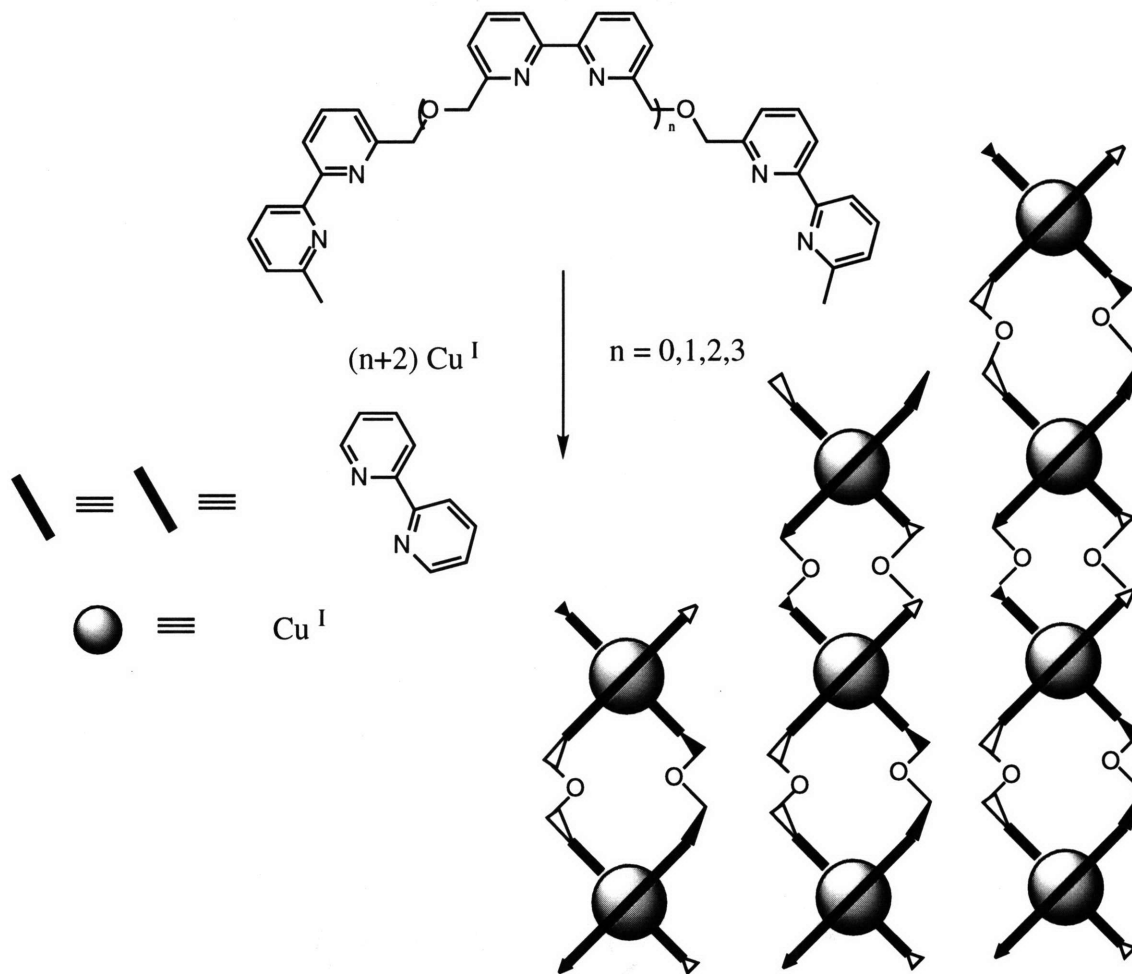
Fujita, Yazaki, and Ogura<sup>17,18</sup> have exploited metal coordination in the formation of macrocycles. When  $[M(en)(NO_3)_2]$  ( $M = Pt, Pd$ ) is treated with bipyridine, a cyclic tetrameric macrocycle - a molecular box - is formed as a thermodynamic product ( Fig. 3). The mechanism presumably involves stepwise displacement of the nitrate by bipyridine. Interestingly, in the reaction of the platinum complex, the kinetic product is an oligomeric species

which is converted slowly into the thermodynamic, tetrameric product when the reaction mixture is heated at 100°C. This observation suggests slow exchange within the ligand set around the metal center. In the palladium complex, ligand exchange must be rapid since no oligomeric products are observed by <sup>1</sup>H NMR spectroscopy and the thermodynamic product is formed immediately. This macrocycle is capable of binding π-electron rich aromatic guests such as 1,3,5-trimethoxybenzene within its cavity.



**Fig.3** Tetrameric bipyridine macrocycles are formed readily through metal directed self-assembly.

A wide variety of macromolecular biological structures display molecular helicity<sup>19-23</sup>, for example, the protein  $\alpha$ -helix. Lehn and co-workers<sup>24,25</sup> have described a series of oligobipyridine ligands, which spontaneously order themselves around an appropriate number of Cu<sup>I</sup> metal centers to give helical complexes (Fig. 4).

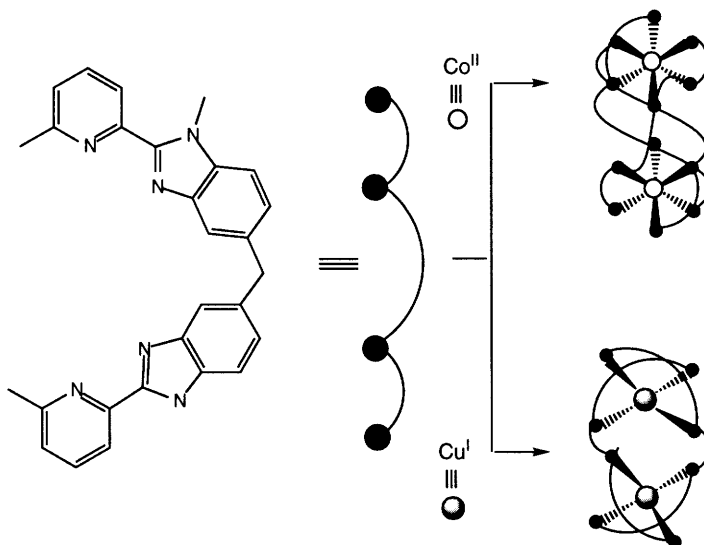


**Fig. 4**  $\text{Cu}^{\text{I}}$  ion directed self-assembly of oligobipyridine-based double helices.

These helical species display many of the features normally associated with self-organizing biological systems. The assembly of the helicates shows positive cooperativity;<sup>26</sup> In other words, the binding of the first  $\text{Cu}^{\text{I}}$  ion facilitates the binding of the second and so on. In addition, the binding of ligands by  $\text{Cu}^{\text{I}}$  displays self-self selection;<sup>27</sup> that is, given a mixture of ligands, a forming helical species will bind selectively a second

ligand of the same size, and thus no overlapping polymeric structures are formed in solution.

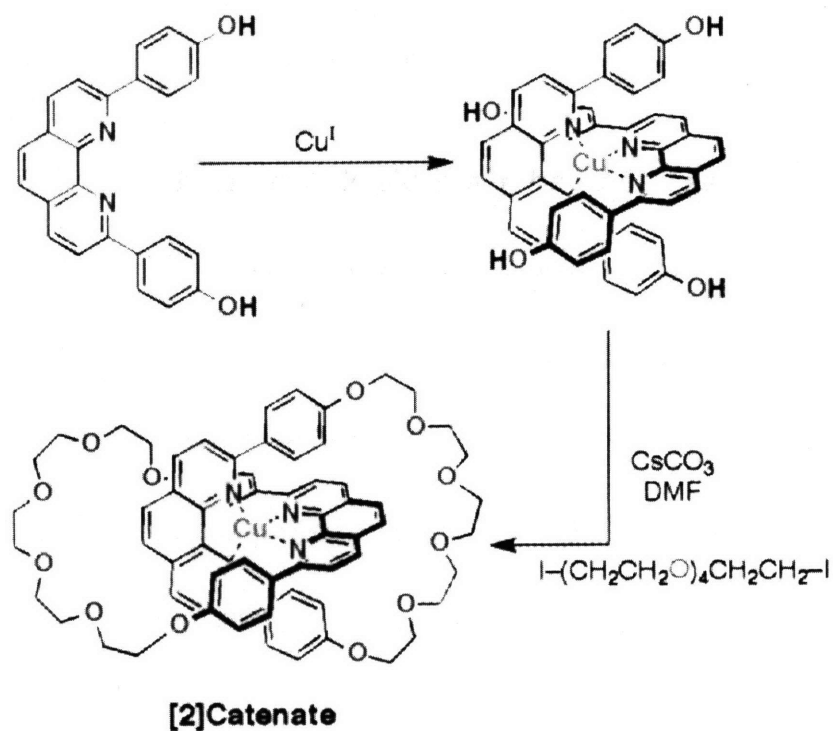
By combining pyridine and benzimidazole subunits within the same ligand, Piguet, Bernardinelli, and Williams have been able to self-assemble a wide range of double and triple helices containing both transition metal and lanthanide centers. <sup>28,29</sup>



**Fig. 5** A double or a triple helical complex can be formed depending on the metal ion employed in the self-assembly process.

A degree of control can be exercised over the outcome of these self-assembly processes. When this ligand is mixed in a 3 : 2 ratio with an appropriate source of Co<sup>II</sup> ions, a dinuclear triple helicate forms spontaneously <sup>30</sup> (Fig. 5). However, the analogous reaction with Cu<sup>I</sup> ions results in spontaneous formation of dinuclear double helicate. In this case, the outcome of the self-assembly process is governed by the coordination geometries of the metal centers.

Sauvage et al. have exploited the coordination geometry of 2,9-disubstituted 1,10-phenanthroline ligands around a  $\text{Cu}^{\text{I}}$  center to provide the first example of a practical, efficient synthesis of a catenated species <sup>31,32</sup>(Fig. 6). The interaction between a  $\text{Cu}^{\text{I}}$  ion and a 9, 10-phenanthroline ligand can be used to direct the formation of a [2]catenane.

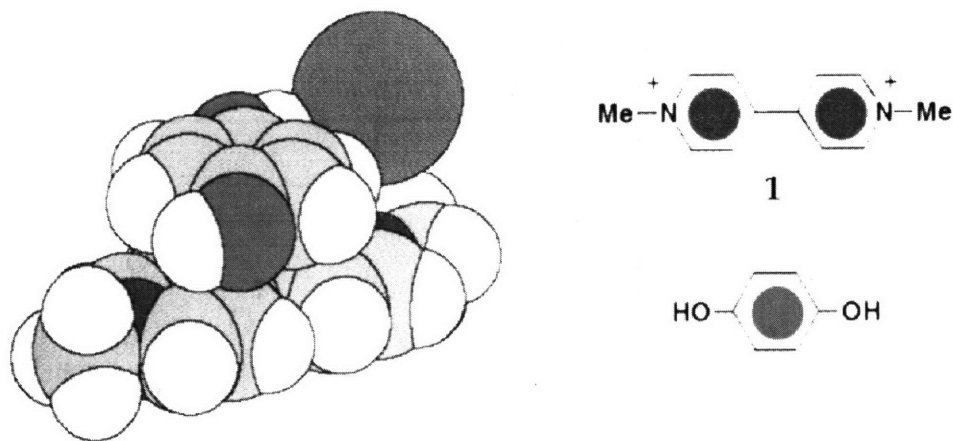


**Fig. 6** The interaction between  $\text{Cu}^{\text{I}}$  ion and a 9,10-phenanthroline ligand can be used to direct the formation of a [2]catenane.

### 1.3.2 Self-Assembling Systems Based on $\Pi$ -donors and $\Pi$ -acceptors

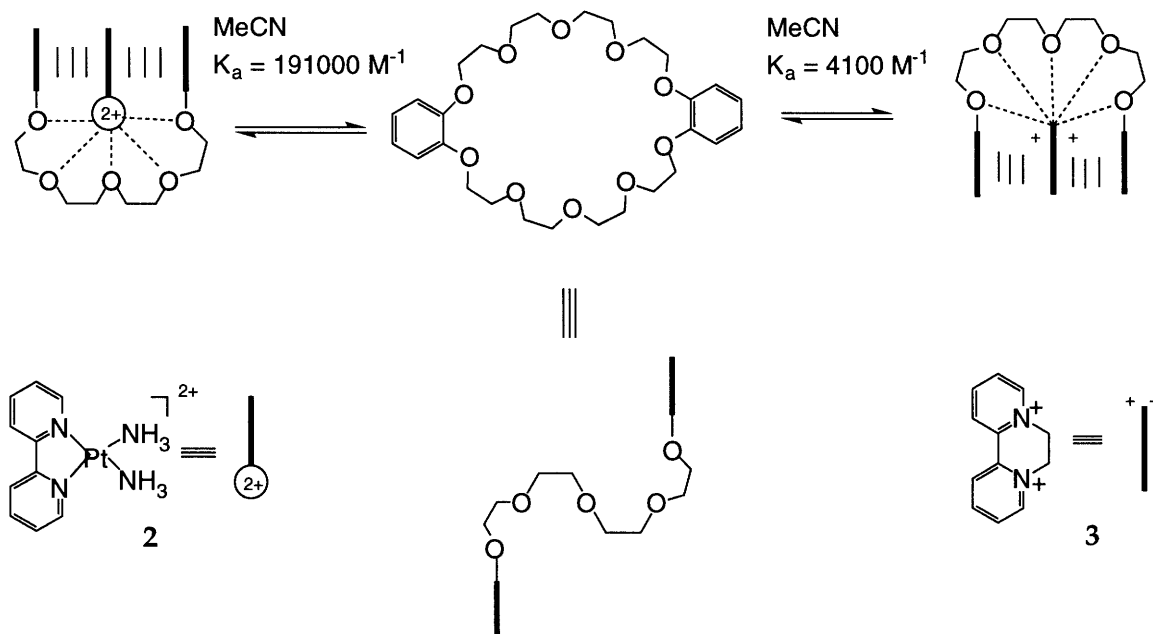
The electron donor-acceptor (EDA) complexes formed between  $\Pi$ -donors and  $\Pi$ -acceptors are believed to be held together by electrostatic, polarization, dispersion, and charge transfer forces. EDA forces are weak and association constants in common organic solvents generally range from 0.1 to 1000  $M^{-1}$ , but are usually less than 10  $M^{-1}$ .

The 1,1'-dimethyl-4,4'-bipyridinium dication  $1^{2+}$ , known as the bipyridinium herbicide paraquat<sup>33-35</sup>, is an extensively studied electron acceptor (Fig. 7). It offers a planar  $\Pi$ -system in which two positive charges are delocalized<sup>36</sup> as well as a rich and reversible electrochemistry<sup>37</sup>. The dication  $1^{2+}$  forms a wide range of electron donor-acceptor complex with aniline, o-phenylenediamine, catechol, and hydroquinone<sup>38</sup>. The bipyridinium herbicides are also capable of forming complexes with macrocyclic  $\Pi$ -donors. The dicationic platinum complex  $2^{2+}$  forms a strong complex ( $K_a = 191000 M^{-1}$ ) with the crown ether dibenzo-[30]crown-10 (DB30C10).



**Fig. 7** The X-ray crystal structure of the paraquat diiodide/hydroquinone complex.

Diquat dication  $3^{2+}$  also forms a strong 1 : 1 complex ( $K_a = 4100 M^{-1}$ ) with dibenzo-[30]crown-10 (Fig.8). The principal stabilizing interactions in the complexes are : 1) the solvation of the positive charge by the oxygen atoms of the polyether chains within DB30C10 through electrostatic interactions including hydrogen bonding and 2) the  $\Pi$ -donor /  $\Pi$ -acceptor and charge transfer (CT) interactions between the electron-rich catechol units of DB30C10 and the electron-deficient  $\Pi$ -system in both dications.

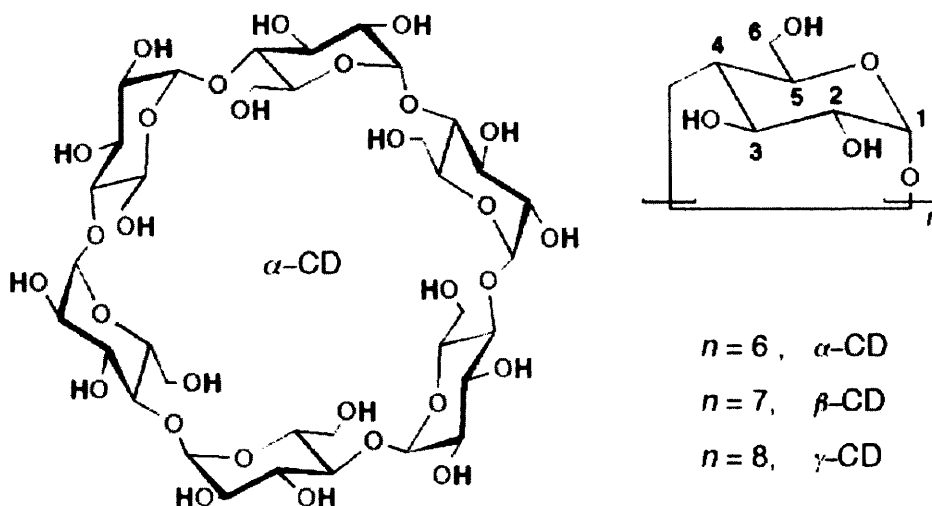


**Fig. 8** The binding of  $[\text{Pt}(\text{bpy})(\text{NH}_3)_2]^{2+}$  and the bipyridinium herbicide diquat by DB30C10. Only one of the tetraethylene glycol chains is shown.

### 1.3.3 Cyclodextrins

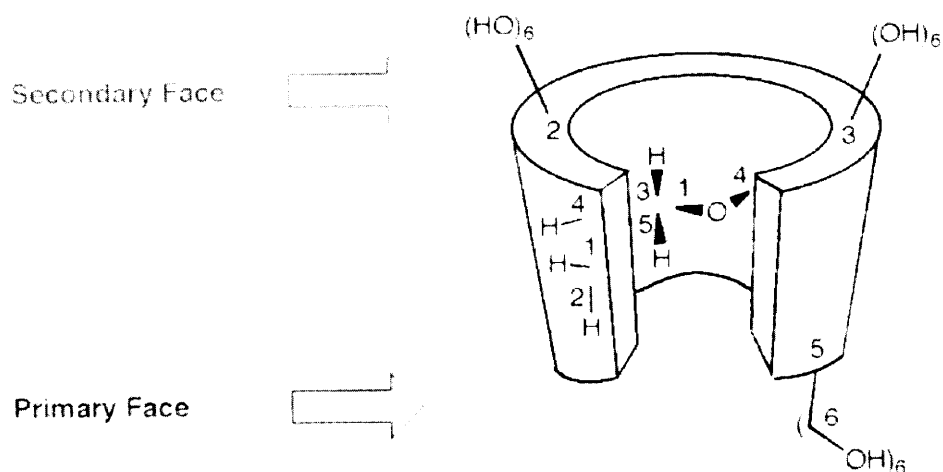
The cyclodextrins are a series of cyclic oligosaccharides consisting of six or more  $\alpha$ -1,4-linked D-glucopyranose rings. (Fig.9) <sup>39</sup>. The cyclodextrins are named according to the number of glucopyranose rings present :  $\alpha$ -CD has six,  $\beta$ -CD has seven, and  $\gamma$ -CD has eight. The most immediately apparent structural feature of the smaller cyclodextrin is a rigid, well-defined cavity resulting from the overall bucket-shape of the molecules (Fig.10).





**Fig.9** The chemical structure of cyclodextrins.

The open top of the bucket is rich in secondary hydroxyl groups at the C2 and C3 positions of the glucopyranose residues, and the bottom of the bucket features by the primary hydroxyl groups at C6. The interior of the bucket is linked with the oxygen atoms associated with the glycosidic linkages and the hydrogen atoms located at the C3 and C5 positions on the glucoside residues. The rigid, relatively hydrophobic cavity of the cyclodextrins gives rise to their voracious appetite for molecular guests of all types. The principal binding interaction in a cyclodextrin-guest complex is most likely a summation of several relatively weak effects, for example van der Waals interactions, hydrophobic binding <sup>40,41</sup>, and the release of high-energy water from the cavity <sup>39</sup>.



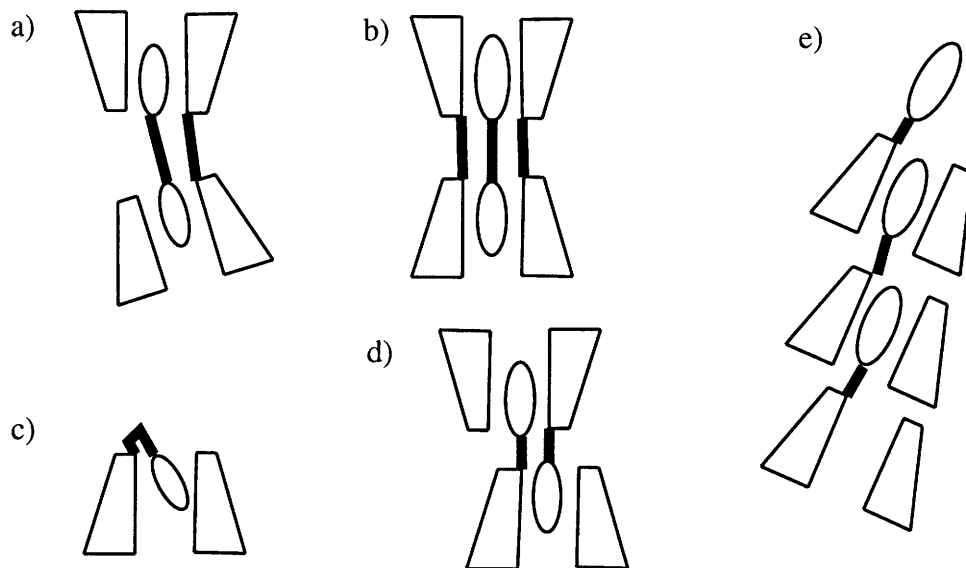
**Fig. 10** The schematic structure of  $\alpha$ -CD.

Cyclodextrins have been known since 1891, and the first detailed description of their isolation was published in 1903 by Schardinger. Since then, these naturally occurring molecular receptors have been exploited in many ways. Cramer<sup>42</sup> demonstrated that cyclodextrin can form inclusion complexes with a wide variety of substrates. Bender<sup>43</sup>, Tabushi<sup>44</sup> and Breslow<sup>45</sup> have extended the role of cyclodextrins as enzyme mimics and catalysts. Recently, however, the focus of cyclodextrin research has shifted towards their use as ready-made components for the construction of nanoscale structures through self-assembly.

Harada et al. and Breslow et al. described the binding potential of singly<sup>46,47</sup> and doubly<sup>48</sup> bridged cyclodextrin dimers (Fig.11). Such molecules are referred to as ditopic hosts<sup>49</sup>, since they are able to include two

hydrophobic guests or a guest with two hydrophobic binding sites (a ditopic guest)<sup>48</sup>.

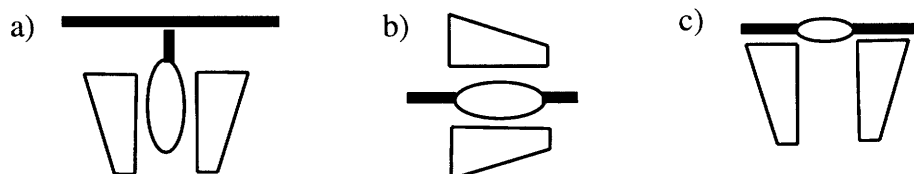
A unique situation arises when a cyclodextrin molecule and a guest molecule are covalently linked. Such cyclodextrin-guest conjugates can organize themselves either intramolecularly to give monomeric inclusion compounds or intermolecularly to give dimeric or polymeric inclusion compounds<sup>50-52</sup>.



**Fig. 11** Topology of inclusion compounds from a) covalently linked hosts and guests and b) ditopic host plus ditopic guest ; c) monomeric, d) dimeric, and e) polymeric complexes of a host - guest conjugate.

A polymer can be complexed by many host molecules if it has a corresponding number of binding sites, in other words, if it functions as a polytopic guest molecule. The binding sites can lie along the main chain as well as in the side chains. Since such polymers can form both inclusion and

addition compounds with cyclodextrins, several arrangements are possible (Fig. 12).



**Fig. 12** Topology of cyclodextrin inclusion compounds with polymeric guest molecules. a) Inclusion of the side chain, b) axial inclusion of the main chain. c) addition to the main chain.

In the interaction between poly(styrenesulfonic acid)<sup>53</sup> or poly(N-alkyl-4-vinylpyridinium bromide)s<sup>54</sup> and cyclodextrins, the side chain undergo inclusion(Fig.12a).

The axial inclusion of the main chain of a polymer(Fig.12b) leads to a special topology : the rings are “threaded” onto a chain. This means that a threaded ring is not undergoing dynamic exchange with the free rings, unless it occupies the position at the end of the chain. The threaded rings can only migrate along the chain or rotate it ; they are thus confined to one-dimensional space with respect to the polymer chain.

Harada et al. constructed polyrotaxane [6] by the threading of a poly(ethyleneglycol)diamine chain with  $\alpha$ -cyclodextrin “beads” and coupling with dinitrophenyl stoppers<sup>55</sup> (Fig.13).

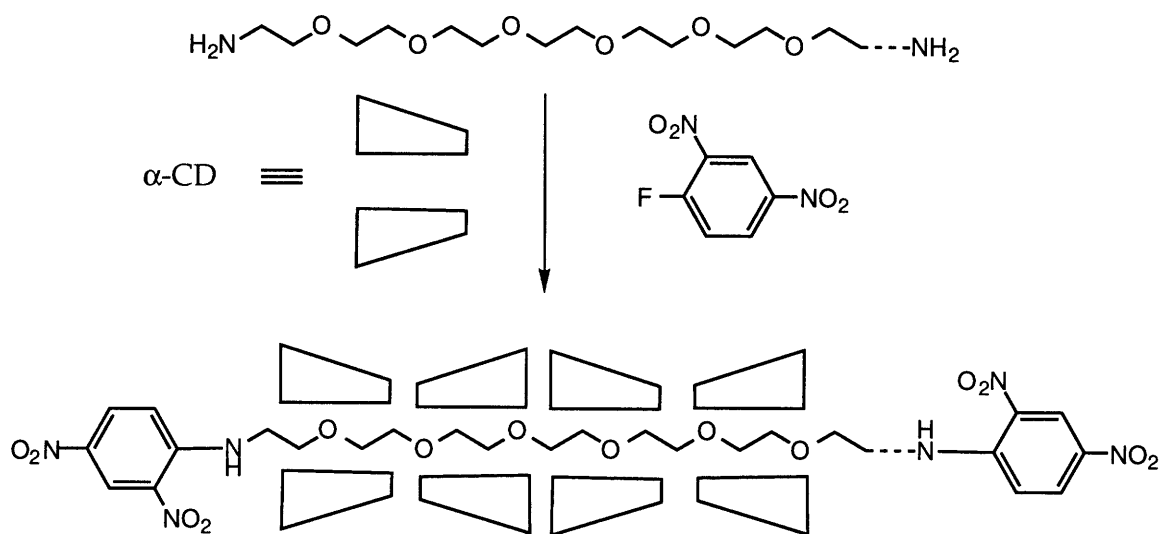
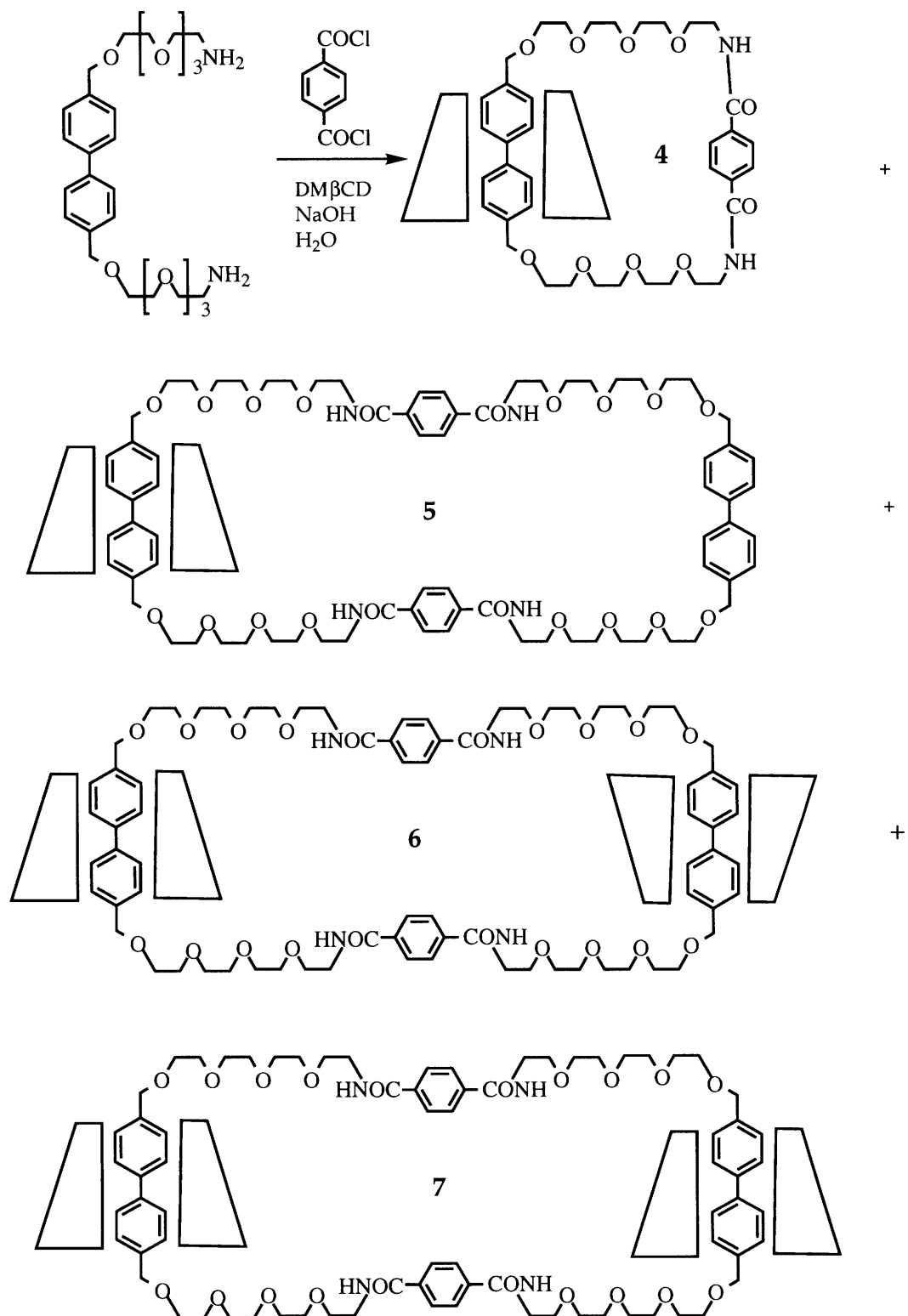


Fig. 13 An  $\alpha$ -CD based polyrotaxane.

Stoddart et al. synthesized two [2]catenanes, 4 and 5, and two [3]catenanes, 6 and 7, from the inclusion compound of the bitolyl derivative 7 in heptakis(2,6-di-O-methyl)- $\beta$ -cyclodextrin (Fig. 14).<sup>56</sup>

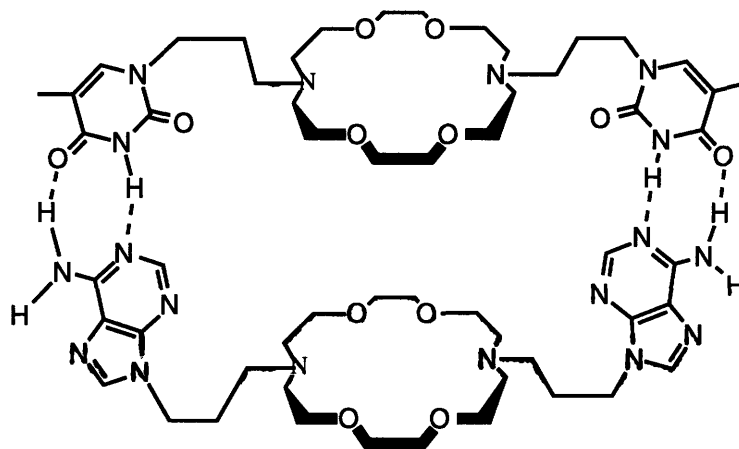
### 1.3.4 The Hydrogen Bond

The highly selective and directional nature of the hydrogen bond makes it ideal for use in the construction and stabilization of large noncovalently linked and supramolecular architectures.



**Fig. 14** Synthesis of [2] and [3] catenane from heptakis(2,6-di-O-methyl)- $\beta$ -cyclodextrin.

The first example for a self-assembling host system dates back to 1987 and was synthesized in the research group of G. Gokel<sup>57</sup>. Mimicking the binding between the two strands of DNA, adenine and thymine groups were used for hydrogen bonding in the synthetic system (Fig.15). Two differently functionalized diaza-18-crown-6 scaffolds, one with thymine sidearms, the other one with adenine sidearms, form four hydrogen bonds upon assembly of the molecular box.

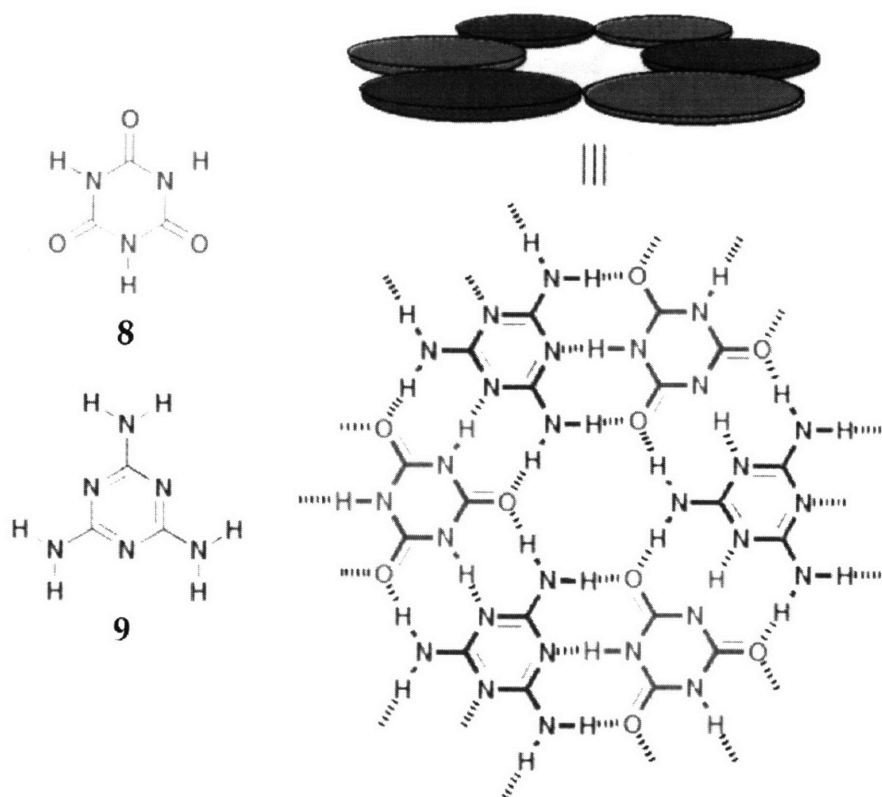


**Fig.15** Hydrogen bonds between thymine and adenine contribute to the stability of the first self-assembled host system.

Vapor phase osmometry indicates that the system forms a labile assembly ( $K_a = 2 \text{ M}^{-1}$ ) in water. The association can be favored by adding appropriate cationic guests which can form additional hydrogen bonds to the crown ethers. Stabilization of the assembly is achieved by addition of  $[\text{H}_3\text{N}-(\text{CH}_2)_{12}-\text{NH}_3]\text{Cl}_2$ , where the dication can form a hydrogen bonded tether across the molecular box between the crown ethers. In chloroform, which in

contrast to water does not compete in the hydrogen bonding, a much higher degree of association is observed ( $K_a = 860 \text{ M}^{-1}$ ). Several different equilibria exist in solution, including Hoogsteen-type bonding and intramolecular interactions between bases linked to the same crown ether scaffold<sup>58</sup>.

Whitesides and co-workers<sup>59-62</sup> have exploited the strong, multiply hydrogen-bonded lattice formed between cyanuric acid **8** and melamine **9** to construct large, nanometerscale structures in solution<sup>59,60</sup>. Reaction of **8** with **9** gives the insoluble 1 : 1 complex [**8•9**] shown in Fig.16 .

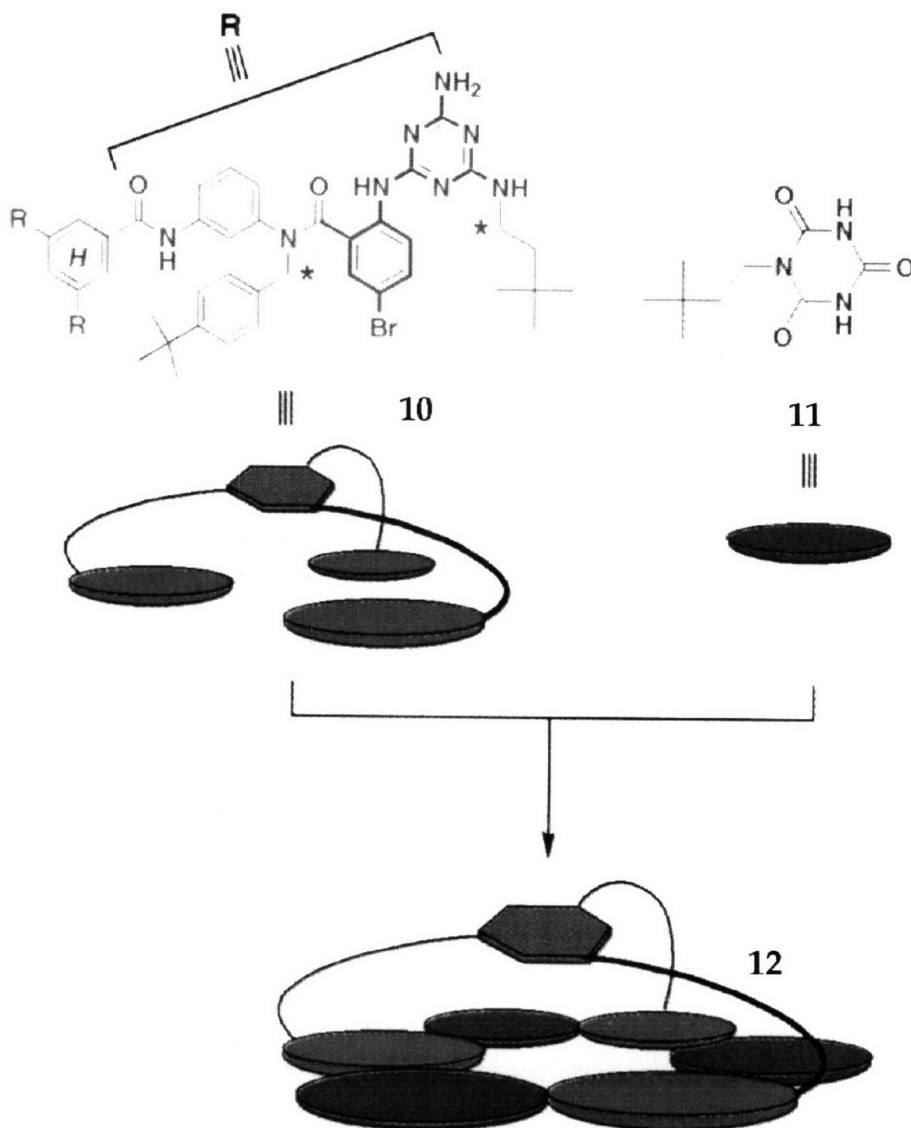


**Fig.16** The stable hexagonal lattice formed between cyanuric acid and melamine.

The linking of three melamine units to a central hub **H** (Fig. 17) affords molecule **10**, which can have a conformation compatible with the cyanuric



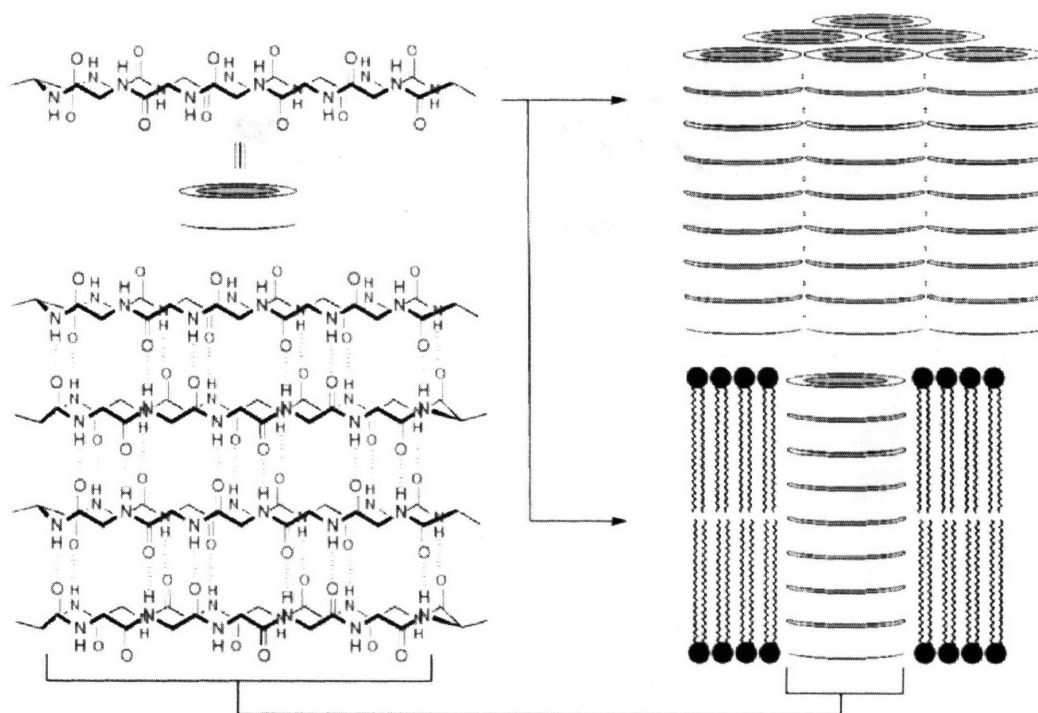
acid/melamine lattice. Thus, mixing **10** with three molar equivalents of the alkyl cyanuric acid **11** gives the extremely stable 3 : 1 complex in  $\text{CDCl}_3$  solution, which contains one layer of the basic structure of the cyanuric acid/melamine lattice capped by the trisubstituted benzene hub **H**.



**Fig. 17** The 3 : 1 complex between the cyanuric acid derivative and the hub, which tethers three melamine units, is stabilized by 18 hydrogen bonds.

The  $^1\text{H}$  NMR spectrum of the  $\text{C}_3$ -symmetric tris(melamine) unit is very broad but becomes completely sharp upon titration with cyanuric acid derivatives once a 1:3 stoichiometry has been reached. Vapor pressure osmometry (VPO) gives a molecular mass for the species in solution of 2720 Da, in close agreement with the calculated value of 2733 Da for 12.

Ghadiri and co-workers have reported the self-assembly of a series of nanoscale tubules based on cyclic peptides<sup>63-65</sup>. The basic design utilizes a cyclic peptide whose primary sequence consists of alternating D- and L-amino acids (Fig. 18).



**Fig. 18** The assembly of a self-complementary cyclic peptide.

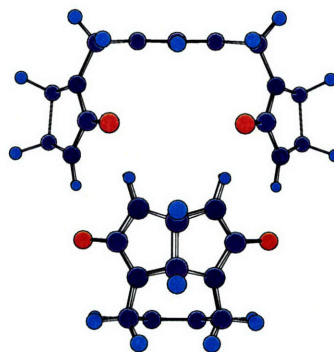
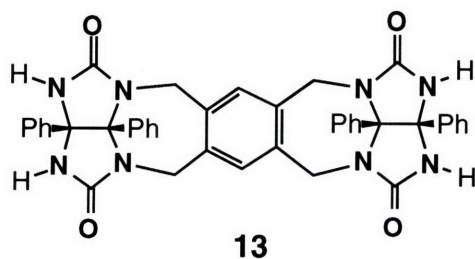
Such peptides possess flat doughnutlike conformations in solution. This conformation promotes the face-to-face association of the cyclic peptides into

nanoscale tubules, which are stabilized along their length by hydrogen bonding interactions between the amide groups in the peptide backbone. Depending on the conditions, such peptides can be assembled into highly ordered aggregates of nanotubules in the solid state or into transmembrane pores.

#### 1.4 Self-Assembling Dimeric Molecule

As discussed above, self-organizing assemblies have been the subject of numerous studies. Recently, new concepts were developed giving molecules that self-assemble to give cavities suitable for encapsulation of selected molecular targets.

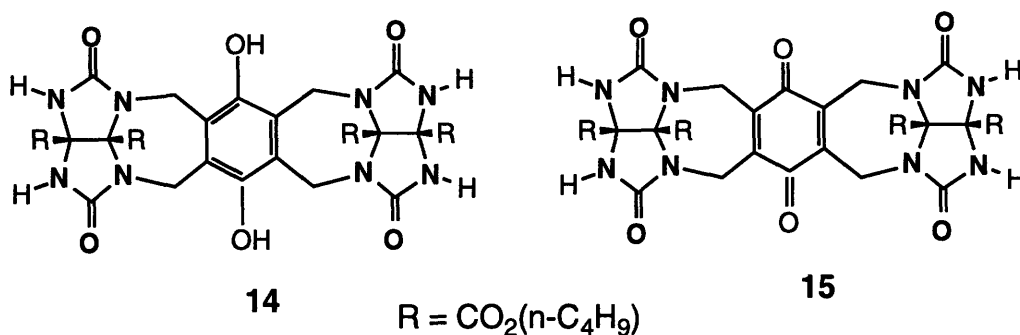
The earliest examples of this strategy was reported by Rebek and co-workers<sup>66</sup>. The compound **13** was prepared by condensing two molecules of diphenyl glycoluril with durene tetrabromide. The curvature of the molecule along its length is consequence of the folding caused by the 7-membered rings when the phenyl units are all on the same face of the structure.



The curvature along its width is caused by cis fusion of the 5-membered rings. The stereochemical features of this molecule impart the necessary curvature for dimeric assembly while lactam functions provide self-complementary hydrogen bond donors and acceptors. These provide the cohesive force along the edge of the molecule to hold the two pieces together. Dimer **13•13** was found to encapsulate small organic molecules such as CH<sub>4</sub>, CH<sub>3</sub>CH<sub>3</sub>, and CDCl<sub>3</sub>. Encapsulation of such guests was observed by <sup>1</sup>H NMR where bound species like CH<sub>4</sub> and CH<sub>3</sub>CH<sub>3</sub> shows signals at -0.91 ppm and -0.39 ppm<sup>67</sup>.

The molecular capsule derived from p-dimethylaminodiphenylglycoluril derivatives offer control of the self-assembly process<sup>68</sup>. The basic sites of the dimethylamino functions are subject to protonation with strong acid such as p-toluenesulfonic acid, and at high acidities the guest (xenon) is released. Neutralization with bases reverses the process and the guest is encapsulated once again. Multiple positive charges that build up on protonation of the periphery force the two halves of the capsule apart through coulombic repulsion.

Using dimers **14•14** and **15•15**, it was found that the electronics of the aromatic spacer influence the binding affinity of guest<sup>69</sup>. Electron rich **14•14** shows a significant increase in affinity over the electron poor **15•15** for species such as CH<sub>4</sub>, C<sub>2</sub>H<sub>6</sub> and CH<sub>3</sub>F.



**Fig. 19** Electron rich and electron poor capsules show altered selectivities.

A study concerned with the systematic variation of shape and size of the spacer was also reported<sup>70</sup>. The monomers **16**, **17** and **18** contain ethylene, naphthalene, and a bridged anthracene, respectively, as their spacer elements. The MM2 energy-minimized structures of the corresponding dimers are compared and calculated O-O distances of the monomers are shown in Fig. 20. The dimerization of these monomers leads to pseudo-spherical structures with cavities smaller or larger than that of **13•13**. In addition to self-assembling as dimers, these new molecules were shown to disproportionate into hybrid species or heterodimers. The resulting new capsules feature internal cavities of varying size and shapes. Formation of hybrid dimers **13•16**, **13•17**, and **17•18** is observed in solutions containing mixtures of two homodimers. The disproportionation equilibria could be manipulated by the addition of appropriately sized solvents as guests. Even the energetically unlikely hybrid **13•17** and **17•18** are found to be dominant species when suitable guests such as CDBr<sub>3</sub> are present.

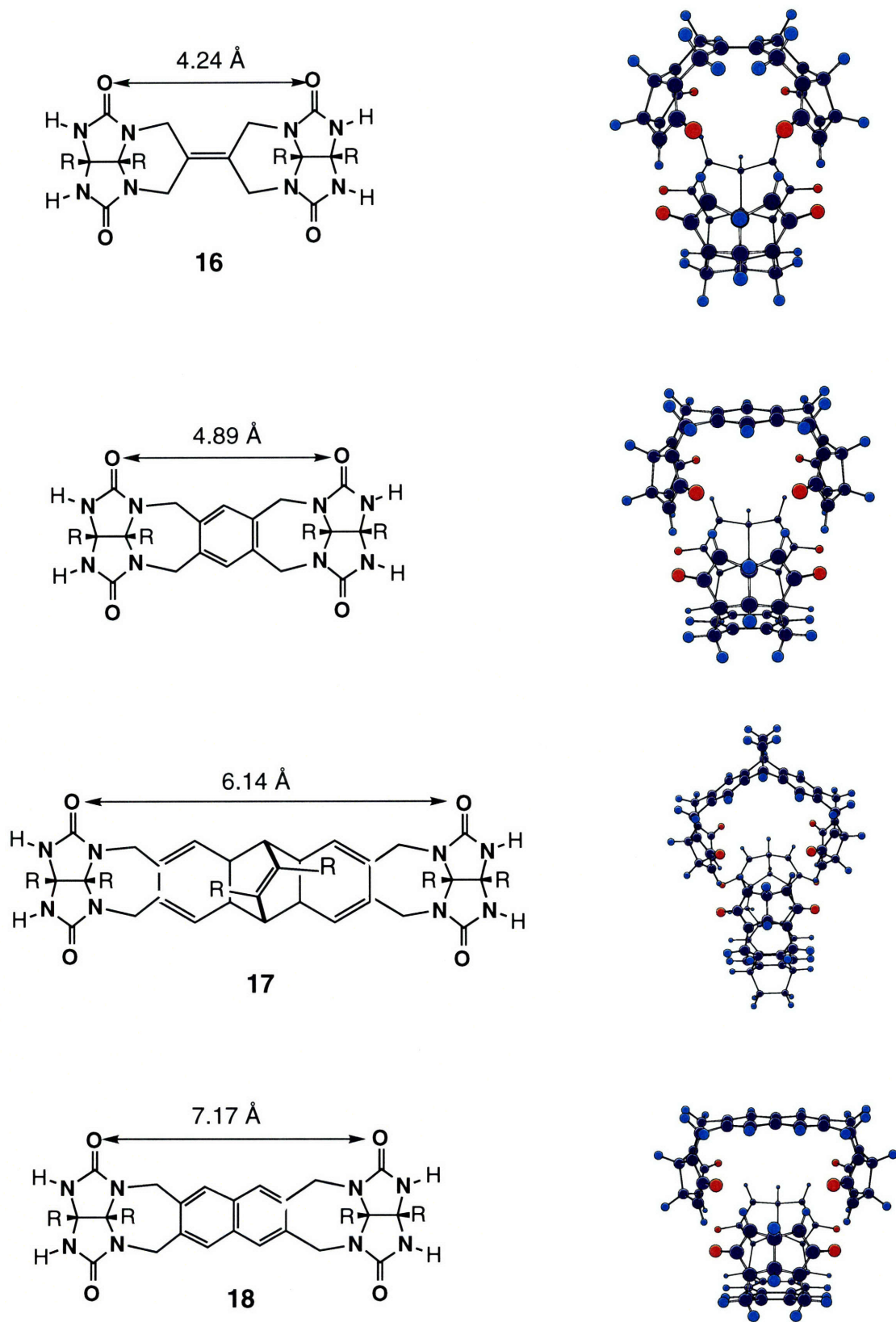
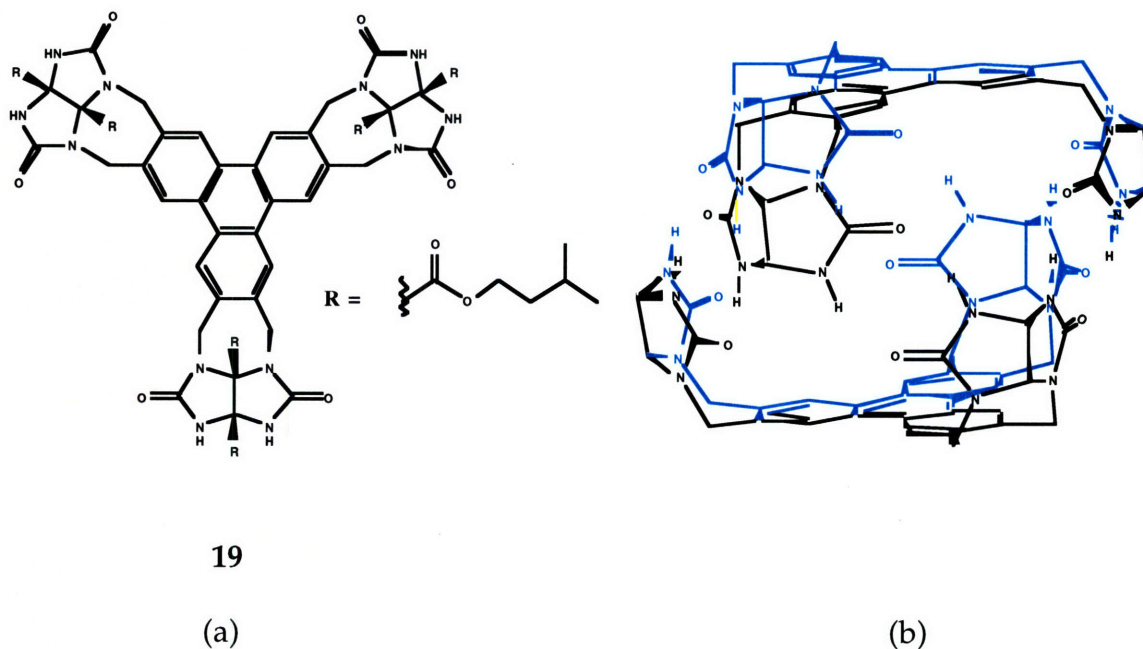


Fig. 20 Dimensions and shapes of new capsules.

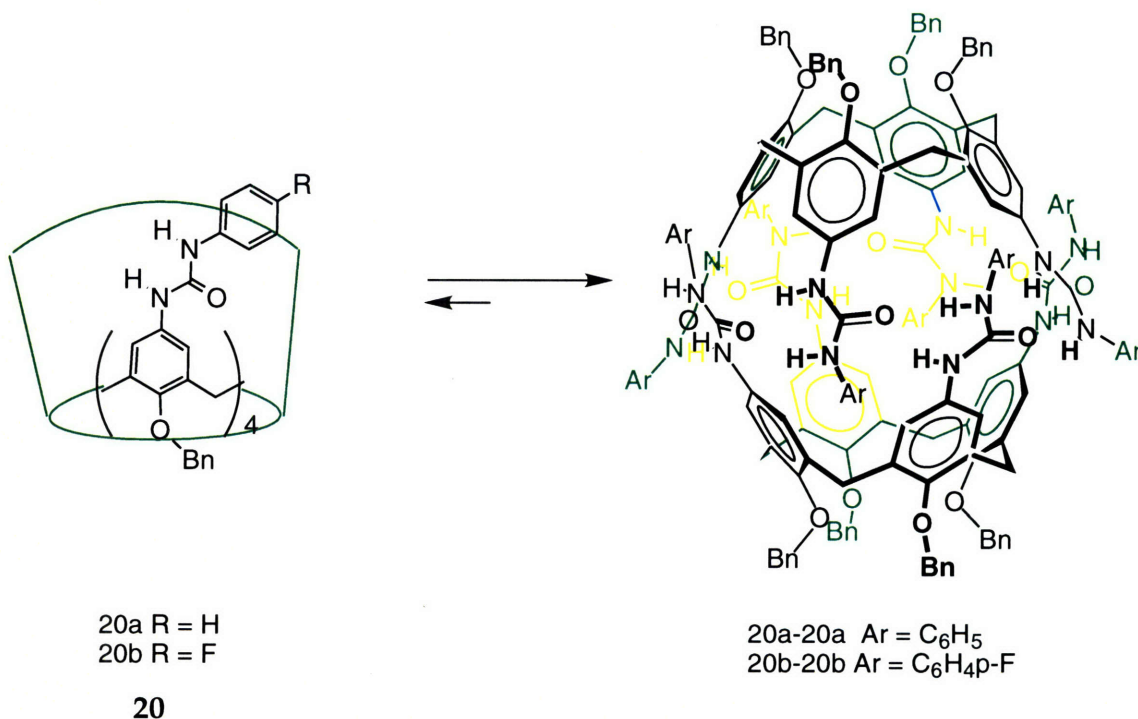
Another variation on the spacer was made by using triphenylenespacer<sup>71</sup>. The ceiling and floor of the assembled capsule consists of aromatic  $\pi$ -surfaces and 12 strong hydrogen bonds hold the two halves together. This dimer features  $D_{3d}$  symmetry and its shape resembles that of Jelly-doughnut. Therefore, flat disc-shaped guests such as benzene and cyclohexane are good complements to the cavity's interior. The spherical solvent  $CDCl_3$  is displaced rapidly by the addition of benzene, suggesting that  $CDCl_3$  is a poor guest. However, when p-xylene- $d_{10}$  is used it takes hours, after the addition of a favorable guest like cyclohexane for the system to reach equilibrium.



**Fig. 21** (a) Two dimensional structure of the jelly doughnut (b) energy-minimized 3-D view of the self-assembled dimer held together by 12 hydrogen bonds.



Rebek and co-workers also synthesized another shape of dimeric capsule which has two bucket shaped calixarenes zippered together along the large rims by hydrogen bonded ureas<sup>72</sup>. With dimerization, the carbonyl oxygens of one urea are buried into NH's of the preceding urea. All eight ureas are fixed in the same direction forming up to 16 hydrogen bonds. Inclusion of solvent molecules in a dimer **20•20** was shown in mixed solvent systems where two distinct calixarene assemblies were observed by <sup>1</sup>H-NMR. Direct observation of the encapsulated guests by <sup>1</sup>H-NMR was also possible with p-xylene, fluorobenzene, p-difluorobenzene and pyrazine. Competition studies of guests with benzene were undertaken and the affinity of the calixarene dimer for these, relative to benzene, is given in Table 1.<sup>73</sup>



**Fig. 22** The dimerization of the tetraurea calix[4]arene through intermolecular forces.



Guest	Affinity (298K)	Guest	Affinity (298K)
$C_6H_6$	1.0	$C_6H_5OH$	0.83
$C_6H_5F$	2.6	$C_6H_5NH_2$	0.32
p- $C_6H_4F_2$	5.8	Pyrazine	3.2
$C_6H_5Cl$	0.3	Pyridine	1.2
$C_6H_5CH_3$	<0.1		

**Table.1** Relative affinities of guests in competition experiments with benzene.

20

## 1.5 References

- 1) Whitesides, G. M.; Mathias, J. P.; Seto, C. T. *Science* **1991**, 254, 1312.
- 2) Nicolaou, K. C.; Sorensen, E. J. *Classics in Total Synthesis*; VCH: Weinheim, 1996.
- 3) Corey, E. J.; Cheng, X. M. *The Logic of Chemical Synthesis*; Wiley: New York, 1989.
- 4) Corey, E. J. *Angew. Chem. Int. Ed. Engl* **1991**, 30, 455.
- 5) Watson, J. D.; Hopkins, N. H.; Roberts, J. W.; Steitz, J. A.; Weiner, A. M. *Molecular Biology of the Gene*; Benjamin/Cummings: Menlo Park, CA, 1988.
- 6) Alberts, B.; Bray, D.; Lewis, J.; Roberts, K.; Watson, J. D. *Molecular Biology of the Cell*; Garland Publisher: New York, NY, 1994.
- 7) Klug, A. *Angew. Chem. Int. Ed. Engl* **1983**, 22, 565.
- 8) Cantor, C. R.; Schimmel, P. R. *Biophysical Chemistry part III*; Freeman: San Francisco, 1980.
- 9) Weissman, J. S.; Kim, P. S. *Science* **1991**, 253, 1386.
- 10) Creighton, T. E. *Biochem.* **1990**, 270, 1.
- 11) Brandon, D.; Tooze, J. *Introduction to Protein structure*; Garland Publishing: New York, 1991.
- 12) Alan, C. *Self-Assembling Architecture*; Liss: New York, 1988.
- 13) Lebeurier, G.; Nicholaieff, A. *Proc. Natl. Acad. Sci. USA* **1977**, 75, 150.
- 14) Lauffer, M. A. *Entropy-Driven Processes*; Springer: New York, 1975.
- 15) Fraenkel-Conrat, H.; Williams, R. C. *Proc. Natl. Acad. Sci. USA* **1955**, 41, 690.

- 16) Barr, R. G.; Pinnavaia, T. J. *J. Chem. Phys.* **1986**, *90*, 328.
- 17) Fujita, M.; Yazaki, Y.; Ogura, K. *Chem. Lett.* **1991**, 1031.
- 18) Fujita, M.; Yazaki, J.; Ogura, K. *J. Am. Chem. Soc.* **1990**, *112*, 5645.
- 19) Geib, S. J.; Vicent, C.; Fan, E.; Hamilton, A. D. *Angew. Chem. Ed. Engl.* **1993**, *32*, 119.
- 20) Constable, E. C. *Tetrahedron* **1992**, *48*.
- 21) Constable, E. C. *Angew. Chem. Int. Ed. Engl.* **1991**, *30*, 1450.
- 22) Constable, E. C. *Nature* **1990**, *346*, 314.
- 23) Bell, T. W.; Jousselein, H. *Nature* **1994**, *367*, 441.
- 24) Lehn, J.-M.; Rigault, A.; Siegel, J.; Harrowfield, J.; Chevrier, B.; Moras, D. *Proc. Natl. Acad. Sci. USA* **1987**, *84*, 2565.
- 25) Lehn, J.-M.; Rigault, A. *Angew. Chem. Int. Ed. Engl.* **1988**, *27*, 1095.
- 26) Pfeil, A.; Lehn, J.-M. *J. Chem. Soc. Chem. Commun.* **1992**, 838.
- 27) Kramer, R.; Lehn, J.-M.; Marquis-Rigault, A. *Proc. Natl. Acad. Sci. USA* **1993**, *90*, 5394.
- 28) Charbonniere, L. J.; Gilet, M. F.; Bernauer, K.; Williams, A. F. *Chem. Commun.* **1996**, 39.
- 29) Williams, A. F.; Piguet, C.; Carina, R. F. *Transition Metals in Supramolecular Chemistry* Kluwer, 1994.
- 30) Piguet, C.; Bernardinelli, G.; Bocquet, B.; Quattropiani, A.; Williams, A. F. *J. Am. Chem. Soc.* **1992**, *114*, 7440.
- 31) Dietrich-Buchecker, C. O.; Sauvage, J. P.; Kern, J. M. *J. Am. Chem. Soc.* **1984**, *106*, 3043.

- 32)Dietrich-Buchecker, C. O.; Sauvage, J. P.; Kintzinger, J. P. *Tetrahedron. Lett.* **1983**, 24, 5095.
- 33)Bard, A. J.; Ledwith, A.; Shine, J. *Adv. Phys. Org. Chem.* **1976**, 13, 155.
- 34)Summers, L. A. *The Bipyridinium Herbicides*; Academic press: London, 1980.
- 35)Summers, L. A. *Heterocycl. Chem.* **1984**, 35, 282.
- 36)Dewar, M. J. S.; Zoebisch, E. G.; Healy, E. F.; Stewart, J. J. P. *J. Am. Chem. Soc.* **1985**, 107, 3902.
- 37)Heyrovsky, M. J. *Chem. Soc. Chem. Commun.* **1987**, 1856.
- 38)Haque, R.; Coshow, W. R.; Johnson, L. F. *J. Am. Chem. Soc.* **1969**, 91, 3822.
- 39)Saenger, W. *Angew. Chem. Int. Ed. Engl.* **1980**, 19, 344.
- 40)Muller, N. *Acc. Chem. Res.* **1990**, 23, 23.
- 41)Blokzijl, W.; Engberts, J. B. F. N. *Angew. Chem. Int. Ed. Engl.* **1993**, 32, 1545.
- 42)Cramer, F. *Cyclodextrins and their Industrial Uses*; Cramer, F., Ed.; Editions de Sante: Paris, 1987, pp 11.
- 43)Griffiths, D. W.; Bender, M. L. *Adv. Catal.* **1973**, 23, 209.
- 44)Tabushi, I. *Acc. Chem. Res.* **1982**, 15, 66.
- 45)Breslow, R. *Acc. Chem. Res.* **1995**, 28, 146.
- 46)Breslow, R.; Greenspoon, N.; Guo, T.; Zarzycki, R. *J. Am. Chem. Soc.* **1989**, 111, 8296.
- 47)Harada, A.; Furue, M.; Nozakura, S.-I. *Polym. J. Tokyo* **1980**, 12.
- 48)Breslow, R.; Chung, S. *J. Am. Chem. Soc.* **1990**, 112, 9659.
- 49)Lehn, J.-M. *Angew. Chem. Int. Ed. Engl.* **1988**, 27, 89.

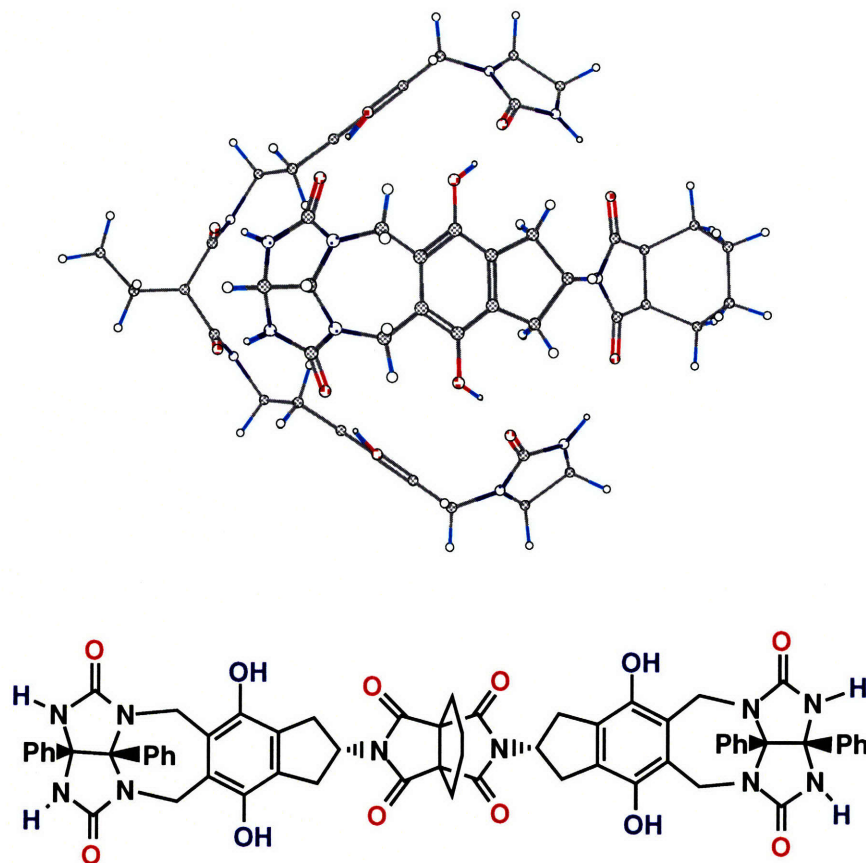
- 50) Kamitori, S.; Hirotsu, K.; Higuchi, T.; Fujita, K.; Yamamura, H.; Imoto, T.; Tabushi, I. *J. Chem. Soc. Perkin Trans.* **1987**, *2*, 7.
- 51) Petter, R. C.; Salek, J. S.; Sikorski, C. T.; Kumaravel, G.; Lin, F.-T. *J. Am. Chem. Soc.* **1990**, *112*, 3860.
- 52) Hirotsu, K.; Higuchi, T.; Fujita, K.; Ueda, T.; Shinoda, A.; Imoto, T.; Tabushi, I. *J. Org. Chem.* **1982**, *47*, 1143.
- 53) Seo, T.; Kajihara, T.; Iijima, T. *Makromol. Chem.* **1990**, *191*, 1665.
- 54) Okubo, T.; Kuroda, M. *Macromolecules* **1989**, *22*, 3936.
- 55) Harada, A.; Li, J.; Kamachi, M. *Nature* **1992**, *356*, 325.
- 56) Armspach, D.; Ashton, P. R.; Moore, C. P.; Spencer, N.; Stoddart, J. F.; Wear, T. J.; Williams, D. J. *Angew. Chem. Int. Ed. Engl.* **1993**, *32*, 854.
- 57) Shall, O.; Gokel, G. W. *J. Am. Chem. Soc.* **1994**, *116*, 6089.
- 58) Kim, M.; Kim, G. W. *J. Chem. Soc. Chem. Commun.* **1987**, 1686. 59) Seto, C. T.; Whitesides, G. M. *J. Am. Chem. Soc.* **1990**, *112*, 6409.
- 60) Seto, C. T.; Whitesides, G. M. *J. Am. Chem. Soc.* **1991**, *113*, 712.
- 61) Zerkowski, J. A.; Seto, C. T.; Wierda, D. A.; Whitesides, G. M. *J. Am. Chem. Soc.* **1990**, *112*, 9025.
- 62) Zerkowski, J. A.; Seto, C. T.; Whitesides, G. M. *J. Am. Chem. Soc.* **1992**, *114*, 5473.
- 63) Khazanovich, N.; Granja, J. R.; McRee, D. E.; Milligan, R. A.; Ghadiri, M. R. *J. Am. Chem. Soc.* **1994**, *116*, 6011.
- 64) Ghadiri, M. R.; Kobayashi, K.; Granja, J. R.; Chadha, R. K.; McRee, D. E. *Angew. Chem. Int. Ed. Engl.* **1995**, *29*, 36.

- 65)Ghadiri, M. R. *Adv. Mater.* **1995**, 7, 675.
- 66)Wyler, R.; Mendoza, J. d.; Rebek. J. Jr. *Angew. Chem. Int. Ed. Engl.* **1993**, 32, 1699.
- 67)Branda, N.; Wyler, R.; Rebek. J. Jr. *Science* **1994**, 32, 1169.
- 68)Branda, N.; Grotzfeld, R. M.; Valdes, C.; Rebek. J. Jr. *J. Am. Chem. Soc.* **1995**, 117, 12733.
- 69)Garcias, X.; Rebek. J. Jr. *Angew. Chem. Int. Ed. Engl.* **1996**, *In press*.
- 70)Valdes, C.; Spitz, U. P.; Toledo, L.; Kubik, S.; Rebek. J. Jr. *J. Am. Chem. Soc.* **1995**, 117, 12733.
- 71)Grotzfeld, R.; Branda, N.; Rebek. J. Jr. *Science* **1996**, 271, 487.
- 72) Shimizu, K. D. ; Rebek J. Jr. *Proc. Natl. Acad. Sci. U.S.A.* **1995**, 92, 12403
- 73) Hamman, B. C. ; Shimizu, K.D. ; Rebek J. Jr. *Angew. Chem. Int. Ed. Engl.* **1996**, 35, 1326

## Chapter 2. Self-Assembling Dimeric Molecule - The First Designed Flexible System

### 2.1 Design

The first designed self-assembling dimeric molecule that can have large cavity was designed by Professor Xavier de Mendoza. This molecule should adopt a C-shaped conformation as depicted in the three dimensional view in Fig. 23.



21

**Fig. 23** The first designed large volume self-assembling dimeric molecule. a) Energy minimized dimeric structure b) Two dimensional monomeric structure.

Not only glycoluril units provide the hydrogen bonding as a donor (from the four N-H bonds to the four carbonyl oxygens in the central ring) but also they provide the hydrogen bonding acceptor (from the four phenolic O-H bonds to the four amidic carbonyl oxygens) in molecule **21** (Fig.23). When two molecules of **21** come together with their concave surfaces facing towards each other, a structure of roughly spherical shape can result from 16 hydrogen bonds. The angle and length of hydrogen bond in the dimeric state from Amber calculation is shown in Table 2.

N—H·····O	O—H·····O
length    2.76 Å	length    2.68 Å
angle        161 ~ 162°	angle        167°

**Table. 2** Hydrogen bond length and angles in self-assembling dimeric molecule **21**

The way the two pieces are assembled in this dimer resembles the structure of a soft-ball. Molecules like adamantane may fit in the cavity of this ball-like structure, and therefore favor or promote the self-assembly leading to the dimer complex. This dimer has some resemblance with carcerand and cryptophanes of Cram<sup>1,2</sup> and Collet<sup>3,4</sup>, but this dimer is formed reversibly.



## 2.2 Retrosynthesis of Molecule 21

The retrosynthetic analysis of this molecule is presented in the following Fig. 24. It should be possible to prepare the target molecule starting from three readily accessible precursors. These are

22: glycoluril      23: 2-indanol derivative

24: the central bicyclic diimide

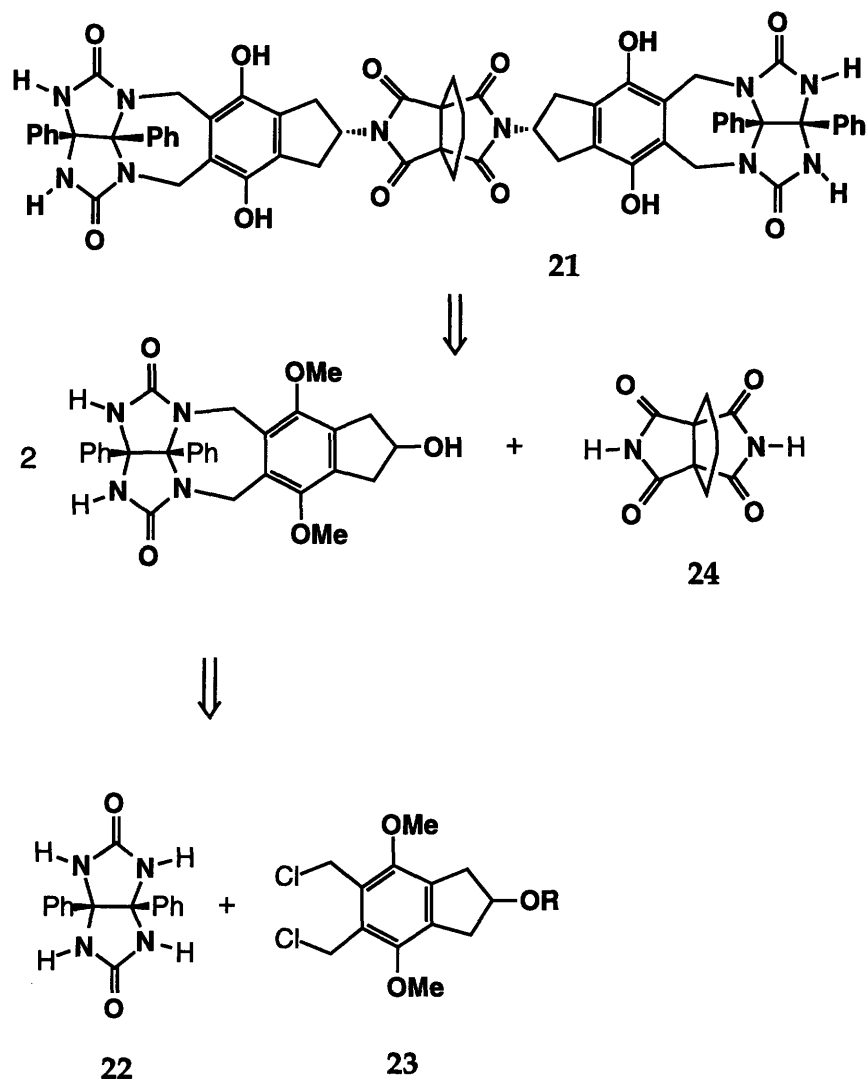
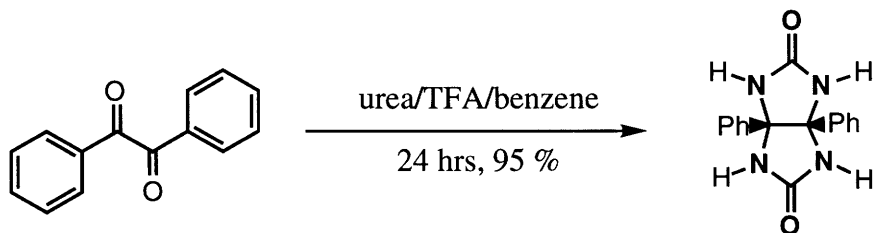


Fig.24 Retrosynthetic analysis of molecule 21.

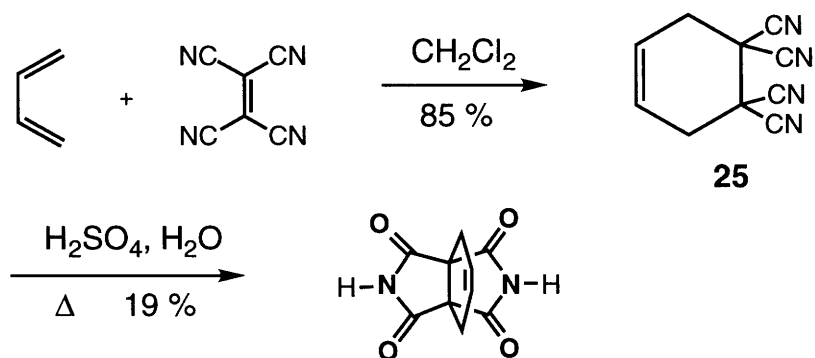
## 2.3 Synthesis

### 2.3.1 Glycoluril and Central diimide

The synthesis of this molecule was developed by the collaboration with Dr. Rene Wyler and Dr. Robert S. Meissner. Glycolurils are easily obtained from urea and 1,2-dioxo compound such as benzil and acid as a catalyst. Diphenyl glycoluril was selected as it was already known although it was not very soluble. Therefore, Diphenyl glycoluril **22** was obtained in high yield and on a 100g scale by condensation of two equiv. of urea with benzil in the presence of trifluoroacetic acid in benzene<sup>5</sup>.



The synthesis of central diimide starts from Diels-Alder reaction of butadiene and tetracyanoethylene. Hydrolysis of Diels-Alder product **25** directly gave the central diimide<sup>6</sup>.



### 2.3.2 The synthesis of 4,7-dimethoxy-2-indanol

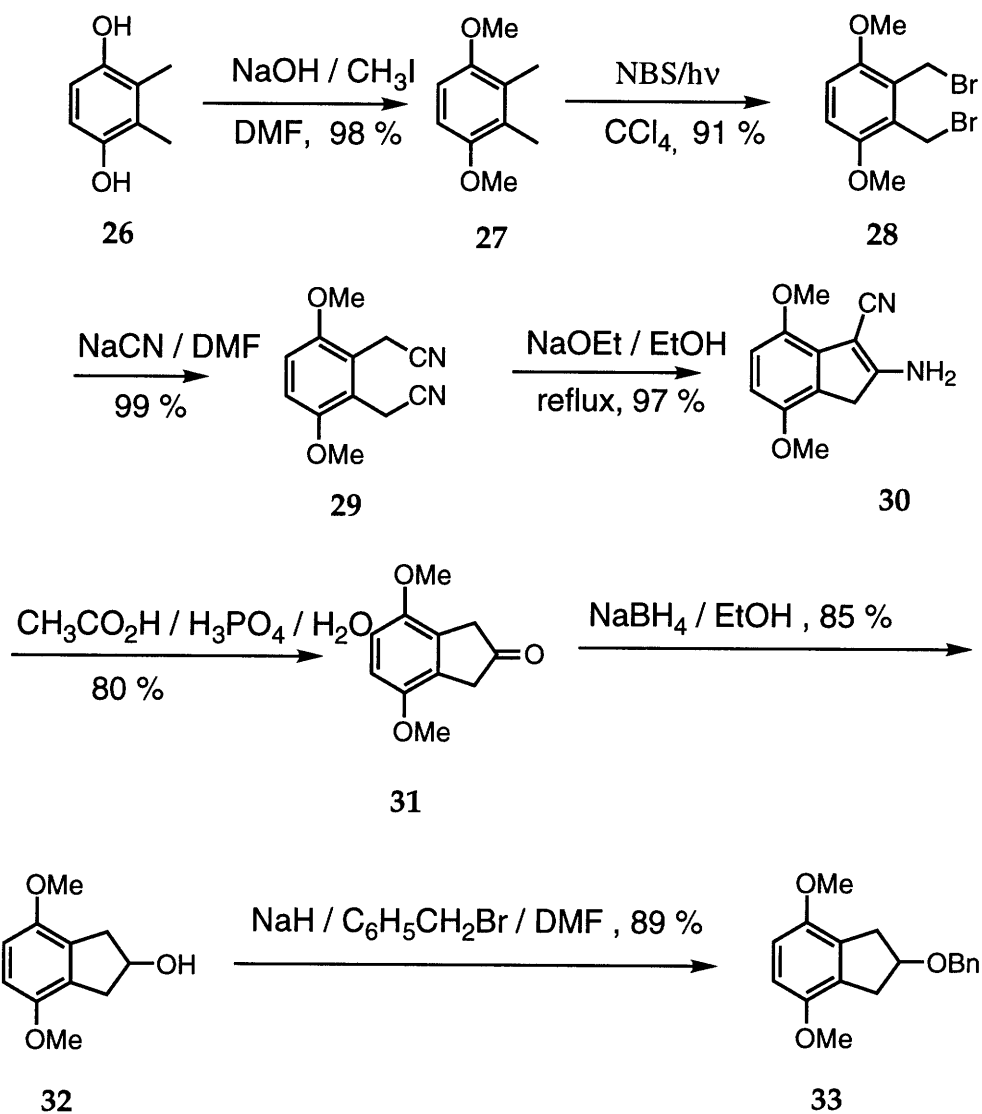


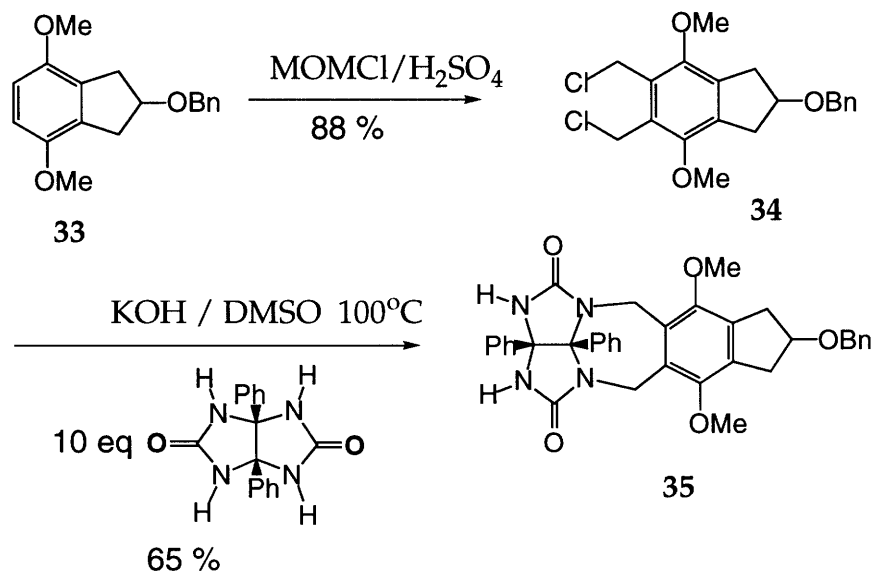
Fig. 25 The synthesis of 4,7-dimethoxy-2-indanol **32**.

The synthesis of 4,7-dimethoxy-2-indanol started from commercially available 2,3-dimethylhydroquinone **26**. Methylation of 2,3-dimethylhydroquinone using sodium hydroxide and methyl iodide in DMF

gave compound **27** in high yield. Radical bromination of compound **27** gave compound **28** and this was followed by the substitution reaction with sodium cyanide to give compound **29**. Cyclization under basic conditions using sodium ethoxide in ethanol solution gave compound **30**. Hydrolysis of compound **30** in mixture of acetic acid and phosphoric acid gave compound **31**. Reduction with sodium borohydride in ethanol gave compound **32** and benzylation with benzylbromide gave the expected protected 2-indanol **33**.

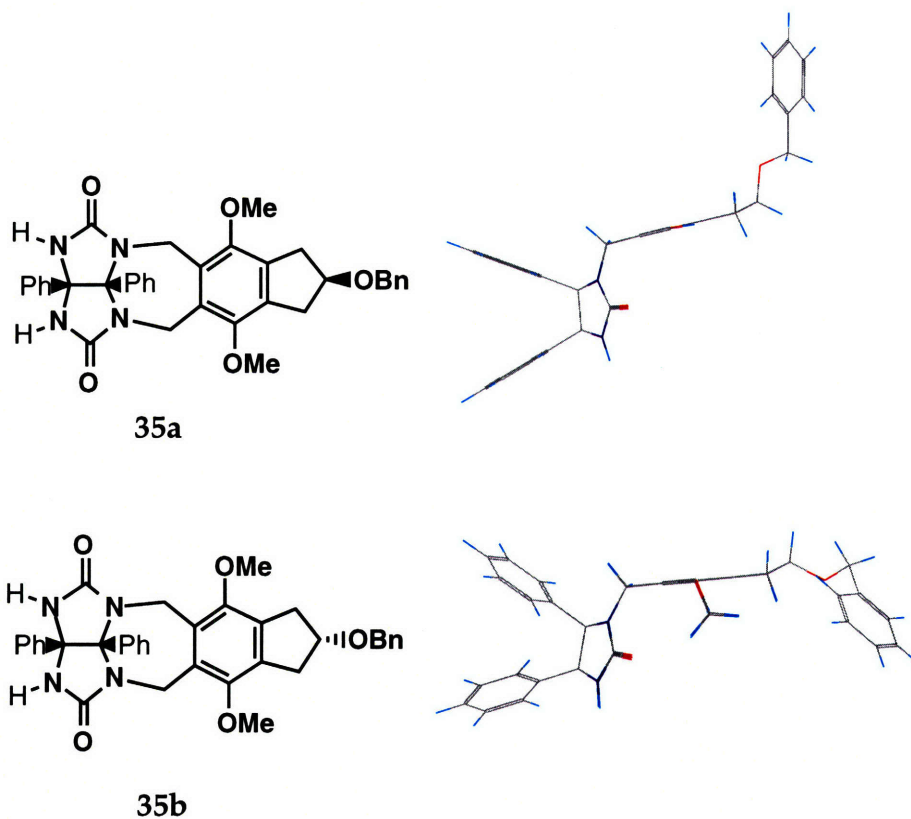
### 2.3.3 Coupling reactions of glycoluril, Central diimide and 2-benzyloxy-4,7-dimethoxyindane **33**

To couple 2-benzyloxy-4,7-dimethoxyindane **33** and glycoluril **22**, **33** was functionalized by double chloromethylation using chloromethyl methyl



**Fig. 26** Coupling reactions between 2-benzyloxy-4,7-dimethoxyindane **33** and diphenylglycoluril.

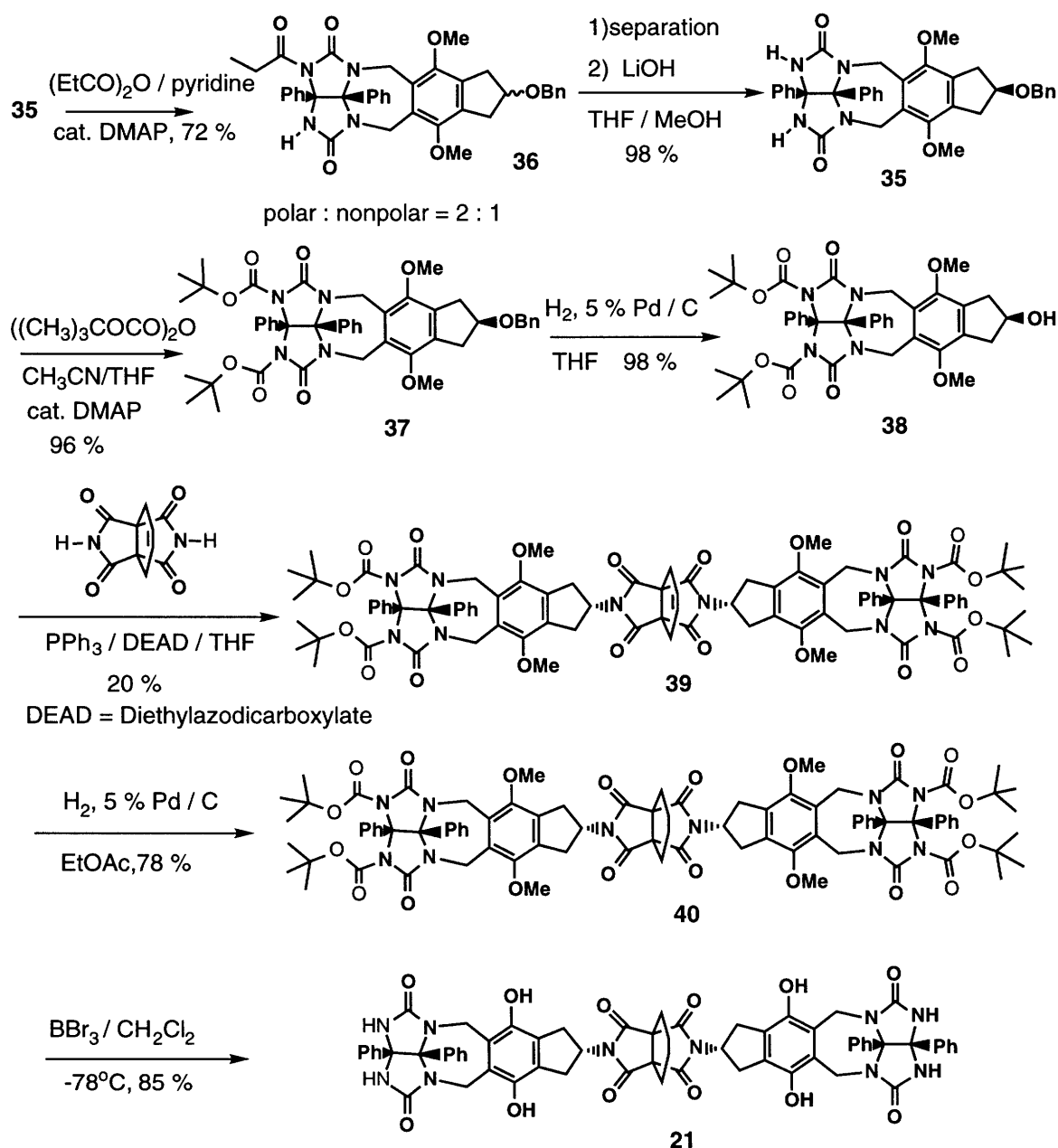
ether<sup>7</sup> with 60 % H<sub>2</sub>SO<sub>4</sub> to give functionalized 2-benzyloxy-4,7-dimethoxyindane **34**. Then **34** was coupled with glycoluril using potassium hydroxide in DMSO at 100°C to give compound **35** in 65 % yield.



**Fig. 27** Energy minimized structures of two stereoisomers **35a** and **35b** from Amber calculation.

Coupling reaction of **34** with the glycoluril gave two stereoisomers. As the next Mitsunobu reaction inverts the stereochemistry of alcohol, compound **35a** is the right isomer. However, it was difficult to separate them and even after the separation, it was difficult to properly assign the structure. Therefore, both compounds were taken through the final synthesis and it was expected that only the right isomer would give a self-assembling dimer. To separate

two isomers easily, the glycoluril part of molecule was selectively propionated and the two isomers were separated by flash column chromatography. The ratio of isomers were polar : nonpolar = 2 : 1 (polarity is based on TLC)

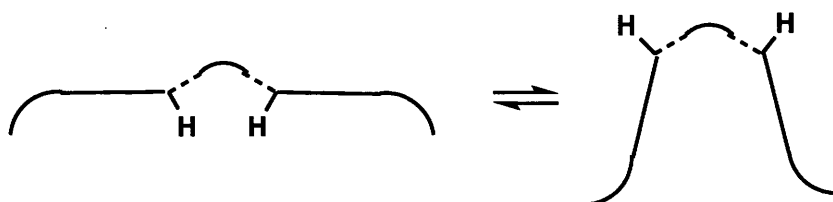
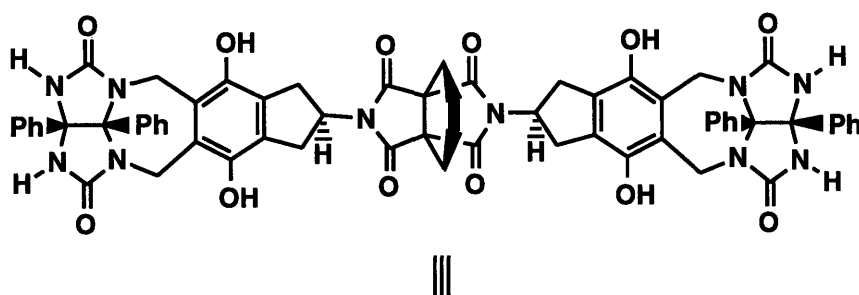
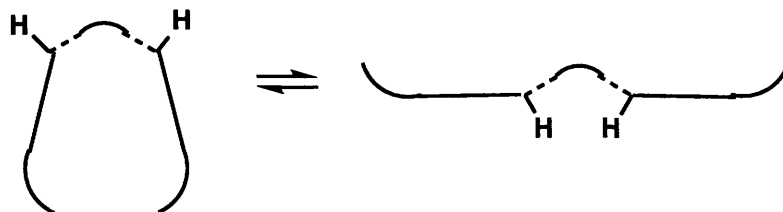
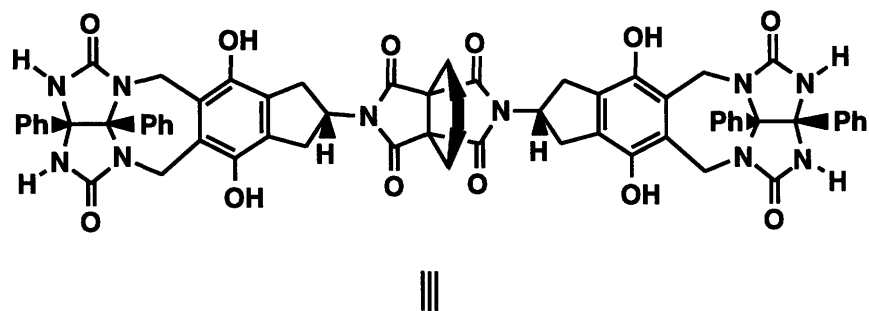


**Fig.28** Coupling reactions of **35** and diimide **24** finally gives the expected compound.

After the separation of isomers, the propionate groups were removed by lithium hydroxide in THF-MeOH to give stereochemically pure compound **35**. As the solubility of compound **35** was low, and the unprotected glycoluril N-H moiety gave complications in Mitsunobu reaction, the tert-butoxycarbonyl (BOC group) was added to compound **35** using di-tert-butylidicarbonate and DMAP. Then the benzyl group was removed using H<sub>2</sub>/ 5 % Pd-C to give compound **38**. Double Mitsunobu reaction<sup>8,9</sup> of compound **38** and central diimide **24** gave the compound **39**. The olefin of the central diimide **39** proved unstable to BBr<sub>3</sub> used in the deprotection of the methyl ethers; therefore it was hydrogenated before the deprotection step. Then, deprotection of the Boc group and methyl group using boron tribromide gave the final compound **21**.

## 2.4 Characterization

Each diastereomer of the intermediate alcohol (**35a** and **35b**) was carried through the synthesis separately, producing two molecules, designated the nonpolar (SB<sub>n</sub>) and polar (SB<sub>p</sub>). The absolute stereochemistry of the two softball diastereomers has not been determined unequivocally. However, their properties should differ as a result of their different gross structural shapes as illustrated in Fig. 29.



**Fig. 29** Conformational analysis of two diastereomers. Only one isomer with the right conformation can have dimer or intramolecular hydrogen bond.



### 2.4.1 The polar isomer

1. This isomer was soluble in DMSO-d<sub>6</sub>, DMF-d<sub>6</sub>, and CDCl<sub>3</sub>/MeOD.

This isomer was too polar, it was not soluble in less polar solvents such as chloroform, acetone, benzene or toluene.

2. <sup>1</sup>H NMR spectra in DMSO-d<sub>6</sub> and DMF-d<sub>7</sub> show complete symmetry between the two sides of the molecule. The <sup>1</sup>H NMR spectra in DMF-d<sub>7</sub> and DMSO-d<sub>6</sub> are shown in Fig. 30.

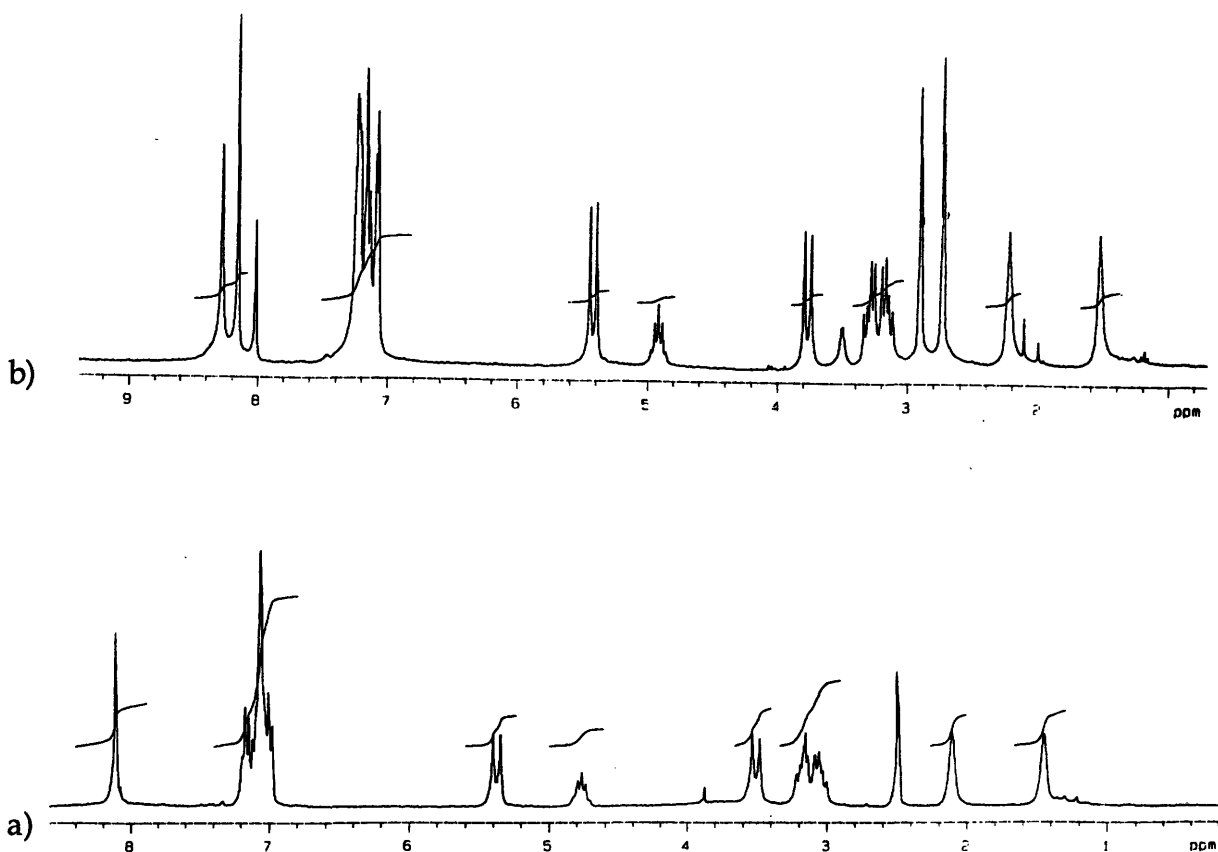


Fig.30 <sup>1</sup>H NMR spectrum of polar isomer in a) DMSO-d<sub>6</sub> and b) DMF-d<sub>7</sub>.

3. Plasma desorption mass spectrometry shows only the monomer is present under the instrumental conditions.

### 2.4.2 Nonpolar Isomer

1. This isomer was soluble in DMSO-d<sub>6</sub>, DMF-d<sub>7</sub>. The <sup>1</sup>H NMR of nonpolar isomer in this solvent is shown in Fig.31.

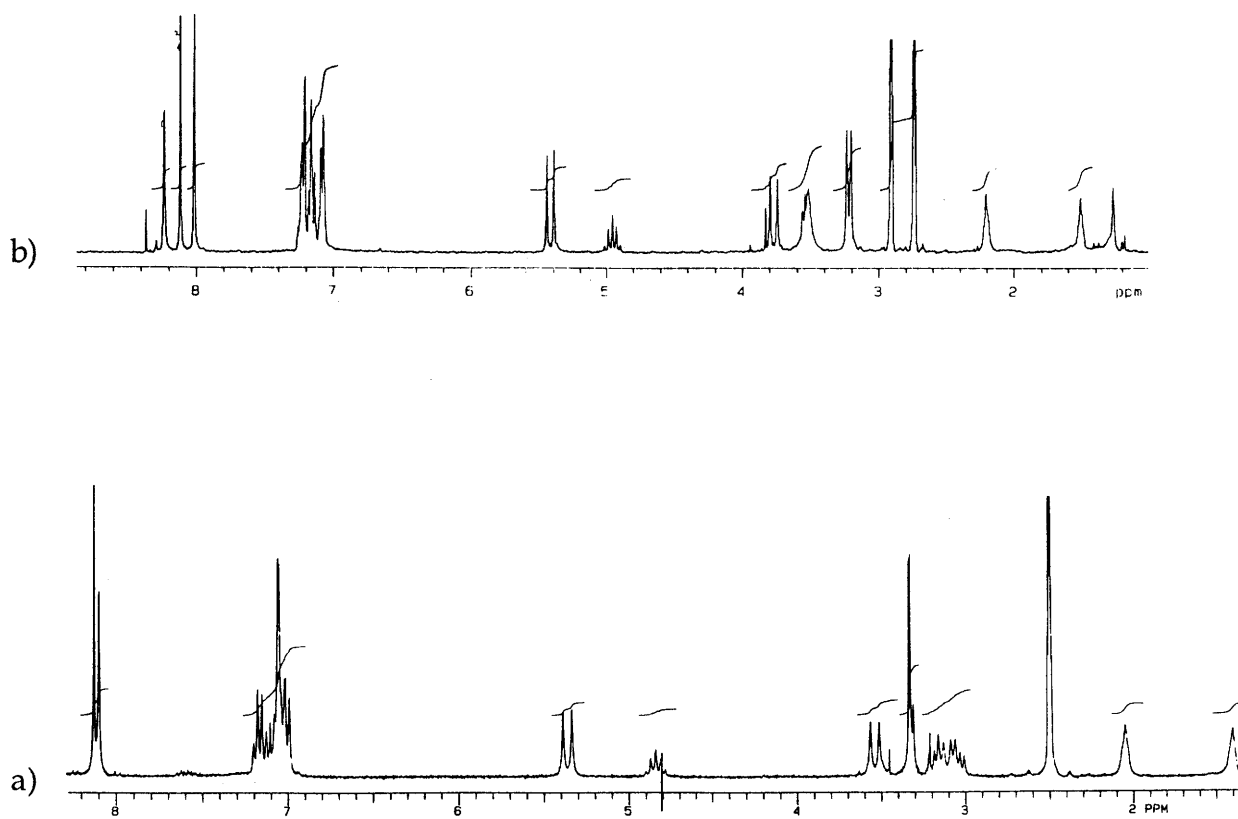
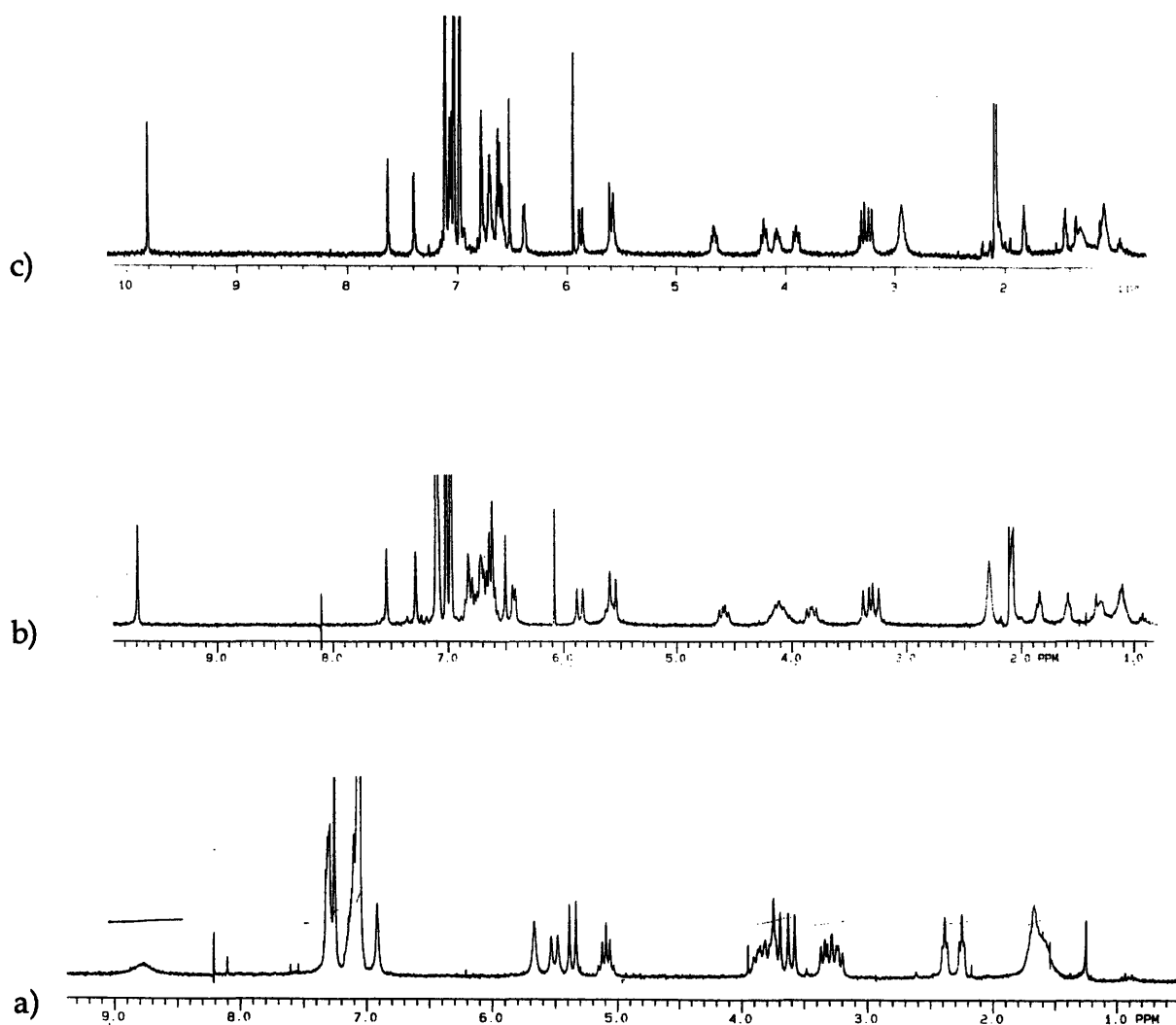


Fig.31 The <sup>1</sup>H NMR spectrum of nonpolar isomer (21) in a) DMSO-d<sub>6</sub> b) DMF-d<sub>7</sub>.

2. In addition, the nonpolar isomer was soluble in  $\text{CDCl}_3$ ,  $\text{CD}_2\text{Cl}_2$ ,  $\text{C}_6\text{D}_6$ , toluene- $d_8$ , THF- $d_8$ , and acetone- $d_6$ . The  $^1\text{H}$  NMR spectra in  $\text{CDCl}_3$ ,  $\text{CH}_2\text{Cl}_2$ ,  $\text{C}_6\text{D}_6$ , toluene- $d_8$ , THF- $d_8$ , acetone- $d_6$ , <50% DMF- $d_6$  /  $\text{CD}_2\text{Cl}_2$ , and <50% DMSO- $d_6$  /  $\text{CDCl}_3$  shows a loss of  $\text{C}_2$  symmetry between the two sides of the molecule (two sets of peak for each hydrogen). Two of the urea N-H bonds appear to be hydrogen bonded, and two do not. The  $^1\text{H}$  NMR of the nonpolar isomer in these solvents are shown in Fig.32. These characteristics are temperature independent between  $-40^\circ\text{C}$  and  $40^\circ\text{C}$ , and concentration independent. The presence of adamantane, tetramethyl adamantane, and Kemp's methyl ester-imide had no effect on the NMR spectra. At >50% DMF- $d_6$  /  $\text{CD}_2\text{Cl}_2$ , and >50% DMSO- $d_6$  /  $\text{CDCl}_3$  there is a retention of  $\text{C}_2$  symmetry between the two sides of the molecule.

3. Plasma desorption mass spectrometry shows only the monomer is present under the instrumental conditions.



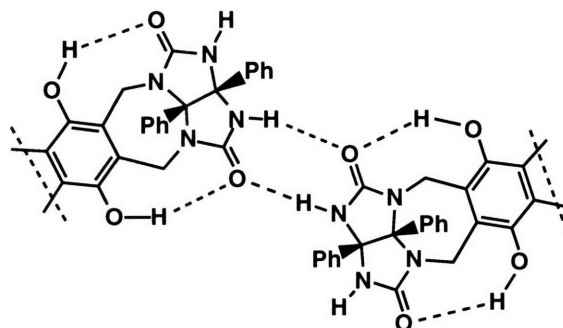
**Fig.32** The  $^1\text{H}$  NMR spectrum of nonpolar isomer (21) in a)  $\text{CDCl}_3$  b) toluene- $\text{d}_8$  at 298K c) toluene- $\text{d}_8$  at 273K.

## 2.5 Conclusion

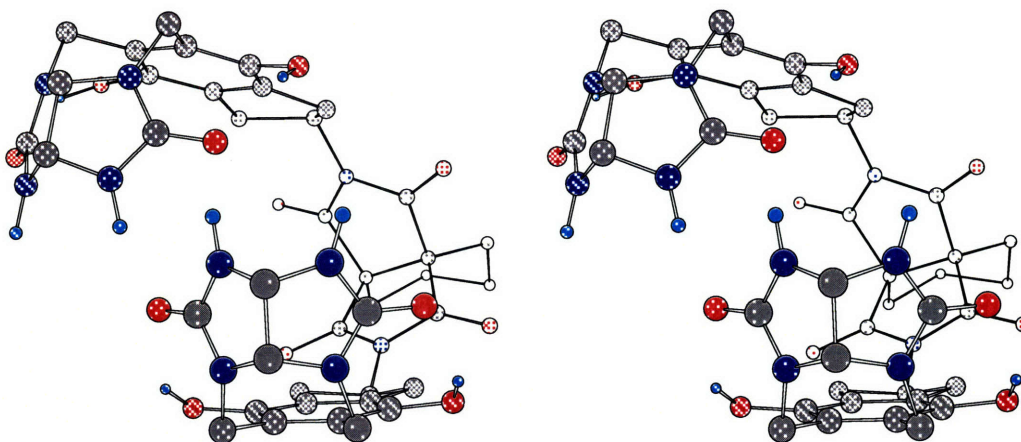
The most important observation from the spectral data is that  $^1\text{H}$  NMR of the nonpolar isomer showed two kinds of peaks for the each

hydrogen and the ratio of two peaks was about 50 : 50. The  $^1\text{H}$  NMR also showed that only 50 % of the N-H bonds are hydrogen bonded. It can be interpreted as 50 % of molecule stays as dimer and 50 % of the molecule stays as monomer. However, the ratio was always same with different solvents and the ratio was temperature independent. If the two kinds of peaks from the  $^1\text{H}$  NMR came from the monomer and dimer and it reflected the ratio of monomer to the dimer, the ratio of the peaks should depend on the solvent and the temperature. Therefore, it seemed more plausible that the downfield signals came from intramolecular hydrogen bonding rather than intermolecular hydrogen bonding. In addition, no guest inclusion was observed and no dimeric mass peak was observed in the plasma desorption mass spectrum. Therefore it was concluded that the nonpolar isomer was the C-shaped isomer as only C-shaped isomer can have intramolecular hydrogen bonds (Fig.29). It was also concluded that C-shaped isomer was collapsing on itself, forming hydrogen bonds within monomer rather than forming a dimer, as shown in Fig. 33.

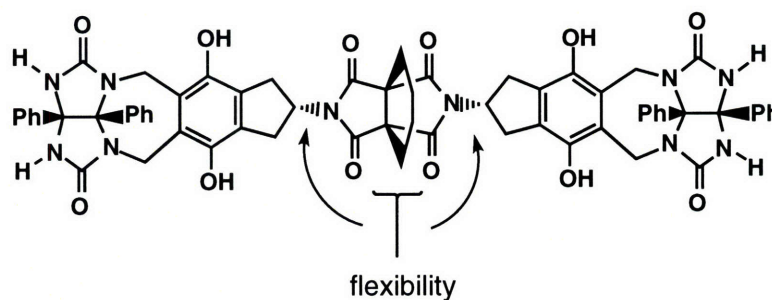
a)



b)



c)



**Fig.33** Intramolecular collapse of the C-shaped isomer ; the stereo view is given in b).

Analysis of the molecular model of the collapsed C-shaped molecule indicates that the central diimide is the structural feature that contains the majority of the molecule's flexibility. This flexibility is apparently too great, allowing the molecule to fold on itself, at least under

the experimental conditions employed. The central diimide is able to twist significantly at the fusion of the three rings, it is apparently too curved to prevent collapse, and the C-N imide single bond allows excessive rotation of the two glycoluril surfaces toward each other.

## 2.6 Experimental

### Diphenyl glycoluril (22)

To a solution of urea( 36.03 g, 0.6 mol ) and benzil ( 63.06 g, 0.3 mol) in benzene ( 1200 ml ) was added trifluoroacetic acid ( 60 ml ) and refluxed with Dean - Stark trap until no water was formed. White solid product was filtered and washed with cold ethanol. Drying with high vacuum gave 83.5g ( 95 % ) of product.  $^1\text{H}$  NMR (300MHz ; DMSO) 7.70 (s, 4H, NH) 7.01 (m, 10H, arom) HRMS (FAB) calculated for  $\text{C}_{16}\text{H}_{14}\text{N}_4\text{O}_2\text{H}^+$ , 295.1195 ; found for 295.1184

### 4,4,5,5-Tetracyanocyclohexene (25)

Butadiene(0.84 g, 15.5 mmol) from gas tank was condensed with cold finger at  $-78^\circ\text{C}$ . Then tetracyanoethylene ( 2 g, 12.6 mmol ) in tetrahydrofuran ( 15 ml ) was added at  $-78^\circ\text{C}$ . Temperature was raised to room temperature and stirred 30 min. Evaporation of THF and washing the residue with ether gave 1.83 g (85 % ) of product.  $^1\text{H}$  NMR (300MHz ;  $\text{CDCl}_3$ ) 5.93 (t, 2H,  $J=1.6$ , -CH=CH-) 3.16 (d, 4H,  $J = 1.6$ ,  $\text{CH}_2$ ) HRMS (EI) calculated for  $\text{C}_{10}\text{H}_6\text{N}_4$  182.0592 ; found for 182.0538



#### **4-Cyclohexene-1,1,2,2-tetracarboxylic diimide (24)**

4,4,5,5-Tetracyanocyclohexene **24** (4.03 g, 22.1 mmol) was refluxed in conc. H<sub>2</sub>SO<sub>4</sub> (25 ml) for 5 h. The reaction mixture was cooled in freezer in 1 hr. White crystal precipitate. The crystals were filtered. Washing the solid product with cold water (10 ml) gave 0.93 g (19 %) of product. <sup>1</sup>H NMR (300MHz ; DMSO) 11.80 (s, 2H, NH) 5.92 (t, 2H, J=2.8, -CH=CH-) 2.59 (d, 4H, J = 2.8, CH<sub>2</sub>) HRMS(FAB) calculated for C<sub>10</sub>H<sub>8</sub>N<sub>2</sub>O<sub>4</sub>Na<sup>+</sup> 243.0382 found for 243.0379

#### **1,4-Dimethoxy-2,3-dimethylbenzene (27)**

To a heated (60°C) solution of 5 g (89.1 mmol) of crushed potassium hydroxide in 100 ml of DMF was added 5g (36.1 mmol) of commercially available 2,3-dimethylhydroquinone **26**. The mixture was stirred for 10 minutes then cooled to 0°C. A solution of 11.78 g(83.0 mmol) of methyl iodide in 50 ml of DMF was added dropwise at 0°C. After 2 hr, the reaction mixture was poured to 1l of water and extracted with 4 X 100 ml of diethyl ether. The ether layer was washed with 2 X 100 ml of water then dried over MgSO<sub>4</sub>. Evaporation of the solvent and recrystallization of the residue in methanol gave 6.0 g (98 %) of product **27**. : mp 74 - 75°C <sup>1</sup>H-NMR (300 MHz ;

CDCl<sub>3</sub>) 6.61 (s, 2H, arom) 3.72 (s, 6H, OCH<sub>3</sub>) 2.11 (s, 6H, CH<sub>3</sub>) HRMS (FAB)

calculated for C<sub>10</sub>H<sub>14</sub>O<sub>2</sub>H<sup>+</sup>, 166.0994 ; found for 166.0990

### **1,4-Dimethoxy-2,3-dibromomethylbenzene (28)**

A solution of 15g (90.3 mmol) of compound **27** and 32.1g (180.3 mmol) of N-bromosuccinimide in 500 ml of CCl<sub>4</sub> was irradiated with sun lamp for an hour. Filtration of succinimide and evaporation of CCl<sub>4</sub> gave 29.3g (91 %) of product **28**. <sup>1</sup>H-NMR (300 MHz ; CDCl<sub>3</sub>) 6.79 (s, 2H, arom) 4.70(s, 4H, CH<sub>2</sub>Br) 3.82(s, 6H, OMe) HRMS(EI) calculated for C<sub>10</sub>H<sub>12</sub>Br<sub>2</sub>O<sub>2</sub>, 321.9203 ; found for 321. 9274

### **1,4-Dimethoxy-2,3-dicyanomethylbenzene (29)**

To a solution of 8.13g (25.1 mmol) of compound **28** in 160 ml DMF was added 2.70g (55.1 mmol) sodium cyanide and stirred for an hour. DMF was evaporated at reduced pressure and residue was washed with 500 ml of CHCl<sub>3</sub>. Evaporation of CHCl<sub>3</sub> gave 5.41g (99 %) of product **29**. <sup>1</sup>H-NMR (300 MHz ; CDCl<sub>3</sub>) 6.83 (s, 2H, arom) 3.79(s, 6H, OMe) 3.77 (s, 4H, CH<sub>2</sub>CN) HRMS(EI) calculated for C<sub>12</sub>H<sub>12</sub>N<sub>2</sub>O<sub>2</sub>, 216. 0899 ; found for 216.0874

### **2-Amino-1-cyano-1,2-ene-4,7-dimethoxyindan (30)**

To a solution of 8.7g (40.2 mmol) of compound **29** in 80 ml of ethanol was added 0.3 ml of NaOEt/EtOH (50 mg of Na in 1 ml of EtOH) and refluxed for 6 hrs. Acetic acid (1 ml) was added to the reaction mixture and stirred for 10 min. Evaporation of ethanol gave the 8.05g (97 %) of product **30**. <sup>1</sup>H-NMR (300 MHz ; CDCl<sub>3</sub>) 6.68 (d, 1H, J = 8.8, arom) 6.46(d, 1H, J = 8.8, arom) 5.03 (br, 2H, NH<sub>2</sub>) 3.79 (s, 3H, OMe) 3.74 (s, 3H, OMe) 3.44 (s, 2H, CH<sub>2</sub>) HRMS(EI) calculated for C<sub>12</sub>H<sub>12</sub>N<sub>2</sub>O<sub>2</sub> , 216. 0899 ; does not give right mass spectrum.

### **4,7-Dimethoxy-2-indanone (31)**

To a solution of 8.05g (37.2 mmol) of compound **30** in 260 ml of acetic acid was added 16 ml of H<sub>2</sub>O and 105 ml of H<sub>3</sub>PO<sub>4</sub>. The reaction mixture was refluxed for 24 hrs. Acetic acid was evaporated at reduced pressure and reaction mixture was poured into 300 ml of water. The resulting mixture was extracted with 100 ml of CHCl<sub>3</sub> 5 times and CHCl<sub>3</sub> layer was washed with 50 ml of sat. NaHCO<sub>3</sub> aqueous solution 3 times and 100 ml of cold water 2 times. Drying organic layer over MgSO<sub>4</sub> and evaporation gave 5.75g (80 %) of

product **31**.  $^1\text{H-NMR}$  (300 MHz ;  $\text{CDCl}_3$ ) 6.70(s, 2H, arom) 3.78 (s, 6H, OMe) 3.45 (s, 4H,  $\text{CH}_2 \times 2$ ) HRMS(EI) calculated for  $\text{C}_{11}\text{H}_{12}\text{O}_3$ , 192.0786 ; found for 192.0723

#### **4,7-Dimethoxy-2-indanol (32)**

To a solution of 2.29g (11.9 mmol) of compound **31** in a mixture of 80 ml of ethanol and 50 ml of  $\text{CH}_2\text{Cl}_2$  was added 0.56g (14.8 mmol) of  $\text{NaBH}_4$  in 100 ml of ethanol dropwise and stirred for an hour. Reaction mixture was poured into 400 ml of 1N  $\text{H}_3\text{PO}_4$  aqueous solution and extracted with 100ml chloroform 3 times. Drying with  $\text{MgSO}_4$  and evaporation gave the 1.84g (85 %) of product **32**.  $^1\text{H-NMR}$  (300 MHz ;  $\text{CDCl}_3$ ) 6.62 (s, 2H, arom) 4.67 (br, 1H, CHOH) 3.75 (s, 6H, OMe) 3.15 (dd, 2H,  $J = 6.2, 6.7$ ,  $\text{CH}_2$  in five membered ring) 2.90 (dd, 2H,  $J = 6.2, 6.7$   $\text{CH}_2$  in five membered ring)

#### **2-Benzyloxy-4,7-dimethoxyindane (33)**

To a solution of 15.14g (78.0 mmol) of compound **32** was added 4.5g (11.2 mmol, 1.4 eq, 60 % dispersion in mineral oil, washed with hexane) of  $\text{NaH}$  and stirred for 30 min. Then, 16g ( 93.5 mmol, 1.2 eq) of benzyl bromide was added dropwise at  $0^\circ\text{C}$ . Temperature of reaction mixture was raised to

room temperature and stirred for 24 hrs. Reaction mixture was poured into 500 ml of water and extracted with 200 ml  $\text{CHCl}_3$  3 times. Evaporation of  $\text{CHCl}_3$  and column chromatography on the silica gel gave 19.7 (89 %) of product.  $^1\text{H-NMR}$  (300 MHz ;  $\text{CDCl}_3$ ) 7.27 (m, 5H, arom) 6.59 (s, 2H, arom) 4.41(m, 1H, CHO-) 4.53 (d, 2H, J = 4.8,  $\text{CH}_2\text{Ph}$ ) 3.74(s, 6H, OMe) 3.15(dd, 2H, J = 15.9, 6.3,  $\text{CH}_2$  in five membered ring) 3.10 (dd, 2H, J = 15.9, 6.3,  $\text{CH}_2$  in five membered ring) HRMS(EI) calculated for  $\text{C}_{18}\text{H}_{20}\text{O}_3$ , 284.1412 ; found for 284.1490

#### **2-Benzyloxy-5,6-dichloromethyl-4,7-dimethoxyindane (34)**

To a solution of 1.09g (3.83 mmol) of compound **33** in 8 ml of chloromethyl methyl ether was added 8 ml of 60 %  $\text{H}_2\text{SO}_4$  at  $40^\circ\text{C}$  and stirred for 24 hrs. Reaction mixture was poured into 200 ml of water and extracted with 100 ml of  $\text{CHCl}_3$  3 times. Drying with  $\text{MgSO}_4$  and evaporation gave 1.27g (88 %) of product.  $^1\text{H-NMR}$  (300 MHz ;  $\text{CDCl}_3$ ) 7.33 (m, 5H, arom) 4.82(s, 4H,  $\text{CH}_2\text{Cl}$ ) 4.58 (s, 2H,  $\text{CH}_2\text{Ph}$ ) 4.45 (m, 1H, CHO) 3.86 (s, 6H, OMe) 3.25 (dd, 2H, J = 16.4, 6.5,  $\text{CH}_2$  in five membered ring) 3.09 (dd, 2H, J = 16.4, 6.5,  $\text{CH}_2$  in five membered ring) HRMS(EI) calculated for  $\text{C}_{20}\text{H}_{22}\text{Cl}_2\text{O}_3$ , 380.0946 found for 380.0996

**1,6-(2-Benzoyloxy-5,6-dichloromethyl-4,7-dimethoxyindane)-tetrahydro-3a,6a-diphenylimidazo[4,5d]imidazole-2,5-(1H,3H)-dione (35)**

To a solution of 9.83 g (33.4 mmol) of diphenyl glycoluril in 300 ml of DMSO was added 5.62 g (100.2 mmol) of KOH at 100°C and stirred for 20 min. 1.27g(3.34 mmol) of compound 34 in 50 ml of DMSO was added dropwise and stirred for an hour. Reaction mixture was poured into 500ml of water and precipitated white solid was filtered. Solid was boiled with 200 ml of CH<sub>2</sub>Cl<sub>2</sub> and filtered. This boiling and filtering was repeated 3 times. Evaporation of CH<sub>2</sub>Cl<sub>2</sub> and chromatography on silica gel gave 0.66g (65 %) of mixture of two isomers. HRMS(EI) calculated for C<sub>36</sub>H<sub>34</sub>N<sub>4</sub>O<sub>5</sub>, 602.2529 ; found for 602.2518

**1,6-(2-Benzoyloxy-5,6-dichloromethyl-4,7-dimethoxyindane)-3-(propionyl)-tetrahydro-3a,6a-diphenylimidazo[4,5d]imidazole-2,5-(1H,3H)-dione (36)**

To a solution of 0.8 g (1.33 mmol) of mixture of two isomer 35a and 35b in 15 ml of pyridine was added 0.85 ml (6.64 mmol) of propionic anhydride and refluxed 7 hrs. Evaporation of pyridine and column chromatography on the silica gel gave 165 mg of nonpolar isomer, 183 mg of polar isomer, and 278 mg of mixture of two isomer(72 % of total yield) **nonpolar isomer** . <sup>1</sup>H-NMR (300 MHz ; CDCl<sub>3</sub>) 7.14 (m, 15H, arom) 6.13(s, 1H, NH) 5.62 (d, 1H, J = 15.6,

CH<sub>2</sub>N) 5.53 (d, 1H, J = 15.9, CH<sub>2</sub>N) 4.61 (s, 2H, CH<sub>2</sub>Ph) 4.41(m, 1H, CHO-) 3.95(s, 3H, OMe) 3.93 (s, 3H, OMe) 3.85 (d, 1H, J = 15.6, CH<sub>2</sub>N) 3.72 (d, 1H, J = 15.9, CH<sub>2</sub>N) 3.25 (m, 2H, CH<sub>2</sub> in five membered ring ) 3.04 (m, 4H, CH<sub>2</sub> in five membered ring + CH<sub>2</sub>C=O) 1.04(t, 3H, J = 7.2) **polar isomer** <sup>1</sup>H-NMR (300 MHz ; CDCl<sub>3</sub>) 7.10(m, 15H, arom) 6.07(s, 1H, NH) 5.57(d, 1H, J = 16.5, CH<sub>2</sub>N) 5.47 (d, 1H, J = 15.9) 4.50 ( s, 2H, CH<sub>2</sub>Ph) 4.40(d, 1H, J = 16.5, CH<sub>2</sub>N) 3.68 (d, 1H, J = 15.9, CH<sub>2</sub>N) 3.10 (m, 6H, CH<sub>2</sub> in five membered ring + CH<sub>2</sub>C=O) 0.98 (t, 3H, J = 7.2) HRMS(FAB) calculated for C<sub>39</sub>H<sub>38</sub>N<sub>4</sub>O<sub>6</sub>H<sup>+</sup>, 659.2870 found for 659.2884

**1,6-(2-Benzyloxy-5,6-dichloromethyl-4,7-dimethoxyindane)-tetrahydro-3a,6a-diphenylimidazo[4,5d]imidazole-2,5-(1H,3H)-dione (35)**

To a solution of 160 mg (0.24 mmol) of compound 36 in 20 ml of THF was added 20 drops of saturated aqueous LiOH and stirred for 20 hrs. 10 drops of saturated aqueous NH<sub>4</sub>Cl was added. Drying over MgSO<sub>4</sub>, filtration and evaporation gave 133mg (98 %) of product. **nonpolar isomer** <sup>1</sup>H-NMR (300 MHz ; CDCl<sub>3</sub>) 7.33 (m, 15H, arom) 5.72 (s, 2H, NH) 5.50 (d, 2H, J = 15.9, CH<sub>2</sub>N) 4.60 (s, 2H, CH<sub>2</sub>Ph) 4.38 (m, 1H, CHO) 3.88 (s, 6H, OMe) 3.67 (d, 2H, J = 15.9, CH<sub>2</sub>N) 3.24 (dd, J = 15.5, 7.2, 2H, CH<sub>2</sub> in five membered ring) 2.99 (dd, J = 15.5, 7.2, 2H, CH<sub>2</sub> in five membered ring) **polar isomer** <sup>1</sup>H-NMR (300 MHz ; CDCl<sub>3</sub>) 7.16 (m, 15H, arom) 5.63(s, 2H, NH) 5.57(d, 2H, J = 15.9, CH<sub>2</sub>N) 4.54 (s, 2H,

CH<sub>2</sub>Ph) 4.45 (m, 1H, CHO) 3.87 (s, 6H, OMe) 3.71 (d, 2H, J = 15.9, CH<sub>2</sub>N) 3.19 (dd, 2H, J = 16.5, 5.8, CH<sub>2</sub> in five membered ring ) 3.07 (dd, 2H, J = 16.5, 5.8, CH<sub>2</sub> in five membered ring )

**1,6-(2-Benzyloxy-5,6-dichloromethyl-4,7-dimethoxyindane)-3,4-(di-tert-butoxycarbonyl)-tetrahydro-3a,6a-diphenylimidazo[4,5d]imidazole-2,5-(1H,3H)-dione (37)**

To a solution of 78 mg (0.13mmol) of compound **36** in a mixture of 3 ml of CH<sub>3</sub>CN and 2 ml of THF was added catalytic amount of DMAP and 56.55 mg(0.26mmol) of di-tert-butyl dicarbonate and stirred for 24 hrs. Evaporation of solvent and column chromatography on the silicagel gave 81,5 mg (96 %) of product. **nonpolar isomer** <sup>1</sup>H-NMR (300 MHz ; CDCl<sub>3</sub>) 7.08 (m, 15H, arom) 5.54(d, 2H, J = 16.3 CH<sub>2</sub>N) 4.56 (s, 2H, CH<sub>2</sub>Ph) 4.34 (m, 1H, CHO) 3.91 (s, 6H, OMe) 3.65(d, 2H, J = 16.3, CH<sub>2</sub>N) 3.20 (dd, 2H, J = 15.5, 7.0, CH<sub>2</sub> in five membered ring ) 2.96 (dd, 2H, J = 15.5, 7.0, CH<sub>2</sub> in five membered ring) 1.33 (s, 18H, C(CH<sub>3</sub>)<sub>3</sub>) **polar isomer** <sup>1</sup>H-NMR (300 MHz ; CDCl<sub>3</sub>) 7.12 (m, 15H, arom) 5.58 (d, 2H, J = 15.7, CH<sub>2</sub>N) 4.56(s, 2H, CH<sub>2</sub>Ph) 4.45(m, 1H, CHO) 3.92(s, 6H, OMe) 3.73(d, 2H, J = 15.7, CH<sub>2</sub>N) 3.18 (dd, 2H, J = 16.4, 5.5, CH<sub>2</sub> in five membered ring) 3.08 (dd, 2H, J = 16.4, 5.5, CH<sub>2</sub> in five membered ring) 1.38 (s,



18H, C(CH<sub>3</sub>)<sub>3</sub>) HRMS(EI) calculated for C<sub>36</sub>H<sub>34</sub>N<sub>4</sub>O<sub>5</sub>, 602.2529 ; found for 602.

2581

**1,6-(4,7-dimethoxy-2-indanol)-3,4-(di-tert-butoxycarbonyl)-tetrahydro-3a,6a-diphenylimidazo[4,5d]imidazole-2,5-(1H,3H)-dione (38)**

To a solution of 0.370 g (0.461 mmol) of the compound 37 in 4 mL THF, 0.5 mL MeOH was added ~50 mg 10% Pd/C, and the mixture stirred under a hydrogen balloon for 14 h. Filtration and evaporation of the solvent gave 0.32 g (98%) of the product as a colorless solid. **nonpolar isomer** <sup>1</sup>H NMR (CDCl<sub>3</sub>): 7.08 (m, 10H, arom), 5.58 (d, 2H, J=15.8, CH<sub>2</sub>N), 4.67 (m, 1H, CHOH), 3.94 (s, 6H, OMe), 3.73 (d, 2H, J= 15.8, CH<sub>2</sub>N), 3.20 (dd, 2H, J=6.4, 16.1, CH<sub>2</sub> in five membered ring), 2.85(dd, 2H, J = 6.4, 16.1, CH<sub>2</sub> in five membered ring) 1.96 (br, s, 1H, CHOH), 1.37 (s, 18H, C(CH<sub>3</sub>)<sub>3</sub>). **polar isomer** <sup>1</sup>H NMR (CDCl<sub>3</sub>): 7.15 (m, 10H, arom) 5.53 (d, 2H, J = 15.8, CH<sub>2</sub>N) 4.68 (br, 1H, CHOH) 3.89 (s, 6H, OMe) 3.69(d, 2H, J = 15.8, CH<sub>2</sub>N) 3.18 (dd, 2H, J = 16.8, 5.4, CH<sub>2</sub> in five membered ring) 2.90 (dd, 2H, J = 16.8, 5.4, CH<sub>2</sub> in five membered ring) 2.05 (s, 1H, OH) 1.38 (s, 18H, C(CH<sub>3</sub>)<sub>3</sub>) HRMS(FAB) calculated for C<sub>39</sub>H<sub>44</sub>N<sub>4</sub>O<sub>9</sub>Cs<sup>+</sup>, 845.2163 ; found for 845.2188

### Compound 39

To a solution of 0.060 g (0.0842 mmol) of the compound **38**, 0.009 g (0.0421 mmol) diimide, and 0.031 g (0.126 mmol) PPh<sub>3</sub> in 1 mL THF was added 0.0198 ml (0.126 mmol) diethylazodicarboxylate. After stirring for 12 h, the solvent was evaporated and the residue chromatographed on silica gel (50-70% ethyl acetate/hexanes) to give 0.034 g (20 %) of the product as a colorless foam. **nonpolar isomer** <sup>1</sup>H NMR (CDCl<sub>3</sub>): 7.04 (m, 20H, arom), 5.97 (m, t, 2H, J=2.2, -CH=CH-), 5.55 (d, 4H, J=15.8, CH<sub>2</sub>N), 5.01 (m, 2H, CHN), 3.88 (s, 12H, OMe), 3.78 (d, 4H, J=15.8, CH<sub>2</sub>N), 3.27 (d, 8H, J=8.2, CH<sub>2</sub> in five membered ring), 2.72 (d, 4H, J=2.4), 1.36 (s, 36H, C(CH<sub>3</sub>)<sub>3</sub>). **polar isomer** <sup>1</sup>H NMR (CDCl<sub>3</sub>): 6.98 (m, 20H, arom) 6.08 (t, 2H, J = 2.7, CH=CH) 5.58 (d, 4H, J = 15.8, CH<sub>2</sub>N) 4.89 (m, 2H, CHN) 3.94 (s, 12H, OMe) 3.73 (d, 4H, J = 15.8, CH<sub>2</sub>N) 3.53(dd, 4H, J = 14.5, 10.3, CH<sub>2</sub> in five membered ring) 3.10 (dd, 4H, J = 14.5, 10.3, CH<sub>2</sub> in five membered ring) 2.85(d, 4H, J = 2.7, =CH-CH<sub>2</sub>) 1.39 (s, 36H, C(CH<sub>3</sub>)<sub>3</sub>) HRMS(FAB) calculated for C<sub>88</sub>H<sub>92</sub>N<sub>10</sub>O<sub>20</sub>Cs<sup>+</sup>, 1741.5544 found for 1741. 5635

## Compound 40

To a solution of 0.040 g (0.0248 mmol) of the compound 39 in 2 ml ethyl acetate was added ~20 mg 5% Pd/C, and the mixture stirred under a hydrogen balloon for 14 h. Filtration and evaporation of the solvent gave 0.040 g (78 %) of the product as a colorless foam. **nonpolar isomer**  $^1\text{H NMR}$  ( $\text{CDCl}_3$ ): 7.05 (m, 20H, arom), 5.55 (d, 4H,  $J=15.8$ ,  $\text{CH}_2\text{N}$ ), 5.03 (m, 2H, CHN), 3.88 (s, 12H, OMe), 3.78 (d, 4H,  $J=15.8$ ,  $\text{CH}_2\text{N}$ ), 3.27 (d, 8H,  $J=8.1$ ,  $\text{CH}_2$  in five membered ring), 2.13 (m, 4H, six membered ring in the center), 1.50 (m, 4H, six membered ring in the center). 1.39 (s, 36H,  $\text{C}(\text{CH}_3)_3$ ) **polar isomer**  $^1\text{H NMR}$  ( $\text{CDCl}_3$ ): 6.98 (m, 20H, arom) 5.58 (d, 4H,  $J = 15.8$ ,  $\text{CH}_2\text{N}$ ) 4.89 (m, 2H, CHN) 3.94 (s, 12H, OMe) 3.73 (d, 4H,  $J = 15.8$ ,  $\text{CH}_2\text{N}$ ) 3.53(dd, 4H,  $J = 14.5$ , 10.3,  $\text{CH}_2$  in five membered ring) 3.10 (dd, 4H,  $J = 14.5$ , 10.3,  $\text{CH}_2$  in five membered ring) 2.09 (s, 4H, six membered ring in the center) 1.43 (s, 4H, six membered ring in the center) 1.39 (s, 36H,  $\text{C}(\text{CH}_3)_3$ ) HRMS(FAB) calculated for  $\text{C}_{88}\text{H}_{94}\text{N}_{10}\text{O}_{20}\text{CS}^+$ , 1743.5538 ; found for 1743. 5592

## Compound 21

To a solution of 0.042 g (0.026 mmol) of the compound **40** in 3 mL CH<sub>2</sub>Cl<sub>2</sub> at -78°C was added 0.10 ml BBr<sub>3</sub>. After warming to RT and stirring for 14 h, 2 mL of MeOH was added and the solvents evaporated. Following three additional MeOH additions and evaporations, the residue was subjected to high vac with mild heating (~50°C) to give 0.030 g (85 %) of the product as a colorless solid.

**nonpolar isomer** <sup>1</sup>H NMR (DMF-d<sub>6</sub>) : 8.24 (s, 4H, OH), 8.12 (s, 4H, NH), 7.16 (m, 20H, arom), 5.42 (d, 4H, J=15.6, CH<sub>2</sub>N), 4.95 (m, 2H, CHN), 3.87 (d, 4H, J=15.6, CH<sub>2</sub>N), 3.22 (d, 8H, J=8.5, CH<sub>2</sub> in five membered ring), 2.21 (s, 4H, six membered ring in the center), 1.53 (s, 4H, six membered ring in the center).

**polar isomer** <sup>1</sup>H NMR (DMSO-d<sub>6</sub>) 8.11 (s, 8H, NH + OH) 7.05 (m, 20H, arom) 5.37(d, 4H, J = 15.5 , CH<sub>2</sub>N) 4.78 (m, 2H, CHN) 3.48(d, 4H, J = 15.5 , CH<sub>2</sub>N) 3.09 (m, 8H, CH<sub>2</sub> in five membered ring) 2.09 (s, 4H, six membered ring in the center) 1.43 (s, 4H, six membered ring in the center) plasma desorption mass spectroscopy calculated for 1154 ; found for 1154 HRMS(FAB) calculated for C<sub>64</sub>H<sub>54</sub> N<sub>10</sub>O<sub>12</sub>Cs<sup>+</sup>, 1287.2979 ; found for 1287. 2963

## 2.7 References

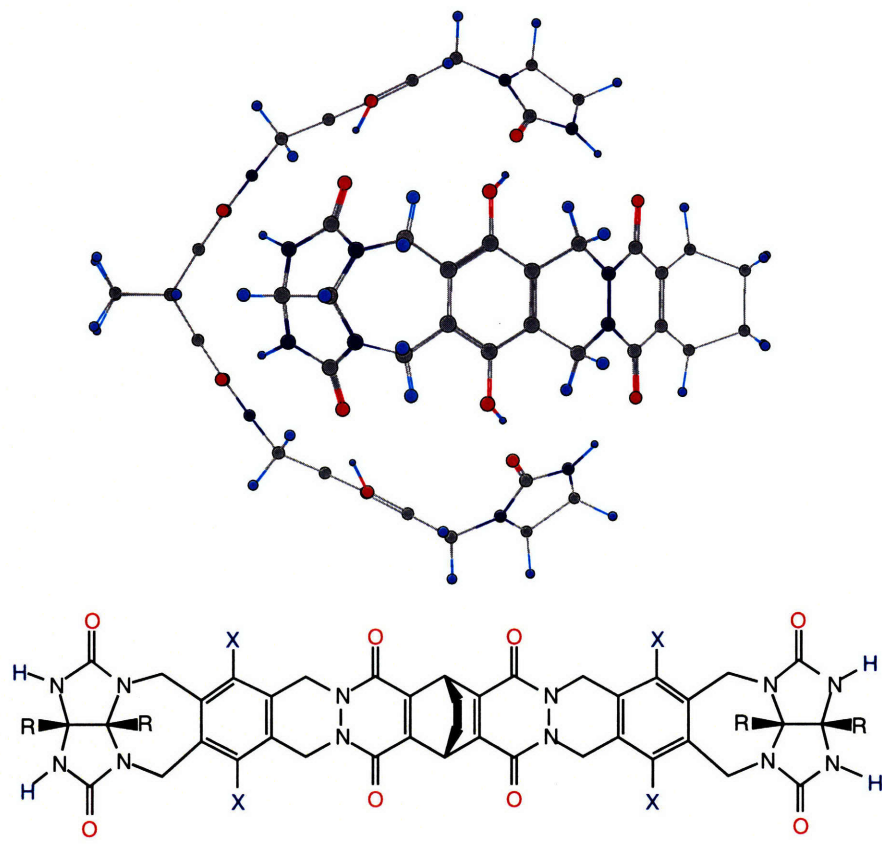
- 1)Cram, D. J.; Choi, H.-Y.; Bryant, J. A.; Knobler, C. B. *J. Am. Chem. Soc.* **1992**, *114*, 7748.
- 2)Cram, D. J.; Blanda, M. T.; Paek, K.; Knobler, C. B. *J. Am. Chem. Soc.* **1992**, *114*, 7765.
- 3)Canceill, J. *Angew. Chem. Int. Ed. Engl.* **1989**, *28*, 1246.
- 4)Collet, A. *Tetrahedron* **1987**, *43*, 5725.
- 5)Butler, A. R.; Leitch, E. J. *Chem. Soc. Perkin Trans. II* **1980**, 103.
- 6)Middleton, W. J.; Heckert, R. E.; Little, E. L.; Krespan, C. G. *J. Am. Chem. Soc.* **1958**, *80*, 2783.
- 7)Suzuki, H. *Bull. Chem. Soc. Japan* **1979**, *43*, 3299.
- 8)Wada, M.; Sano, T.; Mitsunobu, O. *Bull. Chem. Soc. Jpn* **1973**, *46*, 2833.
- 9)Mitsunobu, O.; Wada, M.; Sano, T. *J. Am. Chem. Soc.* **1972**, *94*, 679.

## Chapter 3. The Second Generation Self-Assembling Dimeric Molecule - The Rigid System

### 3.1 Design

As the molecule **21** collapsed rather than forming a dimer, and the cause appeared to be its flexibility, a more rigid system was designed. This system was designed by Dr. Robert S. Meissner. The more rigid bicyclooctane hydrazide was incorporated as the bridged center of the molecule and 13 fused rings gave it an extended, rigid structure (Fig. 34). The stereoisomer shown in Fig. 34 presents the R groups on the same face of the molecule as the central ethylene bridge. This feature permits the structure to assume low-energy conformations of an overall C-shape, with all R groups positioned on its convex surface. Molecular modeling indicates that these molecules are highly preorganized for dimerization. The only significant source of flexibility are the methylenes to which the hydrazide nitrogens are attached; these rings are capable of only small distortions, allowing the glycoluril ends to "breathe" to a small degree. The hydrogen bond distances and angles in the dimers, as listed in Table. 3, are nearly optimal. The molecule **41a** is the first version of this rigid system. It can have 8 hydrogen bonds when it forms a dimer. In the molecule **41b**, the R group in the glycoluril was changed from phenyl group to isoamyl ester group, a change expected to improve the solubility of the molecule as the phenyl derivative was very insoluble. The molecule **42** was designed to give more hydrogen bonds to the dimeric

molecule and at its optimum conformation, the dimeric molecule can have 16 hydrogen bonds.



- 41a** R = phenyl, X = H
- 41b** R = isoamyl ester, X = H
- 42** R= 4-n-heptylphenyl, X = OH

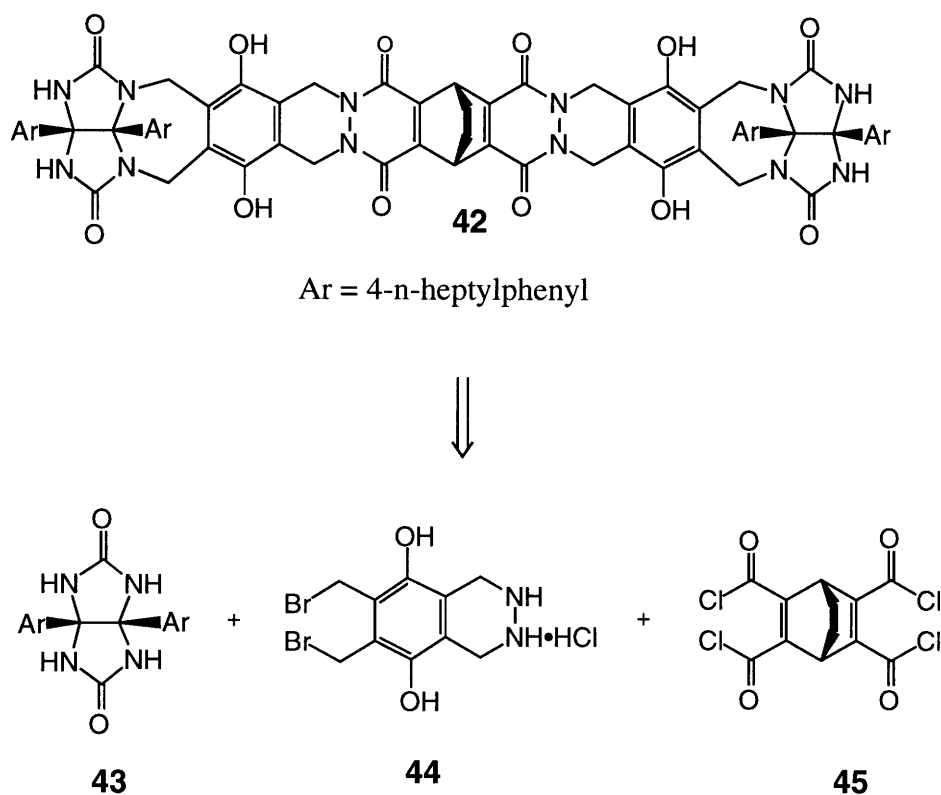
**Fig.34** New self-assembling dimeric system.

$\text{N}-\text{H} \cdots \cdots \text{O}$ <hr style="width: 100%;"/>	$\text{O}-\text{H} \cdots \cdots \text{O}$ <hr style="width: 100%;"/>
length 2.75 ~ 2.76 Å	length 2.69 ~ 2.70 Å
angle 174°	angle 163°

**Table. 3** Hydrogen bond length and angles in the self-assembling dimeric molecule **42** from Amber calculation.

Unfortunately, the isoamyl ester was incompatible with final demethylation step. Therefore, the 4-heptylphenyl group was introduced to meet the requirements of solubility and compatibility during the synthesis. The systems **41a** and **41b** were mainly studied by the Dr. Robert S. Meissner and 16 hydrogen bond system **42** was mainly studied by the author. Therefore this thesis will focus the study of the molecule **42**.

### 3.2 Retrosynthesis of molecule 42



**Fig. 35** Retrosynthetic analysis of the molecule **42**.



The retrosynthetic analysis of this molecule is presented in the Fig.35. It should be possible to prepare the target molecule starting from three readily accessible precursors. These are

**43:** di-(4-n-heptylphenyl)glycoluril

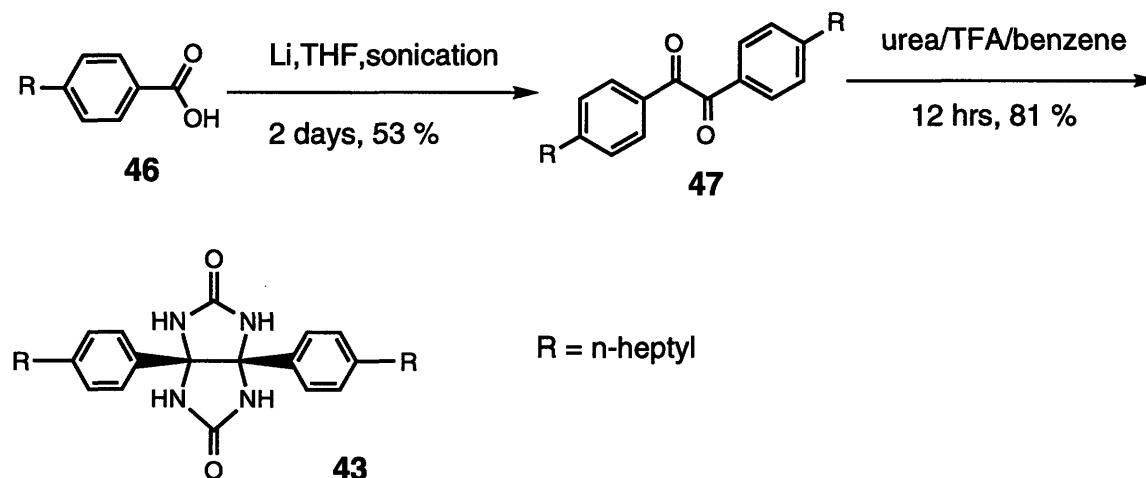
**44:** unsymmetrically functionalized hydroquinone.

**45:** the central bicyclooctatetraacylchloride

### 3.3 Synthesis

#### 3.3.1 The synthesis of di-(4-n-heptylphenyl)glycoluril

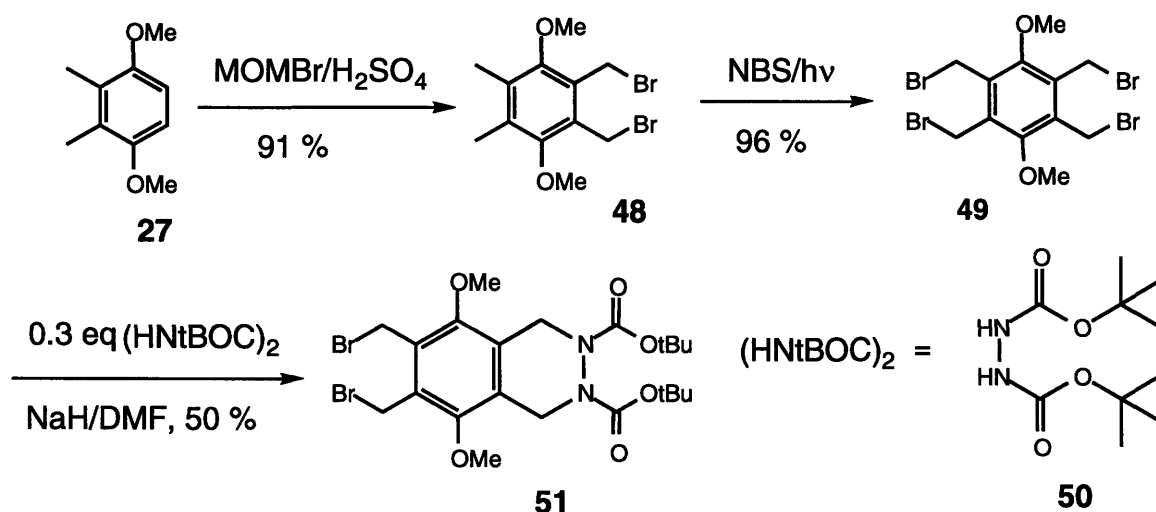
The synthesis began with the reaction of 4-n-heptylbenzoic acid **46** with lithium metal in dried THF to give 4-n-heptylbenzil **47**<sup>1</sup>, which was condensed with urea to give di-(4-n-heptylphenyl)glycoluril **43** (Fig.36) in good yield.



**Fig. 36** The synthesis of di-(4-n-heptylphenyl)glycoluril.

### 3.3.2 The synthesis of 1,4-dimethoxy-5,6-di-bromomethyl -2,3-(di-tert-butyl-1,2,3,4-tetrahydrophthalazine-2,3-dicarboxylate)

The synthesis started with a double bromomethylation of the protected hydroquinone with bromomethyl methyl ether in 60 %  $\text{H}_2\text{SO}_4$  to give compound **48**. This compound was irradiated with NBS in  $\text{CCl}_4$  to give tetrabromide **49**. This tetrabromide was coupled with 0.3 equivalents of hydrazide **50** using NaH in DMF to give compound **51** (Fig. 37). The hydrazide **50** was made from the Mitsunobu reaction between di-tert-butyl azodicarboxylate and methanol.



**Fig. 37** The synthesis of the 1,4-dimethoxy-5,6-di-bromomethyl -2,3-(di-tert-butyl-1,2,3,4-tetrahydrophthalazine-2,3-dicarboxylate).

### 3.3.3 The synthesis of Bicyclo[2,2,2]-octa-2,5-diene-2,3,5,6-tetracarbonyl chloride 59

The synthesis began with esterification of acetylenedicarboxylic acid with p-methoxybenzyl alcohol in benzene to give compound 53. Diels -Alder reaction of compound 53 and furan in a sealed tube at 80°C gave compound

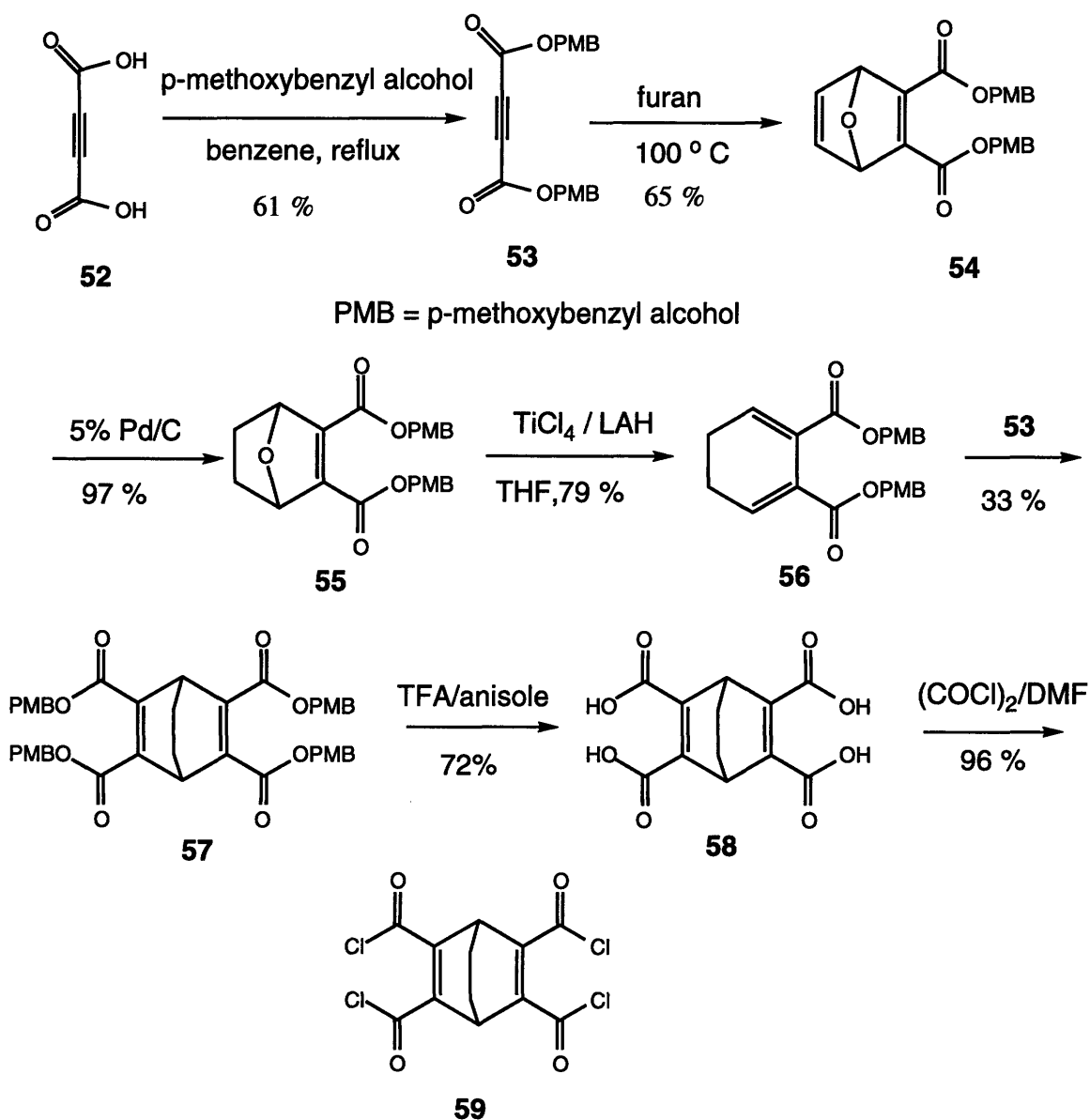


Fig. 38 The synthesis of bicyclo[2,2,2]-octa-2,5-diene-2,3,5,6-tetracarbonyl chloride 59.

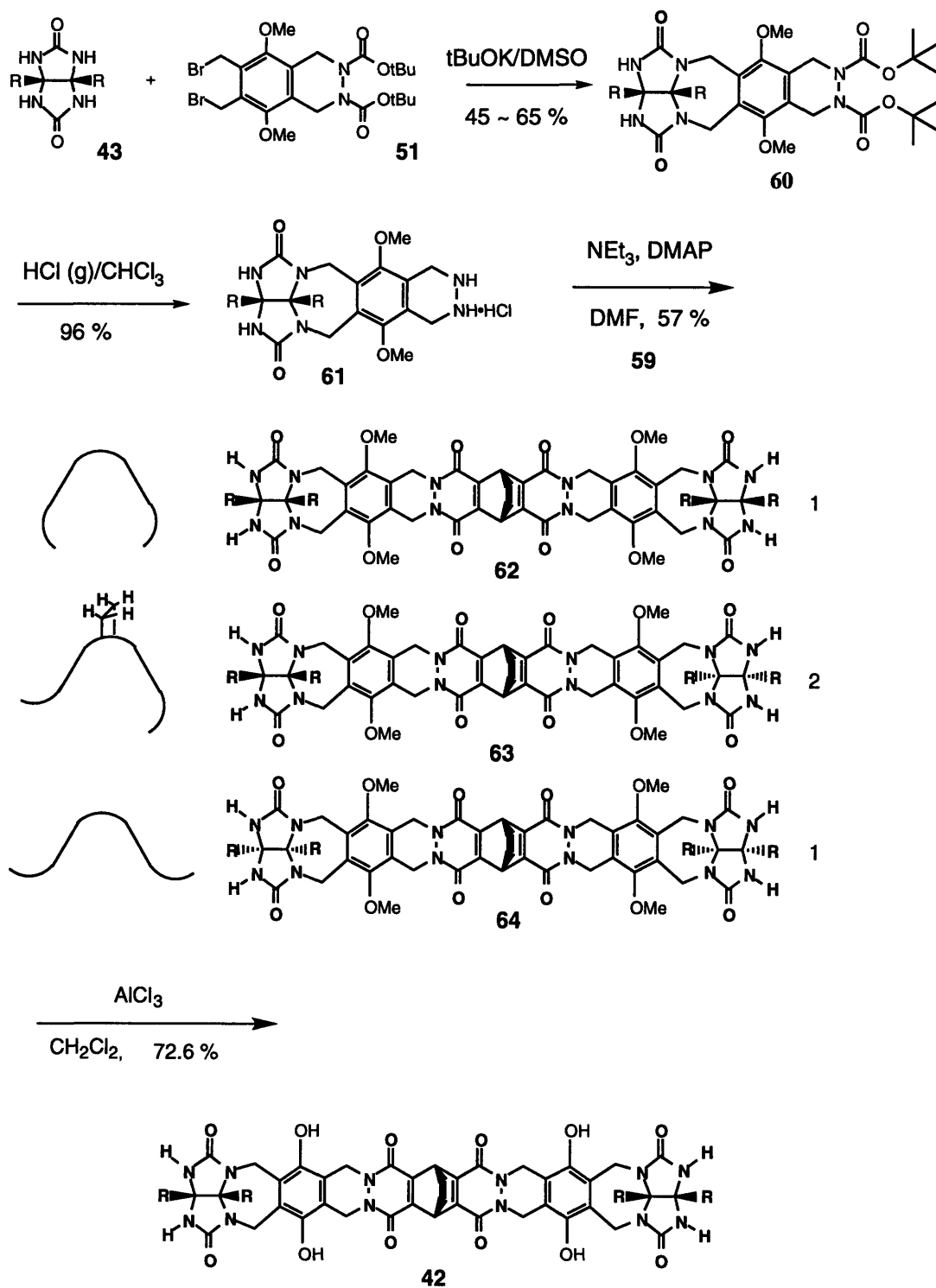
54, which was hydrogenated with 5% palladium on carbon to give compound 55. Deoxygenation reaction of 55 with  $\text{Ti}^0$  metal gave diene 56. Second Diels-Alder reaction of 53 and 56 in toluene gave tetraester 57. The deprotecting reaction with TFA in benzene was followed by treatment with oxalyl chloride to give the expected tetraacyl chloride 59.

### 3.3.4 Coupling reactions of 43, 50, and 59

Coupling the three pieces started with the reaction of 10 equiv. of di-(4-n-heptylphenyl) glycoluril and compound 51 with potassium tert-butoxide in DMSO to give coupled compound 60, which was treated with HCl gas to give hydrazide salt 61. Then compound 61 was coupled with half an equivalent of tetraacid chloride 59 and all three possible stereoisomers were obtained. Isolation of the desired isomer 62 was achieved using column chromatography on silica gel. Deprotection of the phenolic functions to give 42 was accomplished by treatment of 62 with  $\text{AlCl}_3$  in  $\text{CH}_2\text{Cl}_2$  (Fig.39).

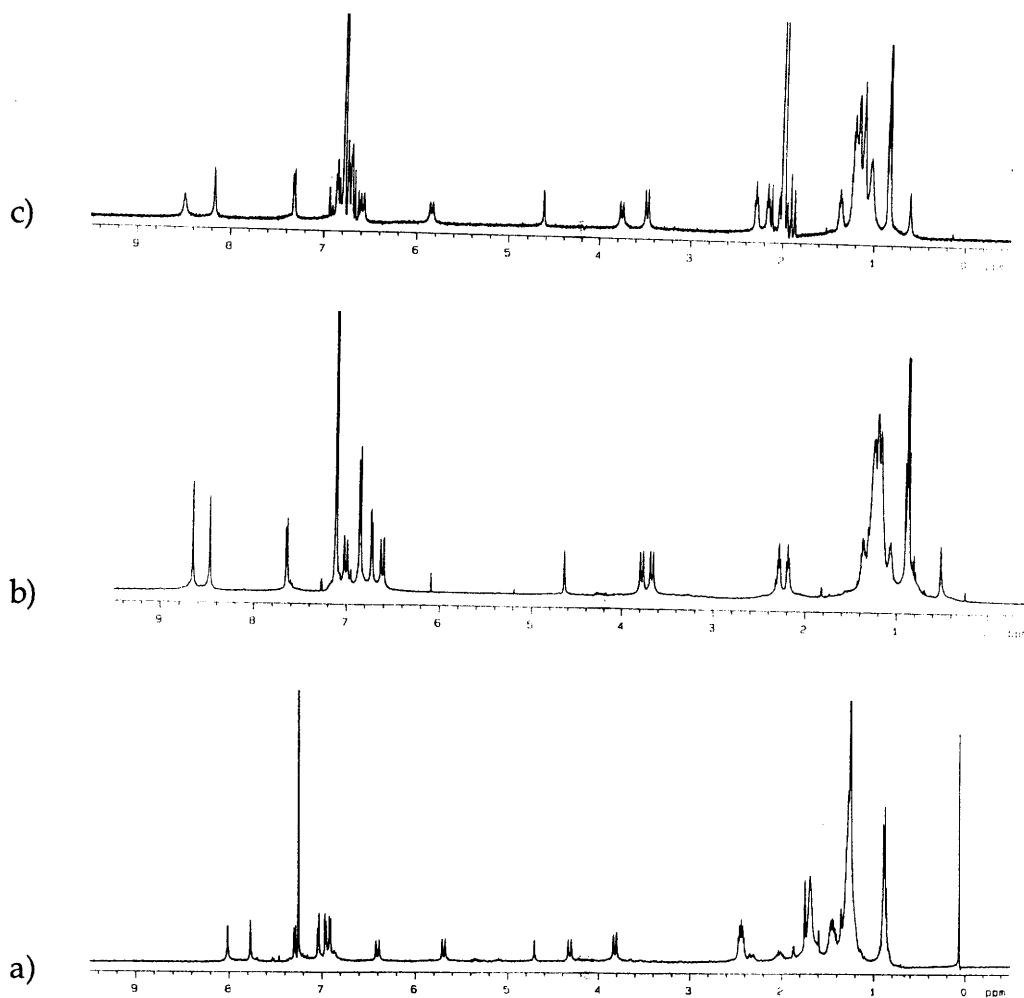
### 3.4 Characterization

Of the three stereoisomers, the S-shaped isomer could be quite easily identified by the NMR spectra because it shows two distinctive N-H peaks and O-H peaks. In addition a complicated N- $\text{CH}_2$  coupling pattern is



**Fig.39** The completion of synthesis was done by couple three pieces of its synthons.

observed. The W-shaped isomer gives broad NMR peaks while the C-shaped isomer gives very sharp and distinctive peaks. For example, in  $\text{CDCl}_3$  the  $^1\text{H}$ -NMR spectrum of dimeric C-shaped molecule **42** shows sharp signals characteristic of an ordered, well-defined system (Fig. 40a). The downfield shifts observed for the glycoluril N-H (7.74 ppm) and O-H (8.00 ppm) resonances in the spectrum of **42** indicate an extensively hydrogen bonded



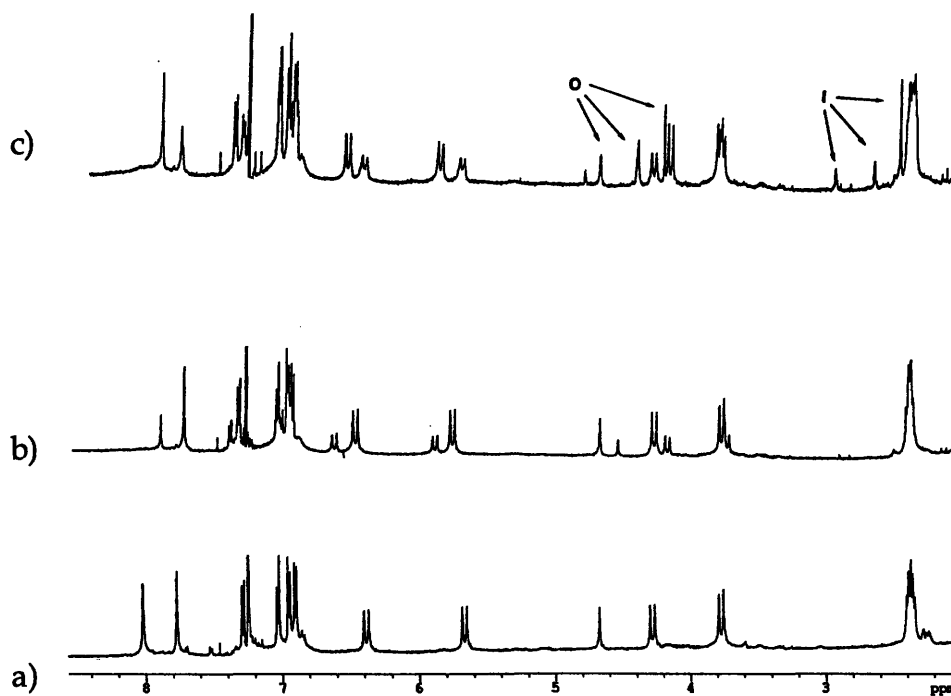
**Fig.40** The  $^1\text{H}$  NMR spectrum of molecule **42** in a)  $\text{CDCl}_3$  b) benzene- $d_6$  c) p-xylene- $d_{10}$

system. The glycoluril carbonyls are the complementary sites for the four phenolic O-H donors (Fig.34), and the constant chemical shift of the O-H peak of **42** (8.00 ppm) indicates consistent hydrogen bonding at these sites. Both the N-H and O-H signals are concentration independent. The N-H resonances of dimeric molecule **42** are not as far downfield as those of other dimeric capsules which were synthesized in our group (~9 ppm)<sup>2</sup>, and it is likely that the hydrogen bonds to this group are somewhat longer in the dimeric molecule **42** than in the other capsules. The shape and volume of the capsule is determined by the average geometries of all the hydrogen bonds involved, i.e. a compromise for the N-H and O-H donors can result in an expanded and more rigid capsule. Again, the molecule **42** shows sharp signals in its NMR spectra (Fig. 40b and 40c) in benzene, toluene and *p*-xylene-*d*<sub>10</sub>. Accordingly, the dominant form of the molecule **42** in these solvents is the dimeric capsule, held together by a network of up to 16 hydrogen bonds.

### 3.5 Encapsulation

Upon addition of adamantane derivatives or ferrocene derivatives to a solution of the molecule **42** in CDCl<sub>3</sub>, a second set of signals appears in the <sup>1</sup>H NMR spectra: a new capsule species is formed (Fig.41). In addition to the second set of signals for the capsule (host) a new set of upfield signals for the encapsulated guests emerge. These appear in the region 0.5 to -0.5 ppm for the adamantane derivatives and 3.5 to 2.5 ppm for the ferrocene

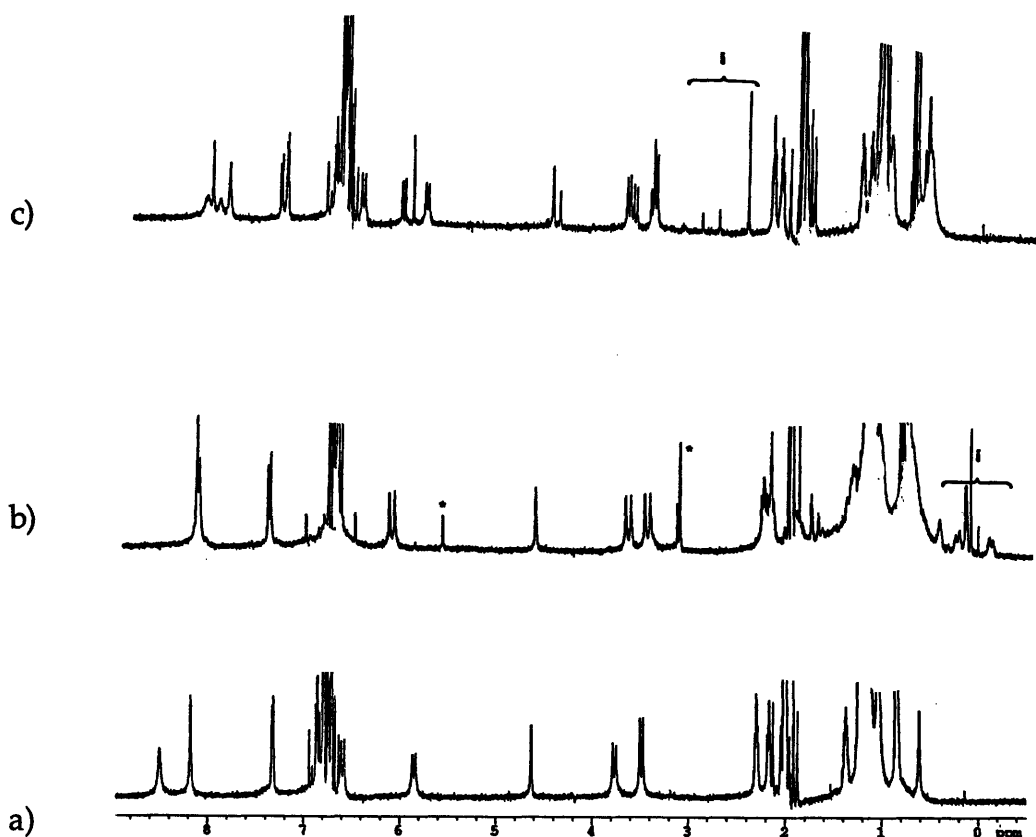
derivatives. Integration shows that the ratio of the new hosts to the encapsulated guests is 1 : 1. Moreover, the widely separated and relatively sharp signals for free and encapsulated guest in the NMR spectra indicate that exchange of guests in and out of the capsule is slow on the NMR scale. Similarly, adamantane derivatives (Fig. 42b) and ferrocene derivatives (Fig. 42c) can be encapsulated in *p*-xylene- $d_{10}$ . The relative concentrations of the original (solvent-occupied) and new (guest occupied) capsules can be determined by NMR integration.



**Fig. 41** The  $^1\text{H}$  NMR spectrum of the molecule **42** a) in  $\text{CDCl}_3$  b) 0.5 equivalents of 1-adamantane carboxylic acid added c) 0.6 equivalents of 1-ferrocenecarboxylic acid added. The signals of the guests inside and outside are labeled with "i" and "o", respectively.



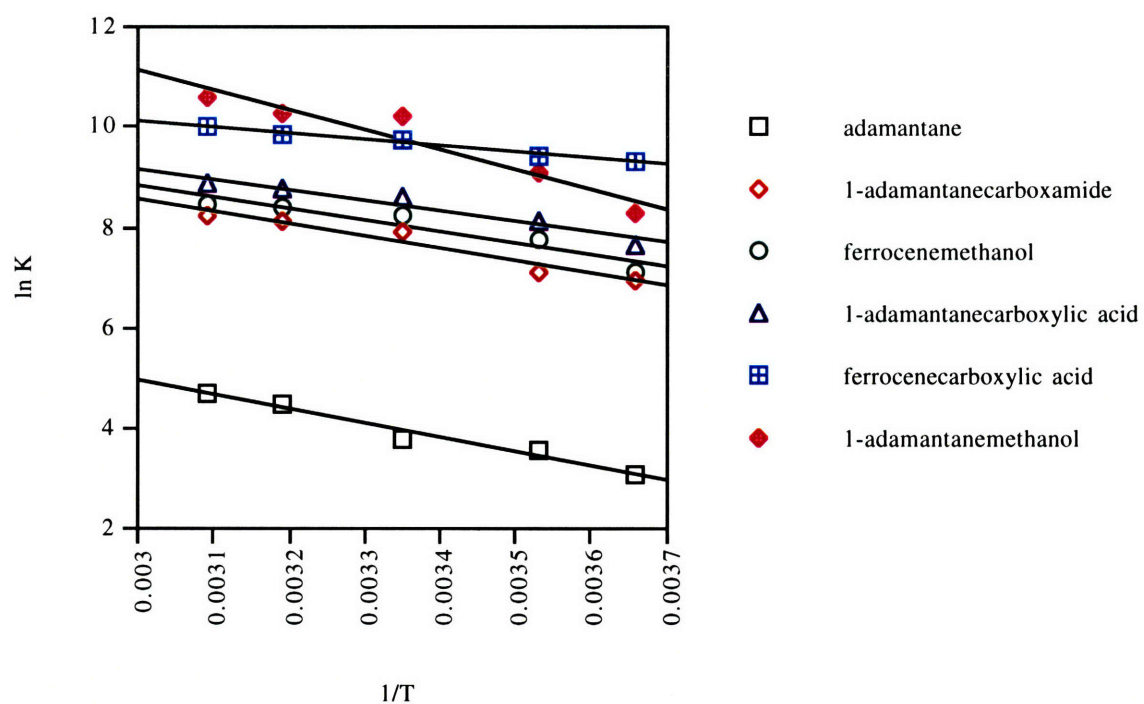
These values can be obtained for various guests as a function of temperature, and equilibrium constants and their thermodynamic parameters could be determined from this procedure (Fig.43 and Table.4). Similar behavior is observed in p-xylene-d<sub>10</sub> and benzene-d<sub>6</sub> solution. In p-xylene, however, the association constant for adamantane encapsulation is about 25 times larger than that observed in CDCl<sub>3</sub> (Fig.44 and Table. 5). While the association constant of adamantane derivative is much lower, the



**Fig. 42** The <sup>1</sup>H NMR spectrum of the molecule 42 a) in p-xylene-d<sub>10</sub> b) 0.9 equivalents of 1-adamantane carboxylic acid added c) 0.4 equivalents of ferrocenecarboxylic acid added. The signals of the included guests are labeled with "i", and signals from internal integration standard(2,4,6-trimethoxybenzaldehyde) are labeled with an asterisk.

association constants for the encapsulation of functionalized adamantanes or ferrocenes in p-xylene-d<sub>10</sub> are too large to be measured with NMR techniques.

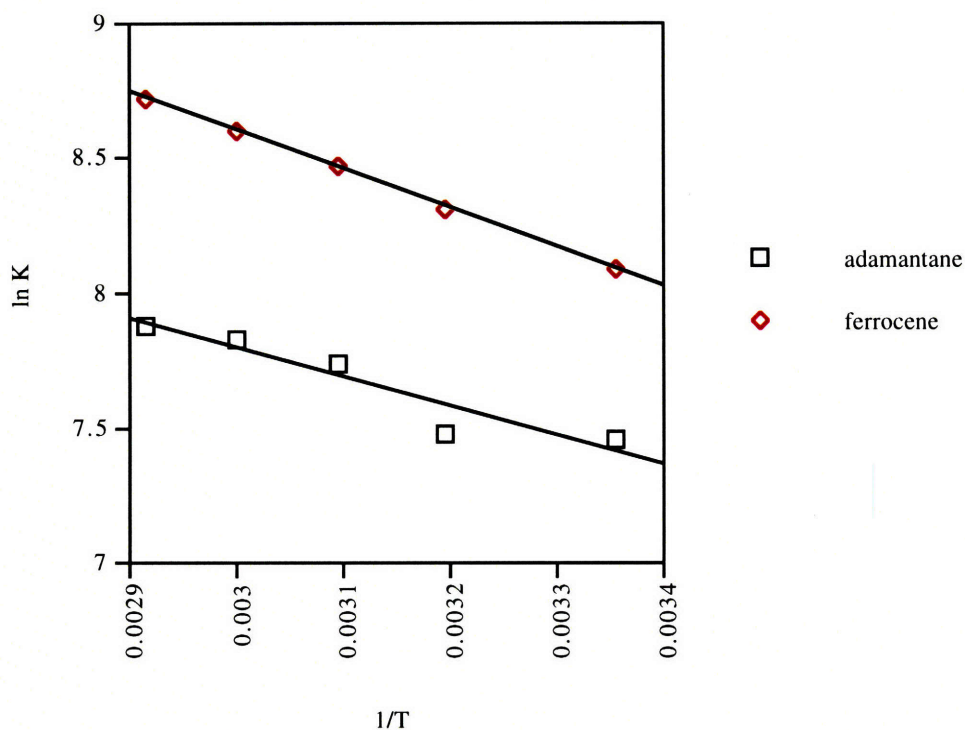
Thermodynamic parameters in benzene are shown in Fig. 45 and Table 6.



**Fig.43** Temperature dependence of encapsulation of adamantane and ferrocene derivatives in dimeric **2** in CDCl<sub>3</sub> solution. The temperature range was from 273 to 323K. (K = association constant).

Guests	$K_{298}$	$\Delta G$ (kcal/mol)	$\Delta H$ (kcal/mol)	$\Delta S$ (e. u. )
adamantane	$4.4 \times 10 \pm 2.2$	$-2.2 \pm 0.1$	$5.6 \pm 0.3$	$26.2 \pm 1.3$
1-adamantanecarboxamide	$2.8 \times 10^3 \pm 1.4 \times 10^2$	$-4.7 \pm 0.2$	$4.9 \pm 0.3$	$32.1 \pm 1.6$
1-ferrocenemethanol	$3.8 \times 10^3 \pm 1.9 \times 10^2$	$-4.9 \pm 0.2$	$4.5 \pm 0.2$	$31.6 \pm 1.6$
1-adamantanecarboxylic acid	$5.6 \times 10^3 \pm 2.8 \times 10^2$	$-5.1 \pm 0.3$	$4.1 \pm 0.2$	$31.1 \pm 1.6$
1-ferrocenecarboxylic acid	$1.7 \times 10^4 \pm 8.5 \times 10^2$	$-5.8 \pm 0.3$	$2.5 \pm 0.1$	$27.9 \pm 1.4$
1-adamantanemethanol	$2.7 \times 10^4 \pm 1.4 \times 10^3$	$-6.0 \pm 0.4$	$7.8 \pm 0.4$	$46.6 \pm 2.3$

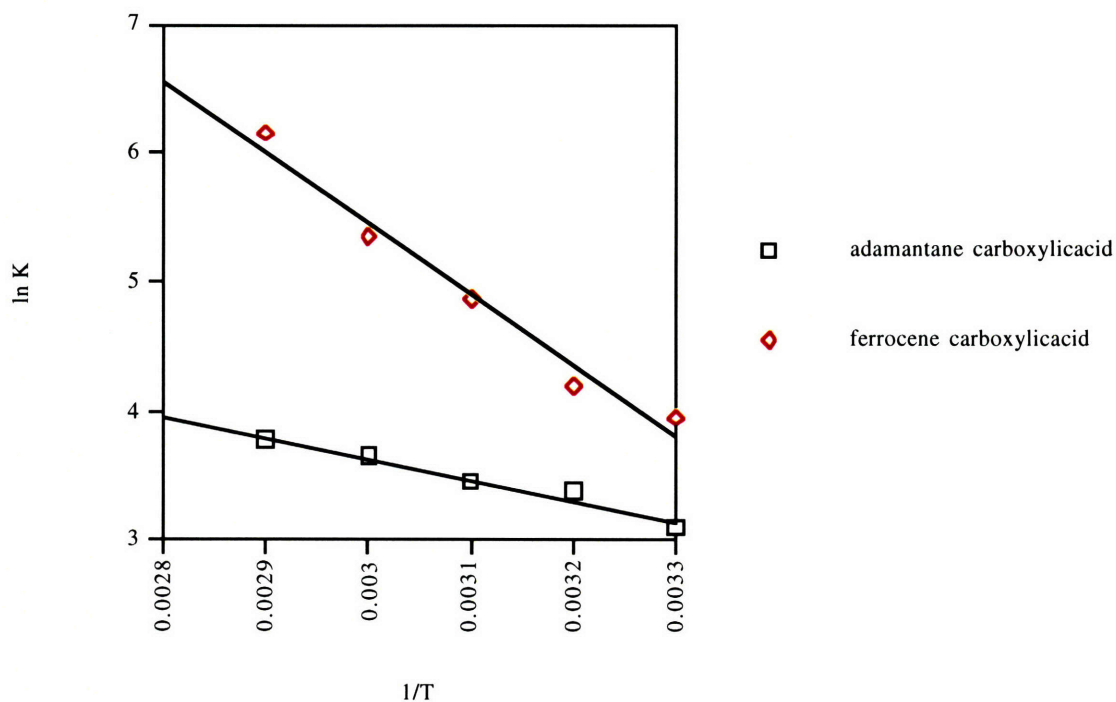
**Table. 4** Thermodynamic parameters of guest inclusion process of the dimer **42** in  $\text{CDCl}_3$ . Abbreviations: K, association constant;  $\Delta G$ , free energy;  $\Delta H$ , enthalpy;  $\Delta S$ , entropy.



**Fig.44** Temperature dependence of encapsulation of adamantane or ferrocene in dimeric **42** in  $p$ -xylene- $d_{10}$  solution. The temperature range was from 298 to 343K. (K = association constant).

Guests	$K_{298}$	$\Delta G(\text{kcal/mol})$	$\Delta H(\text{kcal/mol})$	$\Delta S(\text{e.u.})$
adamantane	$1.7 \times 10^3 \pm 90$	$-4.6 \pm 0.2$	$2.2 \pm 0.1$	$22.6 \pm 1.1$
ferrocene	$3.3 \times 10^3 \pm 170$	$-5.0 \pm 0.3$	$2.3 \pm 0.1$	$24.4 \pm 1.2$

**Table. 5** Thermodynamic parameters for guest encapsulation by dimeric **42** in p-xylene-d<sub>10</sub>.



**Fig.45** Temperature dependence of encapsulation of adamantanecarboxylic acid or ferrocenecarboxylic acid in dimeric **42** in p-xylene-d<sub>10</sub> solution. The temperature range was from 303K to 343K. ( $K$  = association constant).

Guests	K298(benzene-d6)	$\Delta G(\text{Kcal/mol})$	$\Delta H(\text{Kcal/mol})$	$\Delta S$ (e. u.)
1-adamantanecarboxylic acid	$2.3 \times 10 \pm 1.2$	$-1.8 \pm 0.1$	$3.2 \pm 0.2$	$16.9 \pm 0.8$
1-ferrocenecarboxylic acid	$5.3 \times 10 \pm 2.7$	$-2.4 \pm 0.1$	$10.9 \pm 0.5$	$44.7 \pm 2.2$

**Table. 6** Thermodynamic parameters for guest encapsulation by dimeric **42** in benzene-d<sub>6</sub>.

The most significant observation is that guest encapsulation *increases* with temperature (Fig. 46). As most processes involving host-guest association are entropically unfavorable but enthalpically favorable, the trends for **42** are unexpected. Indeed, much has been written about compensating effects of entropy and enthalpy in complex formation<sup>3-5</sup>, but for **42** the inclusion of guests involves an enthalpic cost, which is compensated by a larger entropic gain. This behavior is reminiscent of the classical hydrophobic effect, in which releasing of bound water to the bulk solvent compensates for the association of solutes. In organic media, such behavior is rarely encountered and generally unpredictable<sup>6-8</sup>, even though liberation of solvent is a universal feature of molecular recognition phenomena in solution. It is proposed that for **42**, a single solvent molecule is too small to fill the cavity. Rather, more than one CDCl<sub>3</sub> or p-xylene is required to maximize the intermolecular forces-the van der Waal's interactions- between the convex surfaces of the guests and the concave surface of the host's interior<sup>9,10</sup>.

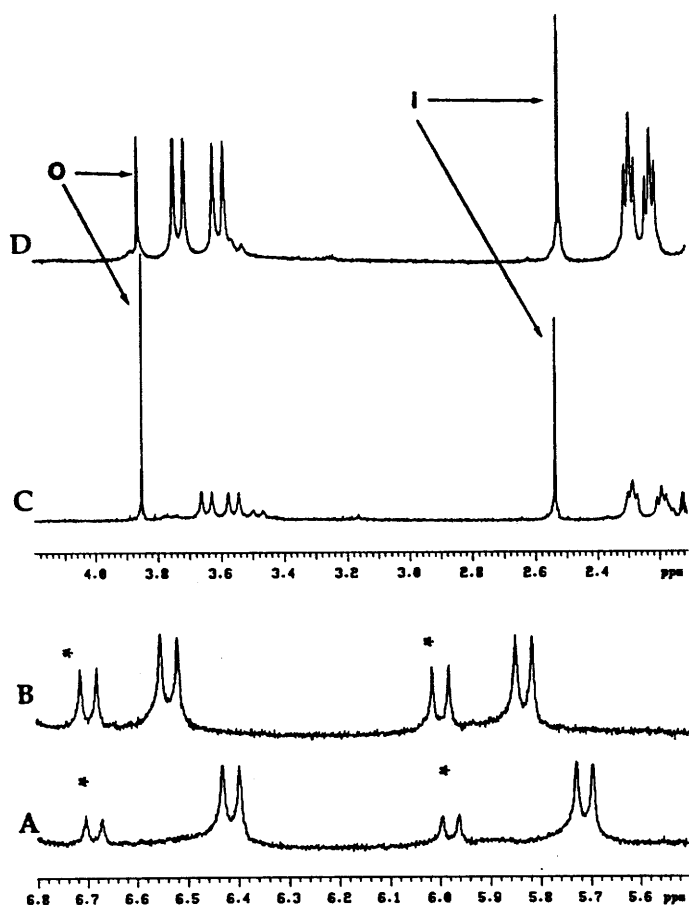
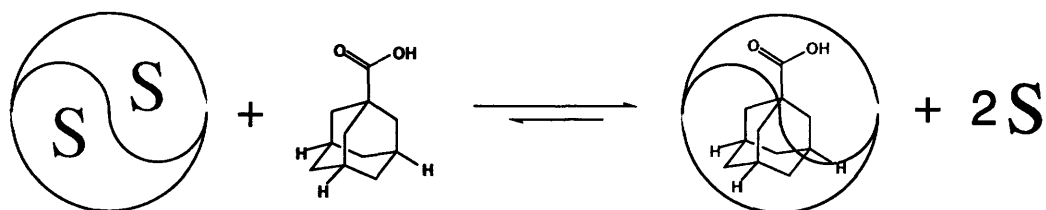


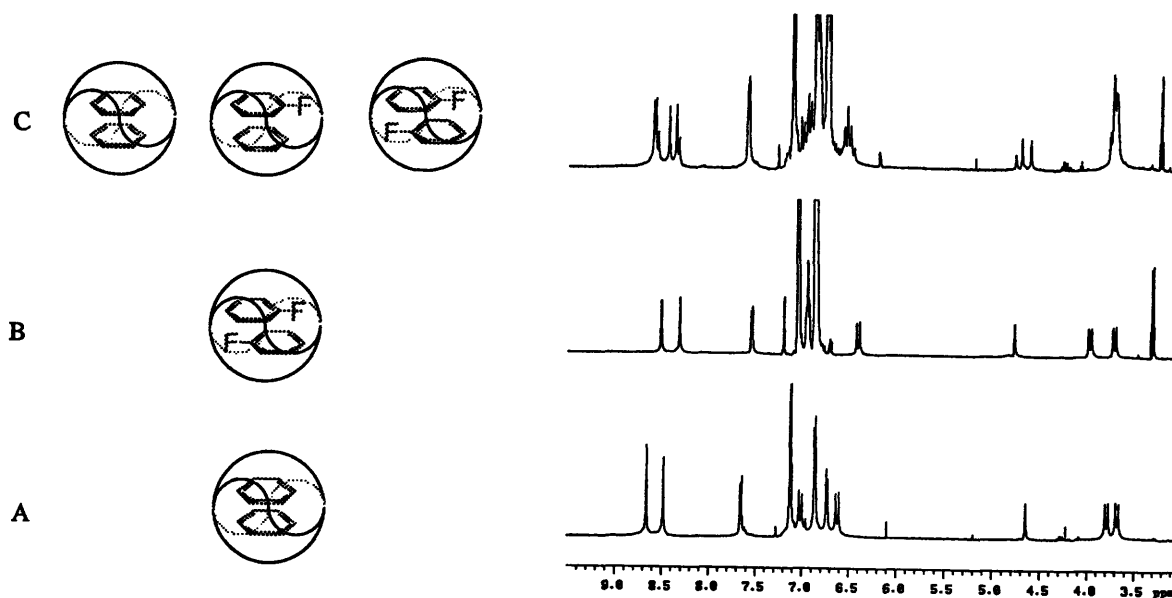
Fig. 46  $^1\text{H}$  NMR spectra of dimeric **42** with guests at different temperatures. Compound **42** with adamantane in  $\text{CDCl}_3$  at 298K (a) and 323K (b) ; Signals of the benzylic protons of demeric **42** with encapsulated adamantane are labeled with an asterisk. Compound **42** with ferrocene in p-xylene- $\text{d}_{10}$  at 298K (c) and 343K (d) ; signals for ferrocene inside and outside are labeled with "i" and "o", respectively.

Now single molecular guests which fill the cavity and offer chemical and structural complementarity are preferred to multiple solvent molecules; one guest releases several solvent molecules. Consequently, the encapsulation of adamantanes or ferrocenes by **42** increases entropy, since more than one encapsulated solvent is released to the bulk solution (Fig. 47).



**Fig. 47** Encapsulation as driven by the liberation of more than one solvent

To prove this hypothesis some two solvent experiments were performed. If molecule **42** can encapsulate two different solvent molecules with similar binding constant, there should be three dimeric species present (Fig 48). Indeed, three dimeric species of molecule **42** are observed at room



**Fig.48**  $^1\text{H}$  NMR spectra of **42** in benzene- $\text{d}_6$  (a), in fluorobenzene- $\text{d}_5$  (b), and in a mixture of two parts benzene- $\text{d}_6$  and one part fluorobenzene- $\text{d}_5$  solvents (c). In the former two cases both guest molecules are equivalent ; in the latter, there are three possible combinations, evident from three signals at 4.5 - 4.8 ppm and the three sets of signals at 8.3 - 8.7 ppm

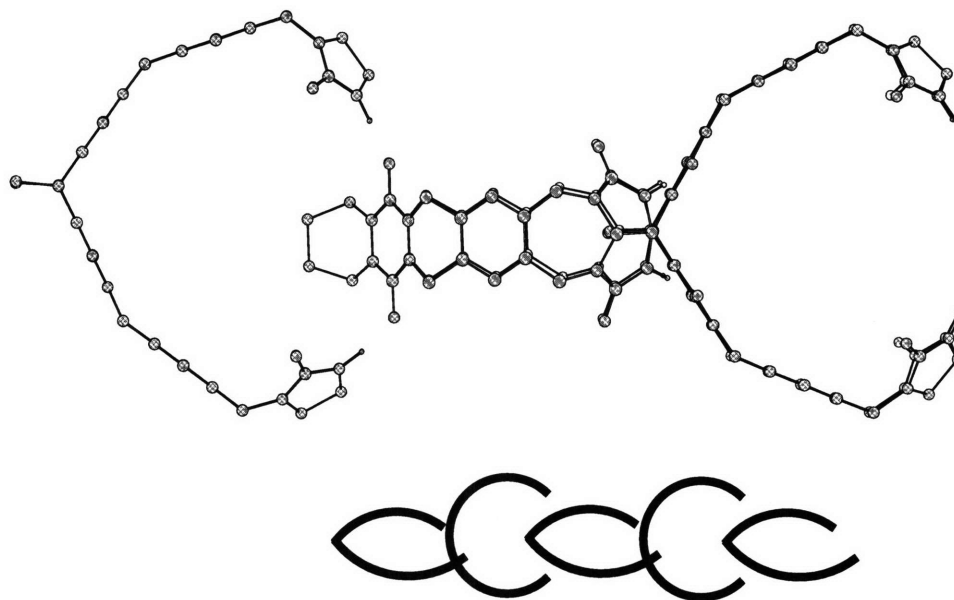
temperature when molecule **42** dissolved in a benzene- $d_6$  and fluorobenzene- $d_5$  mixture (Fig. 48). Other solvents combinations such as (p-xylene, toluene), (p-xylene, 1,4-difluorobenzene), (chloroform, bromoform), (chloroform, dichlorodfluoromethane) and (chloroform, chlorotrifluoromethane) just shows one species that might be due to different binding constant of different solvents, that is, one species dominates or the spectrum unresolved. Although encapsulation of one guest with releasing two solvents was proved, this entropy-driven process should also be reinforced by the release of solvents on the surface of guest as encapsulation proceeds.

### 3.6 Some comparison of molecules **41** and **42**

Molecule **41a** was the first version of these capsules, and it showed low solubility due to the insolubility of diphenyl glycoluril. In  $CDCl_3$ , the molecule **41a** showed an incomprehensibly broadened NMR spectrum and produced a gel-like phase. Although the more soluble molecule **41b** does not produce gel-like phase, it still gives broadened peaks in  $CDCl_3$ . In contrast, molecule **42** forms a clear solution and shows sharp signals characteristic of an ordered, well-defined system. It is expected that molecule **42** favors the dimeric capsule form more than molecule **41a** or **41b** because **42** can have 8 hydrogen bonds more. The fact that the molecule **41a** forms a gel-like phase



indicates that it exists in a polymeric or oligomeric state, as proposed in Fig. 49. The differences in the behavior of **41** and **42** in solution extend to p-xylene-d<sub>10</sub> as solvent. Again, the latter shows sharp signals in its NMR spectra (Fig. 40c) while the former was considerably broadened<sup>11</sup>. Accordingly, the dominant form of **42** in these solvents is the dimeric capsule, held together by a network of up to 16 hydrogen bonds. Molecule **41** and **42** show sharp signals only when it has proper guests inside, that is, when it has nicely ordered state. Therefore, it could be said that p-xylene-d<sub>10</sub> acts as good guest only with molecule **42**.



**Fig. 49** The chain-like oligomeric structure proposed for **41a** in CDCl<sub>3</sub>.

From the above observations, it can be proposed that capsule **42** is larger than capsule **41** from the three lines of evidence. First, The N-H

hydrogen bond length of molecule **42** (7.74 ppm) appears longer than that of molecule **41a**(8.0 ppm). Second, encapsulated guests in **42** are less shielded than encapsulated guest in **41**. In other words, guests inside molecule **42** are not closer to the aromatic surfaces than guests inside molecule **41**.

( encapsulated guest in **41** shift to upfield about 1 ppm while encapsulated guest in **42** shift to upfield to 0.5 ppm). Third, in molecule **42** two p-xylenes can be inside as good guests while molecule **41** apparently cannot accomodate two p-xylenes inside. Consequently, the shape and volume of capsule is determined by the average of all the hydrogen bonds involved, i.e. a compromise for the N-H and O-H donors can result in a expanded and more rigid capsule.

### 3.7 Experimental

#### 4-Heptylbenzil (47)

To a suspension of 2.2g (0.31 mol) of lithium metal (washed with hexane) in 60 ml of dried THF was added 5g (22.7 mmol) of 4-heptyl benzoic acid. This mixture was sonicated for 2 days. After 2 days, the reaction mixture was carefully added to 300 ml of 1N HCl. The resulting mixture was extracted 5 X 60 ml of hexane and dried over MgSO<sub>4</sub>. Evaporation and chromatography on silica gel with 5% ethyl acetate/ hexane gave 2.46g (53 %) of 4-heptylbenzil <sup>1</sup>H-NMR (300 MHz ; CDCl<sub>3</sub>) 7.87 (d, 4H, J=8.25, arom) 7.29 (d, 4H, J = 8.25, arom) 2.67 (t, 4H, J = 7.7, CH<sub>2</sub>-arom) 1.6 (m, 4H, alkyl) 1.28 (m, 16H, alkyl) 0.87 (t, 6H, J=6.6, CH<sub>3</sub>) HRMS (EI) calculated for C<sub>28</sub>H<sub>38</sub>O<sub>2</sub>, 406.2871 ; found 406.2869.

#### 4-Heptylphenyl glycoluril (43)

To 2.46g (6.05 mmol) of 47 was added 0.73g (12.2 mmol) of urea and 2 ml of trifluoroacetic acid and the mixture was refluxed in 100 ml of benzene under a Dean-Stark trap. After 24 hr, the solvent was evaporated and the residue was dissolved in MeOH-CH<sub>2</sub>Cl<sub>2</sub>-THF (10:70:20) solution. Slow evaporation of solvent gave a 2.37g (81 %) white precipitate. : mp > 300°C IR 3231, 2925, 2853, 1718, 1686, 1490, 1229, 1142, 1115, 778 cm<sup>-1</sup> <sup>1</sup>H-NMR (300 MHz ; DMSO) 7.64 (s, 4H, NH) 6.90 (d, 4H, J = 8.3, arom) 6.82 (d, 4H, J = 8.3, arom) 2.35 (t, 4H, J = 7.25,

CH<sub>2</sub>-arom) 1.39 - 1.09 (m, 20H, alkyl) 0.84 (t, 6H, J = 6.9, CH<sub>3</sub>) HRMS (FAB)  
calculated for C<sub>30</sub>H<sub>42</sub>N<sub>4</sub>O<sub>2</sub>H<sup>+</sup>, 491.3386 ; found 491.3377

### **1,4-Dimethoxy-2,3-dimethylbenzene (27)**

To a heated (60°C) solution of 5 g (89.1 mmol) of crushed potassium hydroxide in 100 ml of DMF was added 5g (36.1 mmol) of commercially available 2,3-dimethylhydroquinone. The mixture was stirred for 10 minutes then cooled to 0°C. A solution of 11.78 g (83.0 mmol) of methyl iodide in 50 ml of DMF was added dropwise at 0°C. After 2 hr, the reaction mixture was poured into 1l of water and extracted with 4 X 100 ml of diethyl ether. The ether layer was washed with 2 X 100 ml of water then dried over MgSO<sub>4</sub>. Evaporation of the solvent and recrystallization of the residue in methanol gave 6.0 g (92 %) of product **6**. : mp 74 - 75°C IR 2922, 1481, 1257, 1117, 1099, 800 cm<sup>-1</sup> <sup>1</sup>H-NMR (300 MHz ; CDCl<sub>3</sub>) 6.61 (s, 2H, arom) 3.72 (s, 6H, OCH<sub>3</sub>) 2.11 (s, 6H, CH<sub>3</sub>) HRMS (FAB) calculated for C<sub>10</sub>H<sub>14</sub>O<sub>2</sub>H<sup>+</sup>, 166.0994 ; found for 166.0990

### **1,4-Dimethoxy-2,3-dibromomethyl-5,6-dimethylbenzene (48)**

To a solution of 6.75g (40.6 mmol) of 1,4-dimethoxy-2,3-dimethylbenzene **27** in bromomethyl methyl ether (15 ml) was added 60 % sulfuric acid (15 ml). The reaction mixture was stirred at 40°C for 3 days then was poured into 100 ml of water and extracted with 5 X 50 ml of CH<sub>2</sub>Cl<sub>2</sub>. The organic layer was washed with 3 X 50 ml of 10% sodium bicarbonate solution and 2 X 50 ml of water. The resulting solution was dried over MgSO<sub>4</sub> then evaporated to give 14.30 g (88 %) of product : mp 88 - 89°C IR 2924, 2853, 1459, 1430, 1267, 1086, 1012, 962 cm<sup>-1</sup> <sup>1</sup>H-NMR (300 MHz ; CDCl<sub>3</sub>) 4.80 (s, 4H, CH<sub>2</sub>Br) 3.83 (s, 6H, OMe) 2.21 (s, 6H, CH<sub>3</sub>) HRMS(FAB) calculated for C<sub>12</sub>H<sub>16</sub>Br<sub>2</sub>O<sub>2</sub>H<sup>+</sup>, 350.9516 and [ M - Br ]<sup>+</sup> 271.0334 ; found for [ M - Br ]<sup>+</sup>, 271.0341

### **1,4-Dimethoxy-2,3,5,6-tetrabromomethylbenzene (49)**

A solution of 6.3g (17.89 mmol) of **48** and 6.37g (35.7 mmol) of N-bromosuccinimide in 150 ml of CCl<sub>4</sub> was irradiated with sun lamp for an hour. The CCl<sub>4</sub> was evaporated and the residue was stirred with 20 ml of MeOH for 5 min. Filtration gave 7.42g (82 %) of product. : mp 218 - 219°C IR 2940, 1459, 1410, 1277, 1198, 1025, 928, 831, 753, 623 cm<sup>-1</sup> <sup>1</sup>H-NMR (300 MHz ;

CDCl<sub>3</sub>) 4.76 (s, 8H, CH<sub>2</sub>Br) 4.06 (s, 6H, OMe) HRMS (EI) calculated for C<sub>12</sub>H<sub>14</sub>Br<sub>4</sub>O<sub>2</sub>, 509.8574 ; found for 509.8538

**1,4-Dimethoxy-5,6-di-bromomethyl -2,3-(di-t-butyl-1,2,3,4-tetrahydrophthalazine-2,3-dicarboxylate) (51)**

6.58g (12.9 mmol) of compound **49** was dissolved in 50 ml of THF and 50 ml of DMF mixture at 70 ~ 80°C. After complete dissolution, 1.0g (4.1 mmol) of di-tert-butylazodicarboxylic acid was added, followed by 0.2g (8.2 mmol) of NaH with stirring. After 20 min, the DMF was evaporated and the residue was diluted with ether. Undissolved excess tetrabromide (**49**) was removed by filtration. The trituration was repeated and the excess tetrabromide was filtered again. Chromatography on silicagel with 20% hexane/ethyl acetate gave 1.34g (54 %) of product : mp 210 - 211°C IR 2975, 1706, 1456, 1393, 1367, 1266, 1151, 1023, 754, 665 cm<sup>-1</sup> <sup>1</sup>H-NMR (300 MHz ; CDCl<sub>3</sub>, mixture of rotamers) 5.15 (br, 4H, CH<sub>2</sub>-N) 4.73 (br, 4H, CH<sub>2</sub>Br) 3.89(s, 6H, OMe) 1.49 (s, 18H, C(CH<sub>3</sub>)<sub>3</sub>) HRMS (EI) calculated for C<sub>22</sub>H<sub>32</sub>Br<sub>2</sub>N<sub>2</sub>O<sub>6</sub>, 580.3126 ; found for 580.3214

**Glycoluril coupled compound (60)**

To a solution of 7.56g (15.6 mmol) of di-(4-n-heptylphenyl)glycoluril (**43**) in 300 ml of 20% THF in DMSO was added 3.52g (31.2 mmol) of potassium tert-butoxide. The reaction mixture was stirred for 20 minutes, then 0.91g (1.56

mmol) of dibromide (**51**) in 50 ml of DMSO was added dropwise. After 1 hour, the reaction mixture was poured into 500 ml of water. The precipitate was filtered and washed with ethyl acetate until no further product was detected by TLC. Evaporation and chromatography on silica gel with 50% ethyl acetate/hexane gave 0.77g (55 %) of product. : mp 250 - 251°C <sup>1</sup>H-NMR(300 MHz ; CDCl<sub>3</sub>, mixture of rotamers) 6.8 (br, 8H, arom) 6.15 (br, 2H, NH) 5.42 (br, 2H, CH<sub>2</sub>-N) 5.09 (br, 2H,CH<sub>2</sub>-N) 4.15 (br, 2H, CH<sub>2</sub>-N) 3.80 (br, 8H, OMe, CH<sub>2</sub>-N) 2.78 (m, 4H, CH<sub>2</sub>-Ph) 1.49 (s, 18H, C(CH<sub>3</sub>)<sub>3</sub>)1.25 (m, 20H, alkyl) 0.84 (m, 6H, CH<sub>3</sub>) HRMS (FAB) calculated for C<sub>52</sub>H<sub>72</sub>N<sub>6</sub>O<sub>8</sub>H<sup>+</sup>, 909.5411 ; found for 909.5475

#### **Phthalazine hydrochloride salt (**61**)**

To a solution of 0.70g (0.7 mmol) of **60** in CHCl<sub>3</sub>, HCl gas was bubbled for an hour. The reaction mixture was purged with Ar for 10 min., then evaporated to give 0.56 g (98 %) of product. : mp 268 - 270°C IR 3233, 2925, 2853, 1702, 1460, 1345, 1045, 933, 800, 747 cm<sup>-1</sup> <sup>1</sup>H-NMR (300 MHz ; DMSO) 8.14 (s, 2H, NH) 6.87 (m, 10H, arom) 5.23 (d, 2H, CH<sub>2</sub>-N) 4.13 (s, 4H, CH<sub>2</sub>-NH HCl) 3.79 (s+d, 8H, OMe, CH<sub>2</sub>-N) 2.78 (m, 4H, CH<sub>2</sub>-arom) 1.25 (m, 20H, alkyl) 0.84 (m, 6H,CH<sub>3</sub>) HRMS(FAB) calculated for [C<sub>42</sub>H<sub>57</sub>N<sub>6</sub>O<sub>4</sub>ClCs<sup>+</sup> - HCl ] , 841.3417 ; found for 841.3432

**Di-(p-methoxybenzyl)-acetylenedicarboxylic acid (53)**

To a mixture of 1.0 g (8.77 mmol) of acetylenedicarboxylic acid **52** in 30 mL of benzene at reflux was added 2.8 mL (21.2 mmol) 4-methoxybenzyl alcohol in 4 portions over 15 min. Heated at reflux for 3 h under Dean-Stark trap. After evaporation of the benzene, the residue was chromatographed on silica gel with 15% ethyl acetate/hexane to give 1.89 g (61%) of the ester as a white solid.  $^1\text{H}$  NMR ( $\text{CDCl}_3$ ): 7.30 (d, 4H,  $J=8.7$ , arom), 6.88 (d, 4H,  $J=8.7$ , arom), 5.17 (s, 4H,  $\text{CH}_2\text{-Ph}$ ), 3.81 (s, 6H, OMe). HRMS (EI): calculated for  $\text{C}_{20}\text{H}_{18}\text{O}_6$ , 354.1103; found 354.1100.

**Tetra-(p-methoxybenzyl) 7-oxabicyclo[2,2,1]-2,5-heptadiene-2,3,5,6-tetracarboxylic acid (54)**

A mixture of 3.0 g (8.47 mmol) of the ester **53** and 5 mL of furan was heated in a sealed tube placed in an 85°C oil bath for 4 h. After evaporation of the furan, the residue was chromatographed on silica gel with 30% ethyl acetate/hexane to give 2.33 g (65%) of the ester as a white solid.  $^1\text{H}$  NMR ( $\text{CDCl}_3$ ): 7.31 (d, 4H,  $J=8.4$ , arom), 7.26 (s, 2H,  $-\text{CH}=\text{CH}-$ ), 6.93 (d, 4H,  $J=8.4$ , arom), 5.73 (s, 2H, CHO), 5.16 (dd, 4H,  $J=14.2, 26.5$ ,  $\text{CH}_2\text{-Ph}$ ), 3.87 (s, 6H, OMe). HRMS (EI): calculated for  $\text{C}_{24}\text{H}_{22}\text{O}_7$ , 422.1366; found 422.1369.



**Di-(p-methoxybenzyl) 7-oxabicyclo[2,2,1]-2-heptene-2,3-dicarboxylic acid  
(55)**

A vigorously stirred mixture of 4.5 g (10.7 mmol) of the diene **54** and ~0.5 g of 5% Pd/C in 60 ml of ethyl acetate was hydrogenated at ambient pressure until 260 mL of hydrogen had been consumed. Additional hydrogen was introduced until <sup>1</sup>H NMR analysis showed that the diene was consumed. The mixture was then filtered and the solvent evaporated to give 4.39 g (97%) of the cyclohexene as a white solid. <sup>1</sup>H NMR (CDCl<sub>3</sub>): 7.21 (d, 4H, J=9.0, arom), 6.82 (d, 4H, J=9.0, arom), 5.2 (m, 2H, CHO), 5.04 (dd, 4H, J=13.5, 22.0, CH<sub>2</sub>-Ph), 3.76 (s, 6H, OMe), 1.80 (m, 2H, CH), 1.42 (m, 2H, CH). HRMS (EI): calculated for C<sub>24</sub>H<sub>24</sub>O<sub>7</sub>, 424.1522; found 424.1517.

**Di-(p-methoxybenzyl) 1,2-cyclohexadiene-1,2-dicarboxylate (56)**

To a solution of 15.31 mL (140 mmol) of TiCl<sub>4</sub> in 30 mL of hexane at 0°C was added 125 mL THF over 20 min. A slurry of 1.87 g (49.4 mmol) LAH in 15 mL THF was then added over 10 min. The mixture was then heated at reflux for 30 min, cooled to RT, and a solution of 5.70 g (13.4 mmol) of the cyclohexene **55** in 15 mL THF was added over 5 min. After 2 h, the mixture was poured into 1 L 10 % K<sub>2</sub>CO<sub>3</sub> (aq). The mixture was extracted with ether and the organic extracts were dried over MgSO<sub>4</sub>, and evaporated. The residue was chromatographed on silica gel with 25% ethyl acetate/hexane to give 4.32 g (79%) of the diene as a colorless oil. <sup>1</sup>H NMR (CDCl<sub>3</sub>): 7.23 (d, 4H, J=9.1,

arom), 6.85 (m, 6H, arom), 6.83 (-CH=) 5.02 (s, 4H, CH<sub>2</sub>-Ph), 3.79 (s, 6H, OMe), 2.25 (m, 4H, CH<sub>2</sub>). HRMS (EI): calculated for C<sub>24</sub>H<sub>24</sub>O<sub>6</sub>, 408.1573; found 408.1567.

**Tetra-(p-methoxybenzyl) bicyclo[2,2,2]-octa-2,5-diene-2,3,5,6-tetracarboxylate (57)**

A mixture of 1.75 g (4.28 mmol) of the diene **56** and 1.98 g (5.57 mmol) of the acetylene dicarboxylic acid **52** in 10 mL benzene was heated at reflux for 40 h. Following evaporation of the benzene, the residue was chromatographed on silica gel with 35% ethyl acetate/hexane to give 2.46 g (61%) of a mixture of the starting components and 1.06 g (33%) of the product tetraester as a colorless oil. Resubjection of the recovered starting components to heating and chromatography gave an additional 2.37 g (41%) of the product after 2 additional cycles, for a total of 2.43 g (74%). <sup>1</sup>H NMR (CDCl<sub>3</sub>): 7.17 (d, 8H, J=8.5, arom), 6.84 (d, 8H, J=8.5, arom), 4.97 (s, 8H, CH<sub>2</sub>Ph), 4.42 (s, 2H, CH-CH=), 3.79 (s, 12H, OMe), 1.58 (s, 4H, bridged CH<sub>2</sub>). HRMS (FAB): calculated for C<sub>44</sub>H<sub>42</sub>O<sub>12</sub>, -C<sub>2</sub>H<sub>4</sub>+H<sup>+</sup>=C<sub>42</sub>H<sub>39</sub>O<sub>12</sub>, 737.2598; found 737.2611.

**Bicyclo[2,2,2]-octa-2,5-diene-2,3,5,6-tetracarboxylicacid (58)**

To a solution of 1.33 g (1.74 mmol) of the tetraester **57** in 3 mL of dichloromethane and 3 mL anisole was added 25 ml of TFA in one portion.

After stirring for 15 min, the mixture was diluted with benzene and evaporated. The residue was then diluted with ether and filtered to give 0.355 g (72%) of the tetraacid as a white powder.  $^1\text{H}$  NMR (DMSO- $d_6$ ): 4.27 (s, 2H), 1.45 (s, 4H).  $^{13}\text{C}$  NMR (DMSO- $d_6$ ): d 166.2, 140.8, 40.7, 24.1. HRMS (FAB): calculated for  $\text{C}_{12}\text{H}_{10}\text{O}_8$ , 282.0376; found 282.0371.

#### **Bicyclo[2,2,2]-octa-2,5-2,5-diene-2,3,5,6-tetracarbonyl chloride (59)**

To a suspension of 0.100 g (0.354 mmol) of the tetraacid **58** in 1 mL of dichloromethane was added 1 mL of oxalyl chloride and 1 drop of a 10% v/v mixture of DMF in dichloromethane. The mixture was stirred for 3 h or until complete dissolution occurred, then diluted with benzene and evaporated to give 0.120 g (96%) of the tetraacid chloride as a light brown solid.  $^1\text{H}$  NMR ( $\text{CDCl}_3$ ): 4.77 (s, 4H), 1.92 (s, 4H).

#### **Coupled methoxy compounds (62 and stereoisomers)**

To a solution of 150 mg (0.2 mmol) of **61** and catalytic amount of DMAP in 5 ml of DMF was added 0.2 ml (3 mmol) of  $\text{Et}_3\text{N}$  and 35.8 mg (0.1 mmol) of tetra acyl chloride **59**. The reaction mixture was stirred for 24 hr under argon. DMF was evaporated under reduced pressure and 3 ml MeOH was added with stirring for 10 min. 10 ml of water was added to the solution and the precipitate was filtered. Chromatography on silicagel with chloroform: ethyl acetate : methanol = 6 : 3 : 1 solution gave 50 mg (31 %) of S-shaped isomer **63**,

19 mg (12 %) of C-shaped isomer (**62**) and 24 mg (15 %) of a mixture of C-shaped (**62**) and W-shaped (**64**) isomers. This mixture was difficult to separate at this stage. Therefore, it was directly used in the next demethylation step. IR 3250, 2925, 2853, 1711, 1638, 1462, 1343, 1250, 1115, 1034, 960  $\text{cm}^{-1}$  C-shaped isomer (**62**) : decomp 191 - 192°C  $^1\text{H-NMR}$  (300 MHz ; DMSO) ; 8.12 (s, 4H, NH) 6.90 (m, 16H, arom) 5.54 (d, 4H, J = 15.6,  $\text{CH}_2\text{-N}$ ) 5.27 (d, 4H, J=15.7,  $\text{CH}_2\text{-N}$ ) 4.93 (s+ d, 6H, CH,  $\text{CH}_2\text{-N}$ ) 3.89 (s, 12H, OMe) 3.74 (d, 4H, J= 15.7,  $\text{CH}_2\text{-N}$ ) 2.36 (m, 8H,  $\text{CH}_2\text{-Ph}$ ) 1.14 (m, 44H, alkyl,  $\text{CH}_2$  in middle ring) 0.84 (m, 12H,  $\text{CH}_3$ ) S-shaped isomer (**63**) : decomp 195 - 196°C  $^1\text{H-NMR}$  (300 MHz ; DMSO) ; 8.12 (s, 2H, NH) 8.09 (s, 2H, NH) 6.90 (m, 16H, arom) 5.54 (d, 4H, J = 15.6,  $\text{CH}_2\text{-N}$ ) 5.31 - 5.12 (m, 4H,  $\text{CH}_2\text{-N}$ ) 4.94 (s+d, 6H, CH,  $\text{CH}_2\text{-N}$ ) 3.90 (s, 3H, OMe) 3.88 (s, 3H, OMe) 3.72 (m, 4H,  $\text{CH}_2\text{-N}$ ) 2.36 (m, 8H,  $\text{CH}_2\text{-arom}$ ) 1.14 (m, 44H, alkyl,  $\text{CH}_2$  in middle ring) 0.84 (m, 12H,  $\text{CH}_3$ ) HRMS(FAB) calculated for  $\text{C}_{96}\text{H}_{114}\text{N}_{12}\text{O}_{12}\text{H}^+$ , 1627.8678 ; found for 1627.8654

### Softball (**42**)

To a solution of 20 mg (0.012 mmol) of mixture of C-shaped and W-shaped isomers (**62,64**) was added 50 mg (0.37 mmol) of  $\text{AlCl}_3$  with stirring overnight. The reaction mixture was chromatographed directly on silica gel with 7% methanol/chloroform to give a 7 mg (73 %) of C-shaped compound (**42**). decomp 170 - 172°C IR 3265, 2925, 2854. 1692, 1626, 1467, 1251,

1017 cm<sup>-1</sup> <sup>1</sup>H-NMR (300 MHz ; DMSO) 8.69 (s, 4H, OH) 8.10 (s, 4H, NH) 6.89 (m, 16H, arom) 5.52 (d, 4H, J = 15.6, CH<sub>2</sub>-N) 5.32 (d, 4H, J = 15.6, CH<sub>2</sub>-N) 4.97 (s, 2H, bridgehead CH) 4.78 (d, 4H, J = 15.6, CH<sub>2</sub>-N) 3.62 (d, 4H, J = 15.6, CH<sub>2</sub>-N) 2.36 (m, 8H, CH<sub>2</sub>-arom) 1.14 (m, 44H, alkyl, CH<sub>2</sub> in middle ring) 0.84 (m, 12H, CH<sub>3</sub>)

<sup>1</sup>H-NMR (500MHz ; CDCl<sub>3</sub>) 8.02 (s, 8H, OH) 7.74(s, 8H, NH) 6.84 (m, 32H, arom) 6.40 (d, 8H, J = 16.5, CH<sub>2</sub>-N) 5.69 (d, 8H, J = 16.0, CH<sub>2</sub>-N) 4.71(s, 4H, bridgehead CH) 4.32 (d, 8H, J = 16.5, CH<sub>2</sub>-N) 3.82 (d, 8H, J = 16.0, CH<sub>2</sub>-N) 2.44 (m, 16H, CH<sub>2</sub>-Ph) 1.15 (m, 88H, alkyl, bridge CH<sub>2</sub>) 0.88 (m, 24H, CH<sub>3</sub>) For **42-W** decomp 194 - 196°C <sup>1</sup>H-NMR (300 MHz ; DMSO) 8.66 (s, 4H, OH) 8.11 (s, 4H, NH) 6.89 (m, 16H, arom) 5.36 (d, 4H, J=15.1, N-CH<sub>2</sub>) 5.28 (d, 4H, J=15.2, N-CH<sub>2</sub>) 4.97 (s, 2H, bridgeheadCH) 4.94 (d, 4H, J=15.1, N-CH<sub>2</sub>) 3.62 (d, 4H, J=15.2, N-CH<sub>2</sub>) 2.44 (m, 16H, CH<sub>2</sub>-arom) 1.15 (m, 88H, alkyl, bridge CH<sub>2</sub>) 0.88 (m, 24H, CH<sub>3</sub>) For **42-S** decomp 180 - 182°C <sup>1</sup>H-NMR (300MHz ; DMSO) 8.69 (s, 2H, OH ) 8.68 (s, 2H, OH) 8.12 (s, 2H, NH) 8.08 (s, 2H, NH) 6.80 (m, 16H, arom) 5.37 (m, 8H, N-CH<sub>2</sub>) 4.97 (s, 2H, bridgehead CH) 4.87 (m, 4H, N-CH<sub>2</sub>) 3.63(m, 4H, N-CH<sub>2</sub>) 2.44 (m, 16H, CH<sub>2</sub>-Ph) 1.15 (m, 88H, alkyl, bridge CH<sub>2</sub>) 0.88 (m, 24H, CH<sub>3</sub>)

HRMS(FAB) calculated for C<sub>92</sub>H<sub>106</sub>N<sub>12</sub>O<sub>12</sub>H<sup>+</sup>, 1571.8052 ; found for 1571.8038

### 3.8 References

- 1)Karaman, R.; Fry., J. L. *Tetrahedron Lett.* **1989**, 30, 6267.
- 2)Wyler, R.; Mendoza, J. d.; Rebek J. Jr. *Angew. Chem. Int. Ed. Engl.* **1993**, 32, 1699.
- 3)Searle, M. S.; Westwell, M. S.; Williams, D. H. *J. Chem. Soc. Perkin Trans .* **1995**, 2, 141.
- 4)Peterson, B. R.; Wallimann, P.; Carcanague, D. R.; Diederich, F. *Tetrahedron* **1995**, 51, 401.
- 5)Dunitz, J. D. *Chem. Biol.* **1995**, 2, 709.
- 6)Cram, D. J.; Blanda, M. T.; Paek, K.; Knobler, C. B. *J. Am. Chem. Soc.* **1992**, 114, 7765.
- 7)Cram, D. J.; Choi, H.-Y.; Bryant, J. A.; Knobler, C. B. *J. Am. Chem. Soc.* **1992**, 114, 7748.
- 8)Canceill, J. *Angew. Chem. Int. Ed. Engl.* **1989**, 28, 1246.
- 9)Diederich, F. *Angew. Chem.* **1988**, 100, 372.
- 10)Israelachvili, J. *Intermolecular and Surface Forces*; 2nd ed.; Academic Press: London, 1988.
- 11)Meissner, R. S.; Rebek, J. Jr.; Mendoza, J. D. *Science* **1995**, 270, 1485.

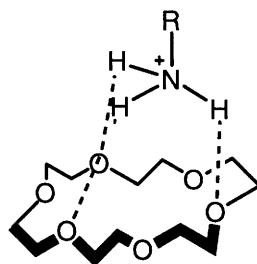
## **Chapter 4. Artificial Receptors Capable of Enzyme-like Recognition**

### **4.1 Introduction**

Molecular receptors bearing both reactive groups and binding sites may complex an appropriate substrate and then react with it. Even more, they may release products, thus regenerating the receptor for a new cycle. The catalytic behavior of molecular receptors represents one of the major challenges of supramolecular chemistry. The catalytic behavior of molecular receptors must involve two steps : selective binding of the substrate and transformation of the substrate into products within receptor-substrate complex. Both steps require the molecular recognition of the productive substrate and the correct molecular information in the reactive receptor. Compared to molecular catalysis, a binding step is involved that selects the substrate and precedes the reaction itself. The design of efficient and selective supramolecular reagents and catalysts may give insight into the elementary steps of catalysis, provide new types of chemical reagents, and effect reactions that are not amenable to enzymatic catalysis<sup>1</sup>.

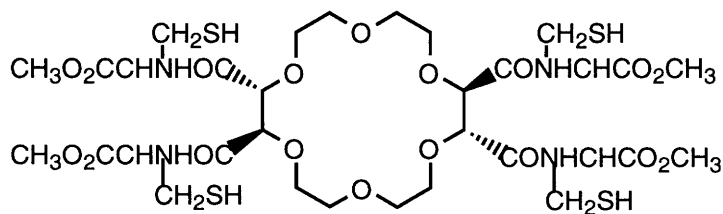
### **4.2 Macrocyclic Polyether**

The classical model for binding of an ion in a crown ether involves

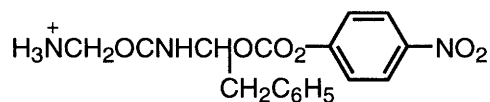


65-NH<sub>4</sub><sup>+</sup>

three point binding as illustrated for ammonium ion complex with [18]crown-6 in 65-NH<sub>4</sub><sup>+</sup>. The most logical method of designing crown ethers capable of mimicking enzyme chemistry is to elaborate the three point binding model. If an ammonium ion with a R group is used as a guest on which reaction can be carried out and then the periphery of the crown ether must be modified to make contact with R. For example, [18]crown-6 fitted with side chains bearing thiol groups cleave activated esters with marked rate enhancements and chiral discrimination between optically active substrate<sup>3-5</sup>.



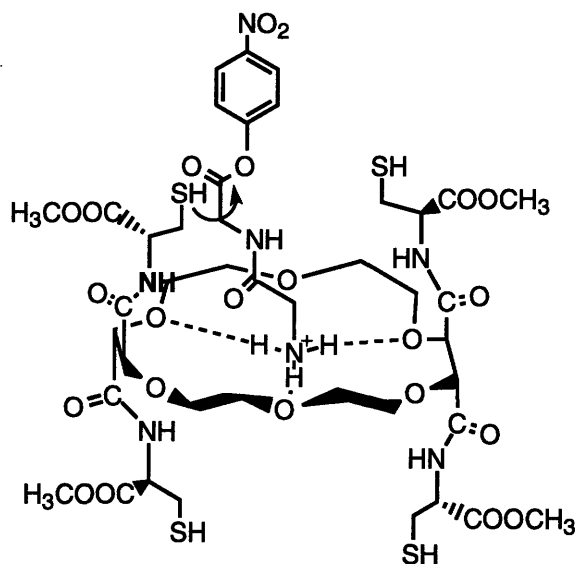
66 (L-cystein derivative)



67



The tetra-cystein derivative of macrocycle **66** binds to p-nitrophenyl(PNP) esters of amino acids and peptides, and reacts with the bound species, releasing p-nitrophenol as shown in Fig. 49<sup>4</sup>.

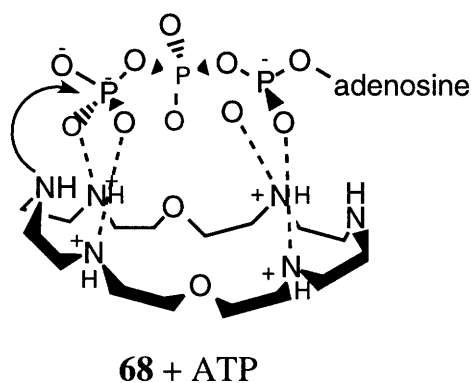


**Fig. 49** The ester cleavage by **66**.

In  $\text{CH}_2\text{Cl}_2/\text{CH}_3\text{OH}/\text{H}_2\text{O}$  (97.9/2/0.1ratio) the L-enantiomer of **67** undergoes acyl transfer to **66** about 50 times more rapidly than the D-enantiomer of **67**. L-**67** appears to fit better in the cavity of **66**. A detailed analysis of steric effect is difficult, however, thiolysis occurs in not outside of the complex as established by the inhibitory effect of KBr, which competes for binding sites in **66**. With **66**, there is no turnover because the catalyst is used in excess in order to obtain rate data.

The development of anion coordination chemistry and anion receptor molecules has made it possible to perform molecular catalysis on anionic substrate of chemical and biochemical interest, such as adenosine

triphosphate(ATP). [24]-N<sub>6</sub>O<sub>2</sub> **68** was found to bind ATP strongly and markedly accelerate its hydrolysis to ADP over a wide PH range<sup>6</sup>. The reaction shows first-order kinetics and is catalytic with turnover. Initial formation of a complex between protonated **68** and ATP was followed by an intramolecular reaction as shown in Fig. 50.



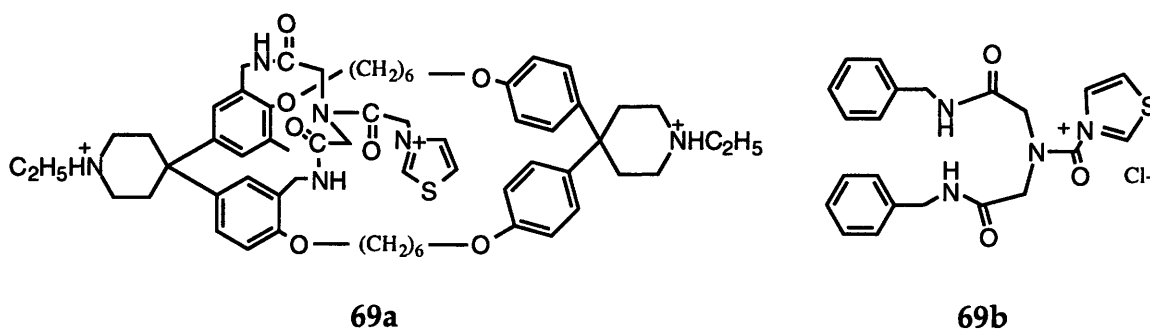
**Fig.50** The catalysis of ATP hydrolysis by **68**.

### 4.3 Cyclophane

The hydrophobic interaction is one of the most important driving forces of molecular recognition in aqueous media. Cyclophanes with a sizable cavity provide good hydrophobic binding sites. This macrocyclic cavity generally provides a stable binding site which is scarcely affected by external factors such as pH, temperature, and ionic strength. A wide synthetic variation of the macrocycles is also possible, so that an appropriate recognition site with regard to size, shape, and microenvironmental property is provided for a target guest molecule. In addition, distinct molecular

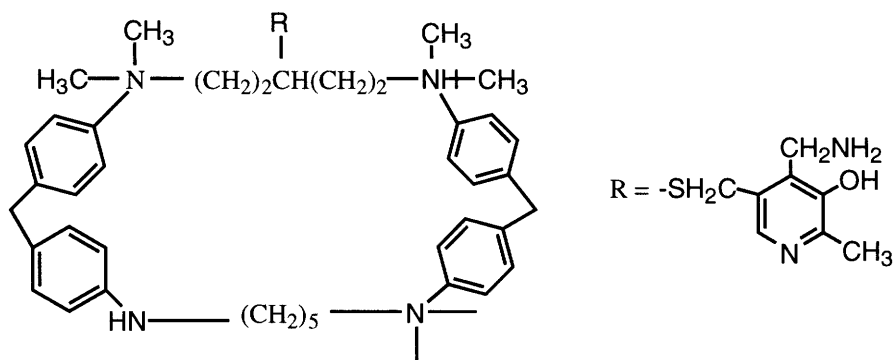
discrimination can be achieved by the introduction of functional groups into appropriate sites of cyclophanes giving additional noncovalent interactions such as electrostatic, hydrogen bonding, charge transfer and metal-coordination interaction.

Diederich et al. studied the benzoin condensation mediated by a thiazolium salt covalently linked to a cyclophane **69a**<sup>7-9</sup>. Molecule **69a** catalyzed the benzoin condensation with turnover behavior more effectively than nonmacrocyclic thiazolium derivative **69b**.



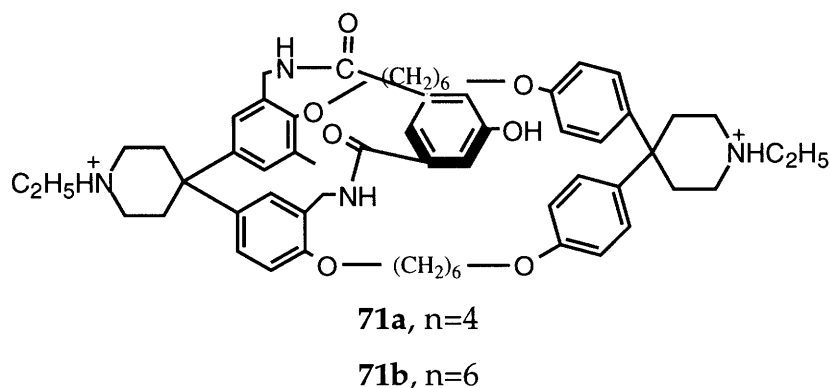
Breslow et al. prepared an cyclophane having a substrate-binding site composed of a tetraaza[1.7.1.7]paracyclophane ring and a covalently bound pyridoxamine moiety **70**<sup>10</sup>. In 2.7 M phosphate buffer at PH 9.3 and 26°C, **70** accelerated the conversion of aromatic  $\alpha$ -keto acids bearing good hydrophobic segments to the corresponding  $\alpha$ -amino acids by more than 1 order of magnitude as compared with the rates for reactions catalyzed by pyridoxamine. The acceleration factors were 31 and 12 for phenyl pyruvic acid and indole pyruvic acid, respectively, while the factor was 6 for  $\alpha$ -ketovaleric

acid. Compound **70** could perform only half of the transamination reactions and a true catalytic cycle was not observed.



**70**

Diederich et al. prepared cyclophanes **71** possessing the phenolic hydroxyl group as a nucleophile positioned in a well defined way atop the macrocyclic binding site<sup>11</sup>. Both macrocycles form complexes of similar stability with naphthalene guests in aqueous solution. In aqueous phosphate buffer at pH 8.0 and 20°C, the acylation of **71a** by the naphthyl ester is only 14 times faster than the hydrolysis in pure buffer, while **71b** shows 178 times the rate of pure buffer.



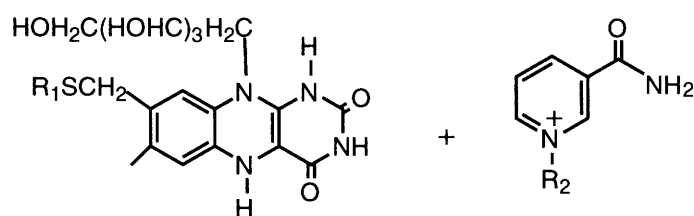
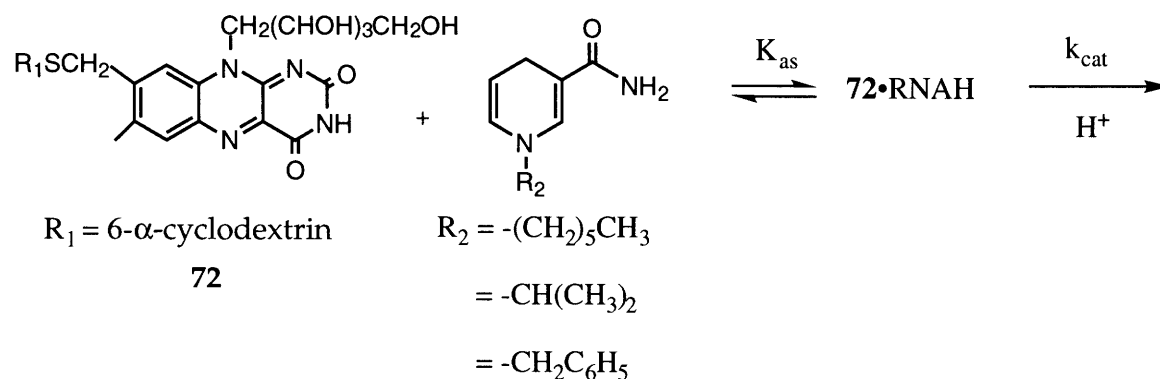
For the acyl transfer, **71b** shows saturation kinetics while **71a** follows second order kinetics . Only **71b** forms a productive complex with a favorable proximity between the phenolic hydroxy group and the substrate carbonyl group. The smaller host **71a** also forms a stable complex with the naphthyl ester. In this complex, the phenol ring completely blocks one side of the cavity. The ester residue of the guest extends in a non-productive manner out of the cavity on the opposite side to the nucleophile and undergoes an intermolecular reaction with the phenol group of another host molecule.

#### 4.4 Cyclodextrins

Cyclodextrins as enzyme models were first reported by the research group of Bender<sup>12,13</sup>, then taken up by others such as Breslow<sup>14-16</sup>, Tabushi<sup>17</sup> and others<sup>18,19</sup> . Modified cyclodextrins were later developed by introducing catalytically active groups selectively into the functions provided the primary or the secondary hydroxyl groups.

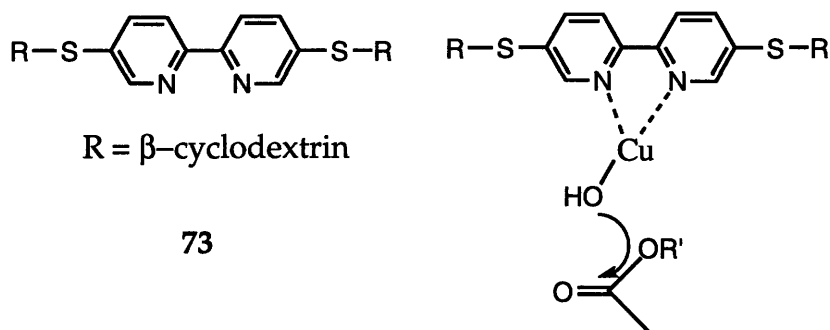
Tabushi et al. prepared a flavo- $\alpha$ -cyclodextrin **72** in which flavin segment is bound to the primary rim of  $\alpha$ -cyclodextrin<sup>20</sup> . Compound **72** binds to N-alkyldihyronicotinamides(RNAH) with large binding constants( $K_a$ ) of 1050, 260, and 2500  $M^{-1}$  for benzyl, isopropyl and n-hexylNAH, respectively, although these are smaller than binding to an artificial flavoprotein, 8 $\alpha$ -S-flavopapain. The overall efficiencies of **72** in dihydroflavin production, as

evaluated by  $k_{\text{cat}}K_{\text{as}}$  were 63, 94 and  $1200\text{M}^{-1}$  with benzyl, isopropyl, and n-hexyl-NAH, respectively ; the first value being larger than that for 8 $\alpha$ -S-flavopapain with benzyl-NAH by 56 times.



**Fig. 51** The catalysis of electron transfer reaction from RNAH to the flavin moiety of 72.

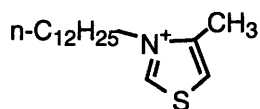
Breslow and Zhang<sup>21,22</sup> prepared a  $\beta$ -cyclodextrin dimer 73 which can bind metal ions with its linker segment. With ester substrates that are bound to 73 with the two cyclodextrin cavities so as to place the ester group next to the metal ion, catalytic hydrolysis was observed to take place with good turnover and a very large rate acceleration. The mechanism involves attack by metal hydroxide species in a manner as proposed with many metalloenzymes.



#### 4.5 Micelles

Micelles are cited as traditional molecular assemblies and can be classified as two categories with regard to the nature of their cores, hydrophobic or hydrophilic. Simulation of enzyme functions has been carried out by utilizing the former type which furnish hydrophobic binding sites in aqueous media.

Tagaki et al. prepared a thiazolium salt bearing an alkyl chain such as N-dodecylthiazolium bromide **74** which forms micelles<sup>23,24</sup>. The H/D exchange rate at the 2-position of **74** was 16 fold faster than that of a nonmicelle forming 3-methyl analog. The high acidity of 2-H proton of thiazolium ring promoted an acyloin condensation of aldehydes, such as benzaldehyde and furfural upon micelle formation.



74

A few examples of Diels-Alder cycloadditions are reported in micellar medium. Singh et al. studied the Diels-Alder reaction of

cyclopentadiene derivatives and quinone derivatives with cetyltrimethylammonium bromide(CTAB).<sup>25</sup> The reaction rate was at least four times faster than conventional Diels-Alder reaction condition like refluxing in toluene and gave better yield. It may be ascribed to the increased concentration of reactants in the core of micellar phase where reactants are more ordered compared to their homogeneous counterpart.

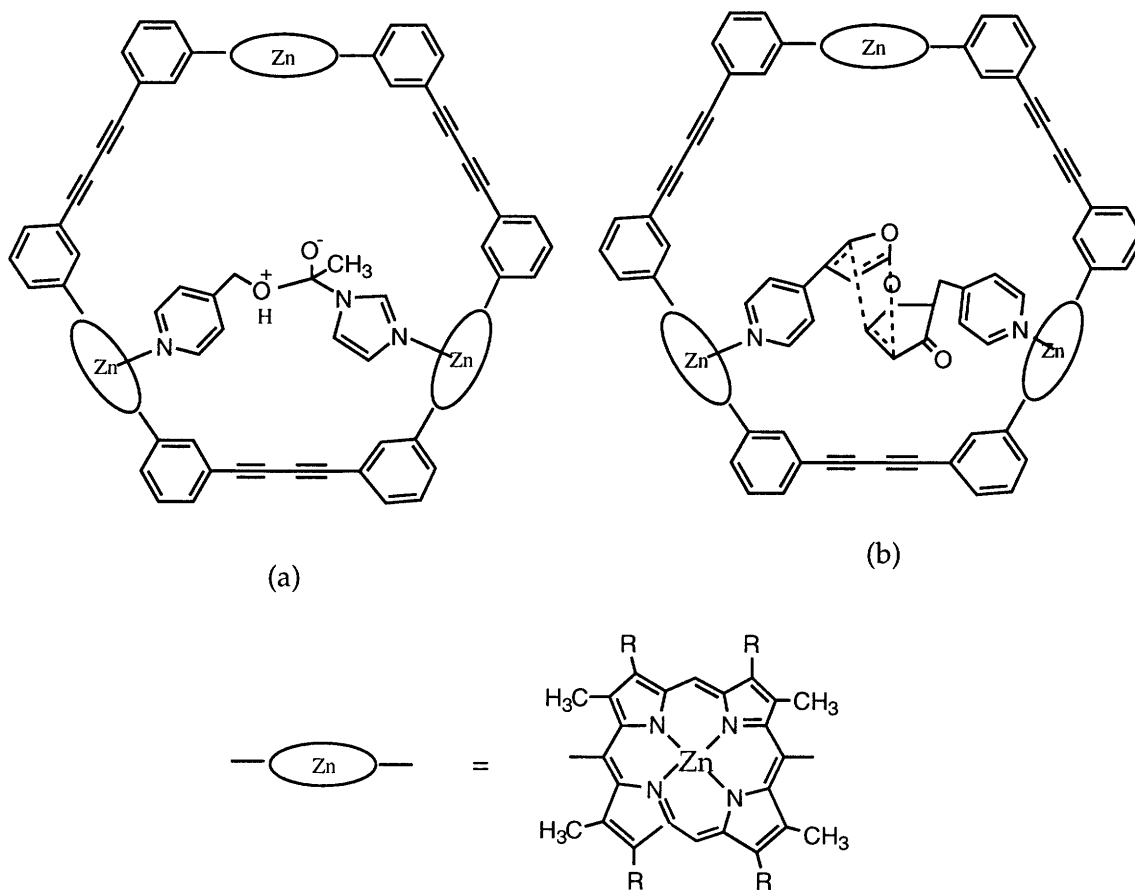
#### 4.6 Template effect by metal-ligand interaction

Sanders and his coworkers created cyclic porphyrin trimer in which convergent binding sites are positioned in such a way that substrate molecules can be held in close proximity through metal-coordination interactions<sup>26</sup>. An acyl transfer reaction of N-acetylimidazole with 4-(hydroxymethyl)pyridine in dry toluene solution at 70°C was effectively catalyzed by porphyrin trimer. This showed turnover behavior via formation of a tetrahedral intermediate doubly bound to the inside the cavity of the trimer (Fig.52) This cyclic porphyrin trimer increased the initial rate by some 16-fold relative to the uncatalyzed reaction.

They also examined a Diels-Alder reaction between a furan derived diene and a maleimide-derived dienophile, both having a pyridine moiety as a ligand to Zn(II) ions(Fig.52)<sup>27-29</sup>. In the absence of any host, the reaction afforded two products, the kinetically favored endo-adduct and the thermodynamically favored exo-adduct in C<sub>2</sub>H<sub>2</sub>Cl<sub>4</sub>. Addition of one



equivalent amount of trimer to the two reactants resulted in acceleration of the forward Diels-Alder reaction by ca. 1000-fold at 30°C and 200-fold at 60°C yielding an exo adduct as the only detectable product. On the basis of the kinetic analysis of the reaction, they claimed that the observed positive templating effect is partly due to increase of concentration of diene and dienophile within the host cavity and partly due to a reduced activation energy caused by preliminary binding of reacting species.

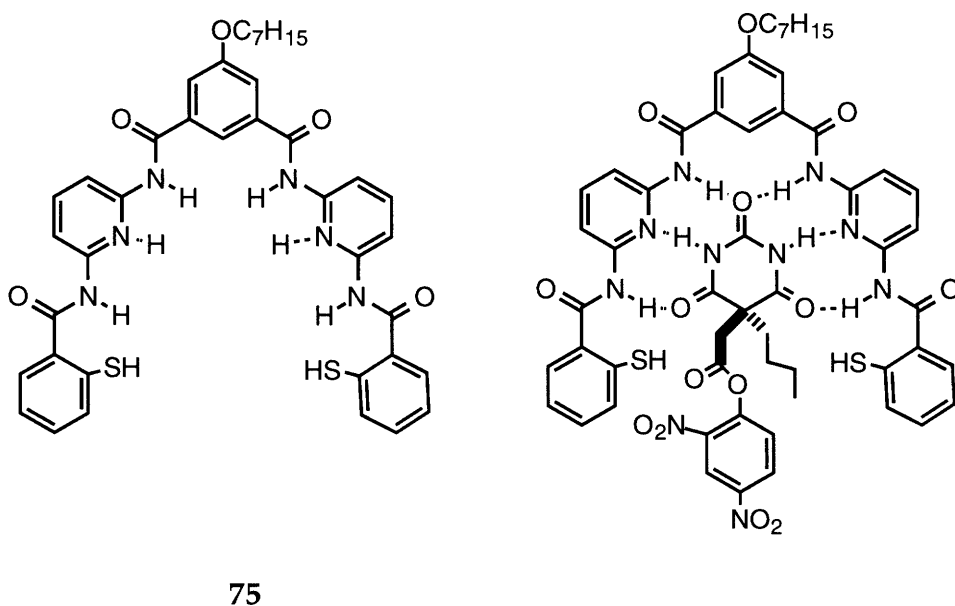


**Fig. 52** (a) The catalysis of an acyl transfer reaction by a porphyrin trimer (b) The catalysis of a Diels-Alder reaction by a porphyrin trimer.

## 4.7 Hydrogen bonding

Artificial receptors capable of recognizing a guest species through multiple hydrogen-bonding interaction with highly directional character were also utilized as enzyme mimics.

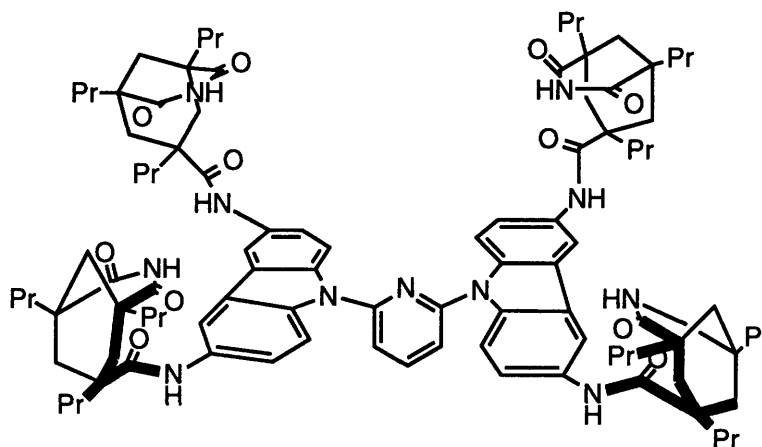
Hamilton et al. prepared receptor **75** that strongly bound barbiturate esters through six hydrogen bonds (Fig.53) and **75** accelerated the ester cleavage in dichloromethane at 25°C by the thiol nucleophile of the receptor placed close to the carbonyl group of the guest. The rate acceleration was more than  $10^4$  when compared with the reaction by a simple thiol<sup>30</sup>.



**Fig. 53** Effective binding of a barbiturate ester by **75** catalyze ester cleavage.

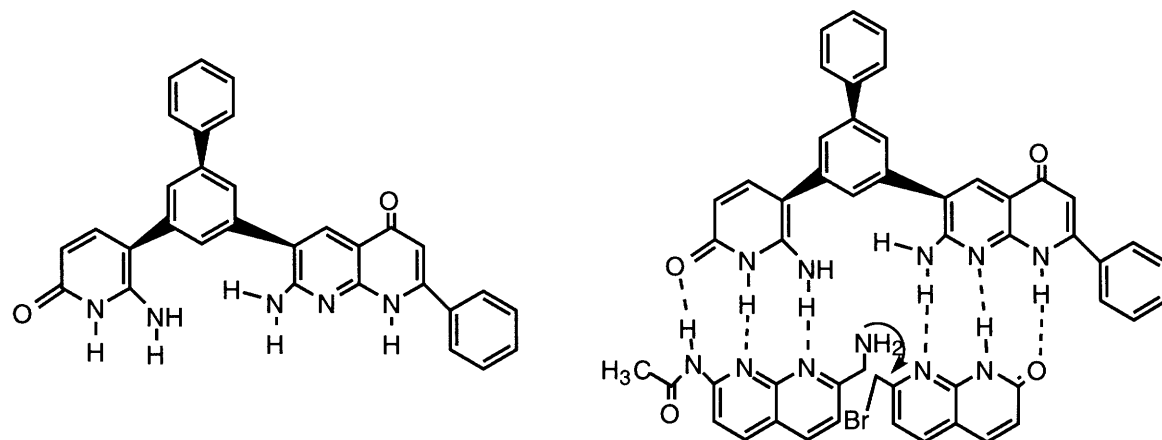
Rebek et al. examined a template effect furnished by synthetic receptors derived from Kemp's triacid in aminolysis of p-nitrophenyl ester with aminoadenosine<sup>31</sup>. They observed a receptor **76** accelerated the reaction

160-fold via formation of a termolecular complex composed of the receptor and two kinds of the substrate.



76

Kelly et al. prepared a reaction template **77** which was designed to use hydrogen-bonding interactions to bind two substrates simultaneously, resulting in the formation of a ternary complex<sup>32</sup>. They studied the Sn2 alkylation of an amine by an alkyl halide in  $\text{CDCl}_3$  at  $26^\circ\text{C}$  and showed that **77** accelerated the reaction by 12-fold. The formation of a ternary complex is favored by complementary hydrogen-bonding interactions(Fig.54)



77

Fig. 54 Reactive ternary complex composed of 77 and two kinds of substrate

#### 4.8 Cavity

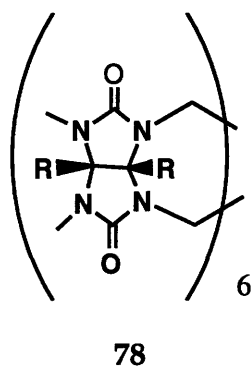
Artificial receptors with a cavity of appropriate size can bind two substrates at the same time, which increases the concentration of two reactant relative to that in the bulk solution. Consequently the reaction rate is increased. Even the transition state of the reaction can be stabilized inside the cavity, which could also result in rate enhancement of the reaction.

Breslow and his coworkers studied the Diels-Alder reaction of cyclopentadiene with butenone and acrylonitrile<sup>33</sup>. They suggested that the transition state of this reaction should be able to fit into the cavity of  $\beta$ -cyclodextrin but not in the smaller cavity of  $\alpha$ -cyclodextrin. Indeed, The two reactions are both 2 ~ 10 times faster when 10 mM  $\beta$ -cyclodextrin is added to the water but slower with 5 or 10mM  $\alpha$ -cyclodextrin. It is not clear whether

the cavity of  $\beta$ -cyclodextrin really stabilizes the transition state but it is clear that catalysis of these Diels-Alder reaction comes from mutual binding of reagents into a cyclodextrin cavity as evidenced by  $\alpha$ -cyclodextrin.

Dessau showed that the Diels-Alder reaction of 1,3-butadiene to 4-vinylcyclohexene is catalyzed by zeolites<sup>34</sup>. The rate of reaction is increased by 2 ~ 200 times depending on zeolite and large pore zeolites are more effective in their rate enhancements. He ascribed this effect to the ability of zeolites to concentrate hydrocarbons within their cavities. He also suggested that the greater effectiveness of large pore zeolites is due to the greater space available within their cavities for the proper alignment of the reactant molecules.

Mock et al. investigated the 1,3-dipolar cycloaddition of alkynes (propargylamine or N-tert-butyl-propargylamine), to an azide (azidoethylamine or N-tert-butylazidoethylamine) to afford the corresponding triazole derivative<sup>35</sup>. This was catalyzed by a polycyclic molecular receptor, cucurbituril **78**, in aqueous formic acid at 40°C.



They found that a catalytic amount of **78** accelerated the reaction  $10^5$  times regioselectively, yielding only the 3,5-disubstituted triazole as a product. This stereospecificity was attributed to the formation of a transient ternary complex between **78** and the substrates. Simultaneous binding of both substrates aligns the reactive groups within the core of **78** so as to facilitate production of triazole. The reaction was claimed to be enhanced by strain-induced compression between these substrates incorporated into the three-dimensionally restricted cavity.

#### 4.9 References

- 1)Lehn, J. M. *Angew. Chem. Int. Ed. Engl.* **1988**, *27*, 89.
- 2)Nagano, O.; Kobayashi, A.; Sasaki, Y. *Bull. Chem. Soc. Jpn.* **1978**, *51*, 790.
- 3)Chao, Y.; Weisman, G. R.; Sogah, G. D. Y.; Cram, D. J. *J. Am. Chem. Soc.* **1979**, *101*, 4948.
- 4)Lehn, J.-M.; Sirlin, C. *New J. Chem.* **1987**, *11*, 693.
- 5)Sasaki, S.; Koga, K. *Heterocycles* **1979**, *12*, 1305.
- 6)Hosseini, M. W.; Lehn, J.-M.; Maggiora, L.; Mertes, K. B.; Mertes, M. P. *J. Am. Chem. Soc.* **1987**, *109*, 537.
- 7)Diederich, F. *Frontiers in Supramolecular Organic Chemistry and Photochemistry*; VCH: Weinheim, 1991.
- 8)Jimenez, L.; Diederich, F. *Tetrahedron Lett.* **1989**, *30*, 2759.
- 9)Lutter, H.-D.; Diederich, F. *Angew. Chem. Int. Ed. Engl.* **1986**, *25*, 1125.
- 10)Winkler, J.; Leppkes, R.; Breslow, R. *J. Am. Chem. Soc.* **1983**, *105*, 7198.
- 11)Diederich, F.; Scvhurmann, G.; Chao, I. *J. Org. Chem.* **1988**, *53*, 2744.
- 12)Bender, M. L.; Komiyama, M. *Cyclodextrin Chemistry*; Springer-Verlag: Berlin, 1978.
- 13)D'Souza, V. T.; Bender, M. L. *Acc. Chem. Res.* **1987**, *20*, 146.
- 14)Breslow, R. *Science* **1982**, *218*, 532.
- 15)Breslow, R. *Adv. Enzymol. Relat. Areas Mol. Biol.* **1986**, *58*, 1.
- 16)Breslow, R. *Pure Appl. Chem.* **1990**, *62*, 1859.
- 17)Tabushi, I. *Acc. Chem. Res.* **1982**, *15*, 66.
- 18)Saenger, W. *Angew. Chem. Int. Ed. Engl.* **1980**, *19*, 344.

- 19)Saenger, W.; Atwood, J. L.; Davis, J. E. L.; Macnicol, D. D. *Inclusion compounds*; Academic Press: London, 1984; Vol. 2.
- 20)Tabushi, I. ; Kodera, M. *J. Am. Chem. Soc.* **1987**, *109*, 4734.
- 21)Breslow, R.; Zhang, B. *J. Am. Chem. Soc.* **1992**, *114*, 5882.
- 22)Breslow, R.; Zhang, B. *J. Am. Chem. Soc.* **1994**, *116*, 7893.
- 23)Tagaki, W.; Hara, H. *J. Chem. Soc. Chem. Com.* **1973**, 891.
- 24)Tagaki, W.; Tamura, Y.; Yano, Y. *Bull. Chem. Soc. Jpn.* **1980**, *53*, 478.
- 25)Singh, V. K.; Raju, B. N. S.; Deota, P. T. *Syn. Comm.* **1988**, *18(6)*, 567.
- 26)Mackay, L. G.; Wylie, R. S.; Sanders, J. K. M. *J. Am. Chem. Soc.* **1994**, *116*, 3141.
- 27)Walters, C. J.; Sanders, J. K. M. *Angew. Chem. Int. Ed. Engl.* **1995**, *116*, 5667.
- 28)Bonar-Law, R. P.; Mackay, L. G.; Walter, C. J.; Marvaud, V.; Sanders, J. K. *M. Pure Appl. Chem.* **1994**, *66*, 803.
- 29)Anderson, H. L.; Anderson, J. K. M. *J. Chem. Soc. Chem. Comm.* **1989**, 1714.
- 30)Tecilla, P.; Hamilton, A. D. *J. Chem. Soc. Chem. Comm.* **1990**, 1232.
- 31)Huc, I.; Pieters, R. J.; Rebek, J. Jr. *J. Am. Chem. Soc.* **1994**, *116*, 10296.
- 32)Kelly, T. R.; Bridger, G. J.; Zhao, C. J. *J. Am. Chem. Soc.* **1990**, *112*, 8024.
- 33)Rideout, D. C.; Breslow, R. *J. Am. Chem. Soc.* **1980**, *102*, 7816.
- 34)Dessau, R. M. *J. Chem. Soc. Chem. Comm.* **1986**, 1167.
- 35)Mock, W. L.; Irra, T. A.; Wepsiec, J. P.; Adhya, M. *J. Org. Chem.* **1989**, *54*, 5302.



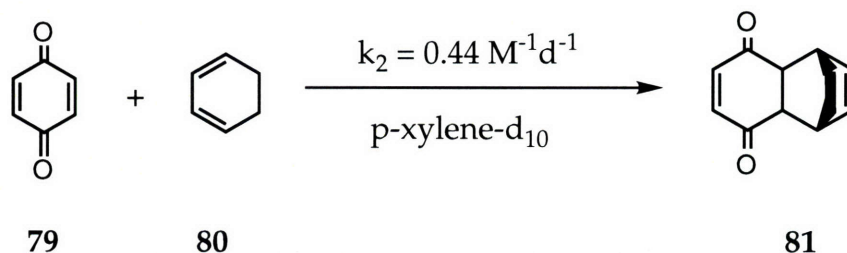
## Chapter 5. Acceleration of a Diels-Alder Reaction by a Self-Assembled Capsule **42**

### 5.1 Introduction

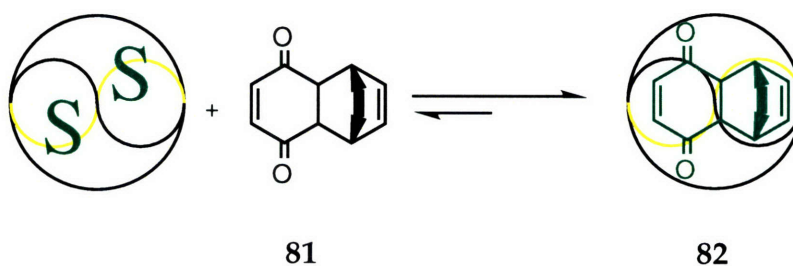
Compound **42** self-assembles in organic solvents to form dimeric capsules. The molecules feature self-complementary patterns of hydrogen bonding sites and a dimeric form emerges when the concave surfaces of two molecules come together. The intermolecular hydrogen bonds hold the two subunits together in much the same manner that the stitches along the seam of a dimeric **42** hold its halves together. In aromatic solvents such as benzene, the dimerization constant is large ( $> 10^6 \text{ M}^{-1}$ ) and the dynamics of assembly are slow on the NMR timescale but fast on the human timescale ( $< \text{seconds}$ ). The dimers can encapsulate molecules of complementary size and shape and do so reversibly. Adamantanes, ferrocene derivatives and [2,2] paracyclophane are among the sizable guests that fit snugly within these capsules. The observation that **two** molecules of solvent benzene are accommodated inside, raises the possibility of the use of these capsules as chambers for bimolecular reactions such as the Diels-Alder reaction. As two benzene shaped molecule seems to be inside, Diels-Alder reactions with two benzene shaped diene and dienophile were selected.

## 5.2 Diels - Alder reaction inside the dimeric capsule 42

The specific Diels-Alder reaction initially examined was that of quinone **79** with cyclohexadiene **80**, which leads to the endo product **81**. The reaction is conveniently slow at room temperature: in p-xylene-d<sub>10</sub> at millimolar concentrations no product is detected by NMR in a week; at molar concentrations a half-life of about two days can be observed ( $k_2 = 0.44$  liters mol.<sup>-1</sup>days<sup>-1</sup>).

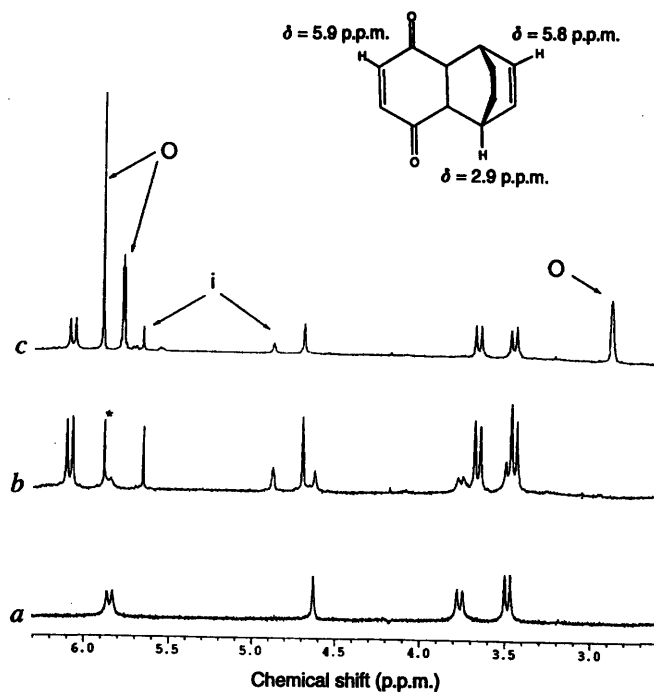


In dilute solution, (e. g. 1 mM) the Diels-Alder adduct **81** is nicely encapsulated by the dimeric **42** (Fig. 55), and NMR signals unique to the encapsulated species **82** can be observed (Fig.56b). The widely separated and relatively sharp signals for the free and bound species indicate slow exchange of the guest into and out of the host capsule (Fig. 56c).



**Fig. 55** Encapsulation of the Diels-Alder adduct by the softball.

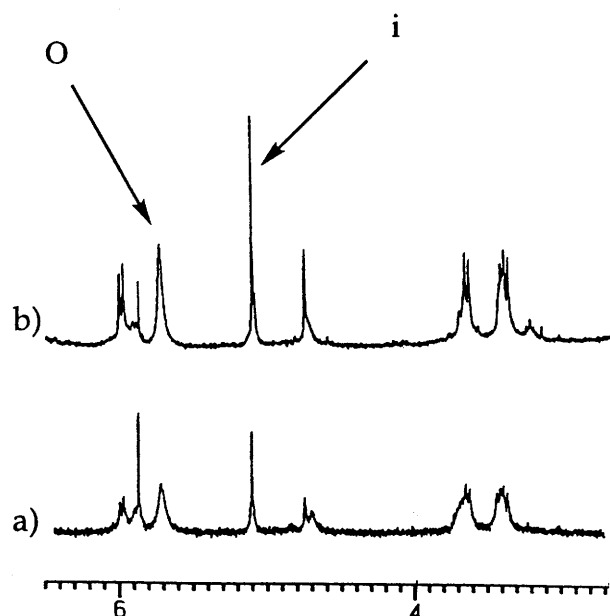
The adduct is an excellent guest; the binding affinity is too large for accurate NMR titrations, and only an estimate ( $K_a = > 10^5 \text{ M}^{-1}$ ) can be made for the association constant.



**Fig.56**  $^1\text{H}$  NMR spectra of **42-42** and its encapsulation complex with the adduct **81** in *p*-xylene- $\text{d}_{10}$ . Signals of the guest inside the capsule and the outside are labeled with "i" and "o", respectively. The signal designated with an asterisk represents chloroform impurity. (a) Compound **42-42** alone (b) Compound **42-42** with 0.7 equiv. of Diels-Alder adduct **81** added ; all of the latter is encapsulated and separate signals are observed for the complex **82** and solvated dimer **42-42** (c) Compound **42-42** with 6 equiv. of Diels-Alder adduct **81** added ; all of the capsule is occupied as complex **82** and separate signals are observed for free and encapsulated adduct **81**. Assignments for resonances of free **81** are shown on the structure.

At millimolar concentrations *p*-quinone alone forms a well-defined complex with the dimer. A new signal for encapsulated quinone can be observed in the spectrum and integration of this signal indicates nearly two equivalents of quinone are inside each capsule (Fig. 57).

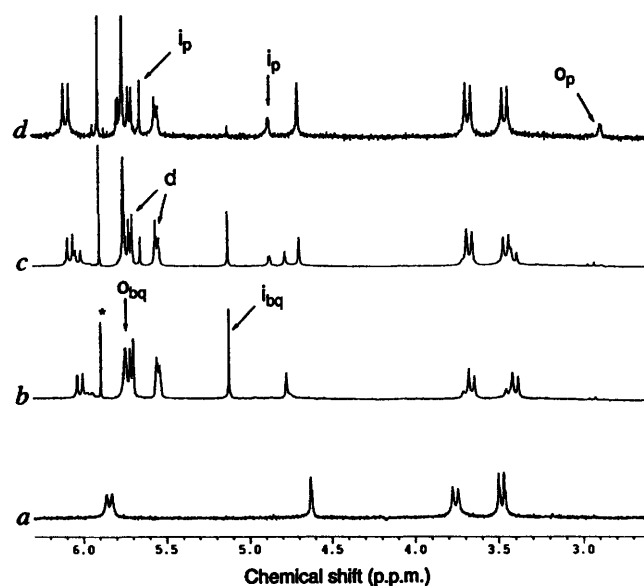
The broadening of the spectrum may be due to intermediate rates of exchange of this guest in and out of the capsules. Lowering the temperature to 0° C (the freezing point of the solution) failed to sharpen the spectra; heating gave somewhat improved resolution of the capsule's signals, while the signal for the free quinone broadened in accord with a classical exchange process. Another cause for the broadening of the spectrum may be the presence of several encapsulated species. The chemical shift differences between the new species and those capsules filled with solvent are small, and



**Fig. 57**  $^1\text{H}$  NMR spectra of **42-42** in the presence of (a) 2 equiv. of p-benzoquinone (b) 4 equiv. of p-benzoquinone. Quinone inside and outside are labeled with "i" and "o", respectively.

broadening may result from the superimposition of the somewhat overlapped spectra. Free quinone is the right size, shape and functionality to complement the hydrogen bond donors at the ends of **42**, and could compete with the assembly of the dimeric form. At the same concentrations

cyclohexadiene alone has little effect on the spectrum of **42**; a slight broadening is observed but no signals attributable to encapsulated cyclohexadiene can be distinguished. Apparently cyclohexadiene alone is unable to compete with solvent to form complexes with the dimeric form. When both paraquinone and cyclohexadiene (4 mM each) are exposed to the dimeric capsule (1 mM) in *p*-xylene- $d_{10}$  at room temperature, the spectra again show the characteristics of quinone encapsulation (Fig. 58b).

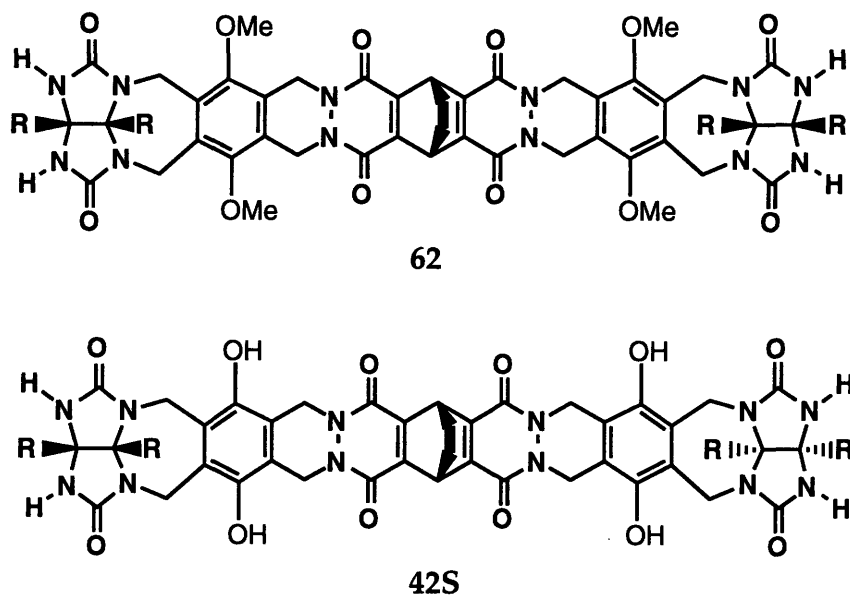


**Fig.58** Change in the  $^1\text{H}$  NMR spectra of **42-42** during the reaction of *p*-benzoquinone **79** and 1,3-cyclohexadiene **80** in *p*-xylene- $d_{10}$ . The signals for *p*-benzoquinone (bq) and Diels-Alder product (p) inside and outside are designated as "i" and "o", respectively. Signals from cyclohexadiene are designated as "d". The signal designated with an asterisk represents chloroform impurity. (a) Compound **42-42** alone (b) Shortly after 4 equiv. of *p*-benzoquinone and 4-equiv. of 1,3-cyclohexadiene were added to the solution of **42-42**. (c) The reaction mixture after 2 days. (d) The reaction mixture after 19 days, showing evidence of released product and **82** as the principal species.

This appears to be the dominant species and no signals unique to encapsulated cyclohexadiene can be assigned. Nonetheless, it must also be present inside, since the signal for the encapsulated adduct emerges within one day, and continues to grow at the expense of the encapsulated quinone (Fig 58c). At 60° C the corresponding changes take place within one hour. The reaction-under these conditions-is accelerated some 200-fold in the presence of **42**.

A number of factors including heat, pressure, acids, antibodies<sup>1</sup>, micelles<sup>2-5</sup>, medium<sup>6,7</sup> and template effects<sup>8</sup> are known to accelerate Diels-Alder reactions, and before reversible encapsulation is added to this list some assurance is required that the rate accelerations provided by **42** are due to encapsulation of the components, rather than some of the effects noted above. For example, carefully designed biphenylenediols<sup>9</sup> that can provide convergent hydrogen bonds to the carbonyl oxygens of some dienophiles, are known to be catalysts for this reaction, and as numerous hydrogen bonding sites are featured on the edges of **42**, control experiments were set up to test this possibility. Molecule **42S** presents the same functionalities as does **42** but it differs in shape: it is S-shaped (Fig. 59). Its ends are too far apart to grasp a quinone at both oxygen atoms with its glycoluril hydrogens. Molecule **62** does have the same shape and the grasping capability of **42** but differs in that the phenols are alkylated. This results in a structure which is prevented from dimerizing into a capsule. Neither **42S** nor **62** had any effect on the rate of the Diels-Alder reaction. Catalysis through hydrogen bonding to the phenols or

the glycoluril functions of a single molecule of **42** cannot be the source of rate acceleration. If this form of acid catalysis is available only within the capsule then there are no obvious controls that are likely to expose it.

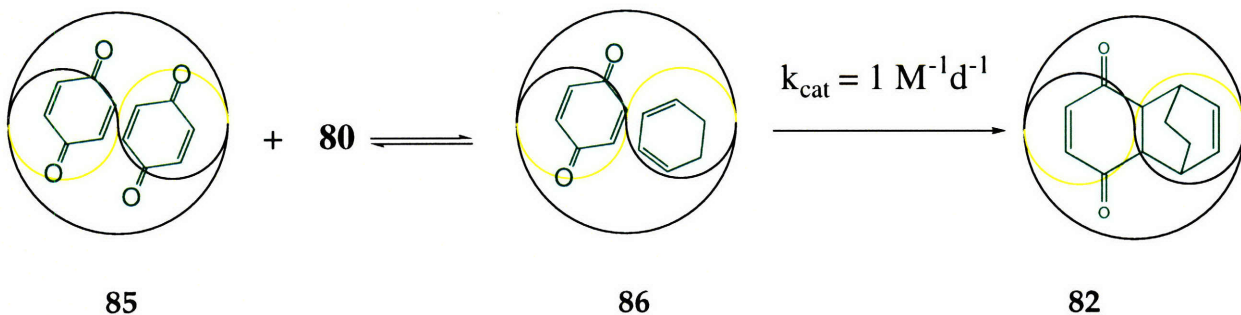


**Fig. 59** Phenol alkylation in **62** or change to an S-shape **42S** abrogates acceleration of the Diels-Alder reaction.

In addition, 1,4-naphthoquinone **83** (Fig. 60) and its reaction with cyclohexadiene was studied. The Diels-Alder adduct **84** forms at a background rate about half of that seen with quinone, as might be expected on statistical grounds. There were no spectroscopic changes when **83** was added to a solution of **42** and no acceleration of the reaction was observed in the presence of **42**. The naphthoquinone is too large a molecule to fit into the capsule, but could have been grasped by the monomeric form of **42**. Based on this admittedly limited sampling, we conclude that there is a size selectivity



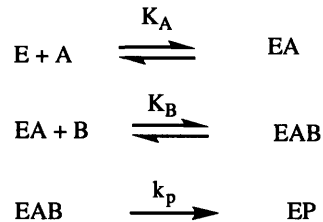




**Fig. 61.** The likely mechanism of the Diels-Alder reaction within the dimeric **42**.

After several days at ambient temperature some of the adduct appears outside the capsule, and in the longest run of 19 days some turnover was evident. Specifically, about 1 equiv. free adduct and 1 equiv. encapsulated adduct were present (starting with 4 equiv. each diene and dienophile and 1 equiv. capsule) as the reaction rate ground to a halt. (Fig. 58d).

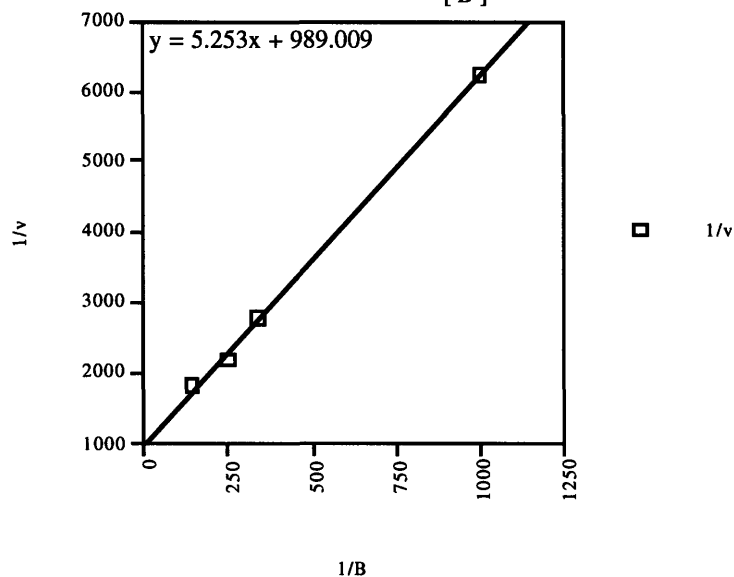
It is clear that product inhibition is the cause of this problem. Indeed, addition of adduct **81** or other good guests (benzene, [2,2] paracyclophane) effectively shuts down the reaction. From the considerations of entropy, the replacement of two reactants by one well-accommodated product is more reasonable than the reverse, and this prevents the system from turning over and offering true catalysis. Thus, product inhibition, size selectivity and saturation kinetics all support a reaction that takes place within the capsule.



E : softball    A: p-benzoquinone    B: 1,4-cyclohexadiene

$$\frac{1}{v} = \frac{K_B}{V_{\max}} \left( 1 + \frac{K_A}{[A]} \right) \frac{1}{[B]} + \frac{1}{V_{\max}}$$

plot  $\frac{1}{v}$  vs.  $\frac{1}{[B]}$



$$\frac{1}{V_{\max}} = 989 \quad V_{\max} = 0.00101 = k_p [E_t]$$

$$k_p = 1.01$$


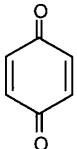
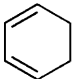
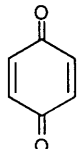

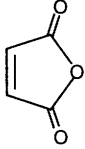
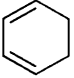
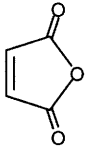
$$\text{Effective molarity} = k_p/k = 1.01/0.44 = 2.30$$

**Fig.62** Line-weaver Burke plot of the reaction rate,  $V$ , of 79 with 80 in the presence of 42-42. The concentration of 1,3-cyclohexadiene 80 were changed with a constant concentration(4mM) of p-benzoquinone.

Another line of reasoning, albeit indirect, is also consistent with the proposed acceleration through mere encapsulation, rather than some special stabilization of the transition state. This involves estimating the effective molarity (EM)<sup>10</sup> of the encapsulated reactants. Using a technique described elsewhere<sup>11</sup>, we calculate the interior volume of the capsule to be about 300 Å<sup>3</sup>; when it is occupied with one molecule each of quinone and cyclohexadiene, the concentration of the reactants inside is about 5 M - about a thousand times their concentration in the bulk solution (4 mM). When the first order rate within the capsule (*k*<sub>cat</sub>) is compared to the background bimolecular rate, an EM value of ~2.3 M is obtained, a figure similar to the calculated concentration inside. In other words, the acceleration provided by the capsule is comparable to the "pseudoconcentration" of reagents when they are trapped inside for some time. Notwithstanding the above, it is still uncomfortable with the use of EM's in this context. This treatment has been applied in the past to compare rates of bimolecular reactions with those of their strictly unimolecular counterparts, but this is not the case inside the softball. Somewhat closer in notion, but still inexact, are the many intracomplex reactions favored as enzyme models. In these, rate enhancements can be obtained through comparing reactions of the same molecularity, but reaching the transition state of an intracomplex reaction can be more difficult - by a large margin - than reaching the same point for a (reasonable) unimolecular model, and the enormous EM's seen for the latter

doubtless reflect this fact. The goings on in the capsule, wherein the translational freedom of the reactants is coupled, would seem to be an advantage especially if any reaction geometries are available to the pair.

Other diene dienophile pairs were briefly screened for their suitability as guests in the system. Quinone **79** consistently showed itself a willing reaction partner, a result that further reinforces the probability that its interactions with the interior of the capsule and the rate accelerations are inextricably entwined. The effective molarities and conditions for their calculations are given in the Table.7.

Diene	Dienophile	Temperature	k for control reaction	k <sub>p</sub> inside reaction softball = 1mM substrate = 4mM	effective molarity mol/l
		rt	0.25/mol•min 20 mM	0.7/min	2.8
		rt	0.41/mol•day 1M	1.01/day	2.46
		rt	5.13/mol•min 20mM	0.43/min	0.72
		rt	14.08/mol•day 20mM	7.63/day	0.54

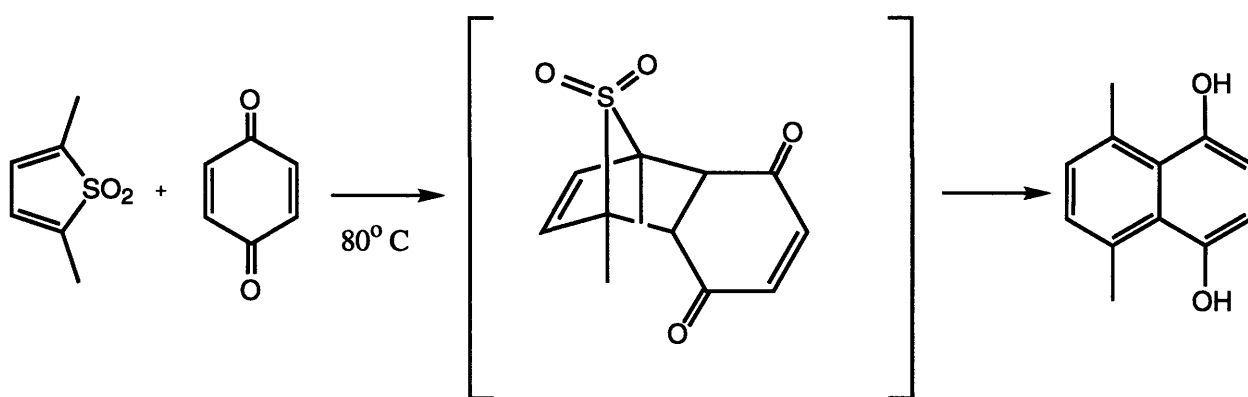
**Table. 7** Rate constant from controlled reaction and initial velocity study.

True catalysis via encapsulation can result if the size and shape selectivity can be extended to preferential recognition of transition states<sup>12,13</sup> or even high-energy intermediates. Dealing with the problem of product inhibition will always be an issue for associative processes but could be avoided in future applications by using dissociative processes, i. e., reactions that result in an increased number of encapsulated species<sup>14</sup>. In the meantime, the results here augur well for the application of reversibly-formed molecular assemblies as reaction chambers.

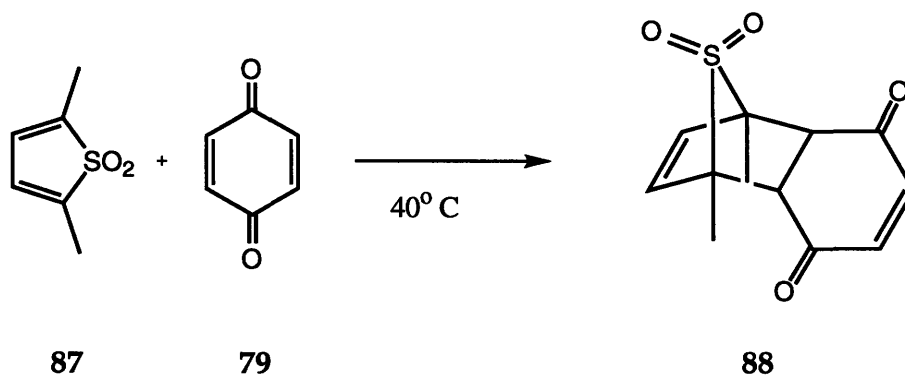
#### **5.4 Turnover in the catalysis of the Diels-Alder reaction by encapsulation**

Because product inhibition prevented true catalysis in above case, a system where turnover can be expected was sought. A reaction in which the initial Diels-Alder reaction is followed by a fragmentation was used with brilliant success by Hilvert in the study of catalytic antibodies<sup>1</sup>. The fragmentation leads to a change in the shape of the product that then escapes the antibodies. It is reasonable to expect that such a change of shape would lead to a product that is no longer accommodated within the molecular capsule.

The reaction involves p-benzoquinone **79** and 2,5-dimethylthiophene dioxides **87** and their adducts **88**. When a large excess of the former is present and high temperatures are used, the initial adduct loses SO<sub>2</sub> and aromatizes<sup>15</sup>. Further oxidation to the naphthoquinone can be observed.

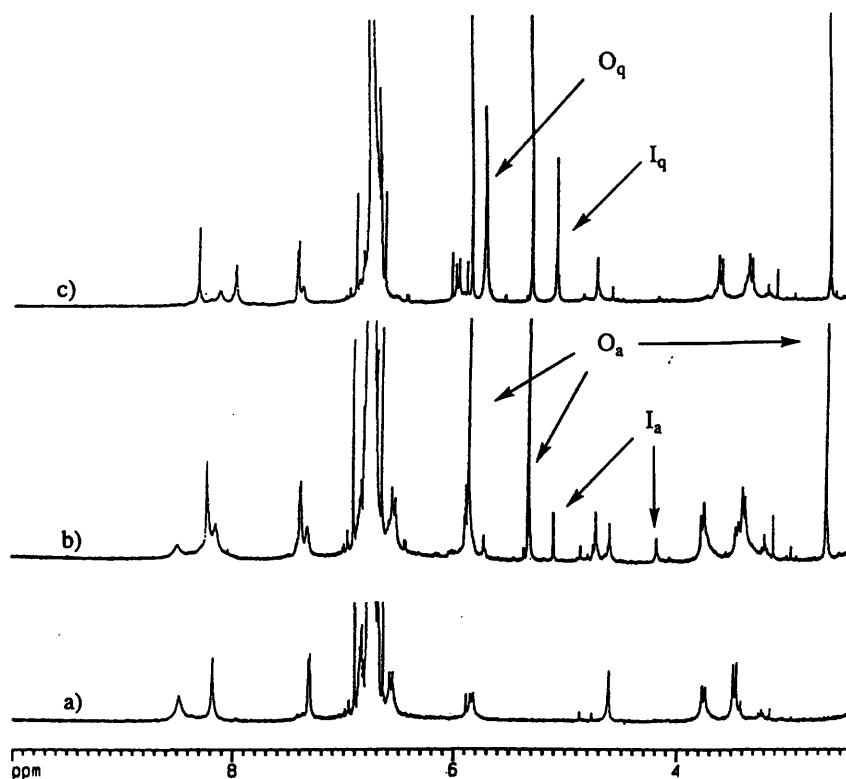


At lower temperatures, however, the initial adduct can be isolated, the product is reasonably stable.



Studies of the encapsulation of this in p-xylylene-d<sub>10</sub> show that it is a poor guest for the "softball" (Fig.63b). The association constant is 155 M<sup>-1</sup>, a number more than an order of magnitude lower than observed for adamantane or ferrocene

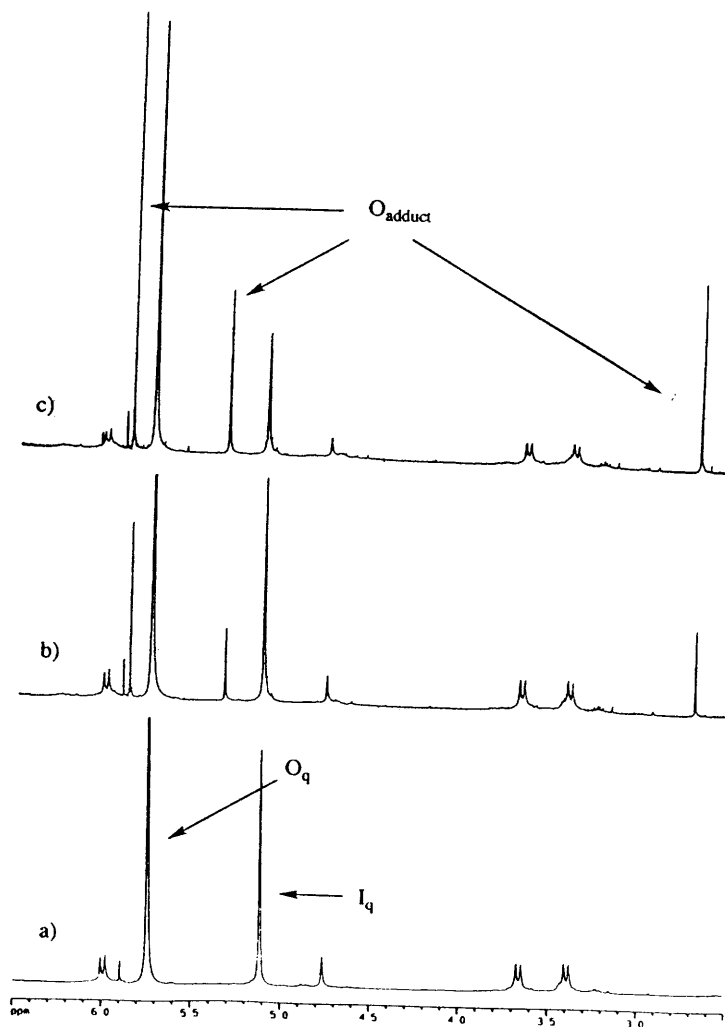
under these conditions.<sup>6</sup> Nonetheless, the resonances for free and encapsulated adduct can be assigned. Moreover, the adduct is driven out of the softball by the relatively good guest *p*-benzoquinone.



**Fig. 63**  $^1\text{H}$  NMR Spectra of 42-42 and its encapsulation complex with adduct 86 in *p*-xylene- $\text{d}_{10}$ . Signals of guest inside the capsule and outside are labeled with "i" and "o", respectively. a) compound 42-42 alone b) compound 42-42 with 8.4 equiv. of Diels-Alder adduct 86 added c) 7 equiv. of *p*-benzoquinone was added to the solution of (b)

Figure. 63c shows that two molecules of *p*-benzoquinone readily displace the adduct at convenient NMR concentrations of 7 millimolar. The corresponding binding studies with the thiophene dioxide showed a much

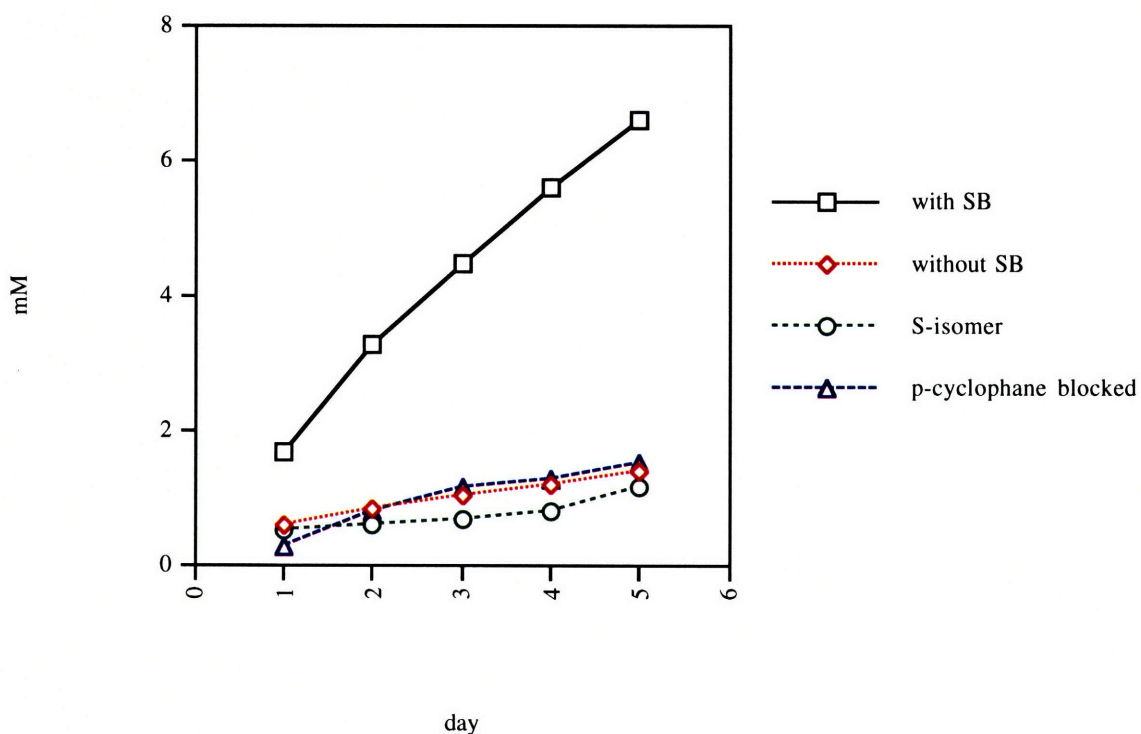
reduced affinity. In the experiment, solutions of diene (8 mM) and dienophile (16 mM) in *p*-xylene- $d_{10}$  solvent were exposed to the softball (1mM)(Fig.64).



**Fig. 64** Change in the proton NMR spectra of **42-42** during the reaction of *p*-benzoquinone **79** and 2,5-dimethylthiopene dioxide **85** in *p*-xylene- $d_{10}$ . The signals for *p*-benzoquinone (q) and Diels-Alder adduct **86** inside and outside are designated as 'i' and 'o' respectively. Signals from 2,5-dimethylthiopene dioxide were overlapped with signals from *p*-benzoquinone inside. a) shortly after 16 equiv. of *p*-benzoquinone and 4 equiv. of 2,5-dimethylthiopene dioxide were added to the solution of **42-42** b) The reaction mixture after 1 day. c) The reaction mixture after 4 days.

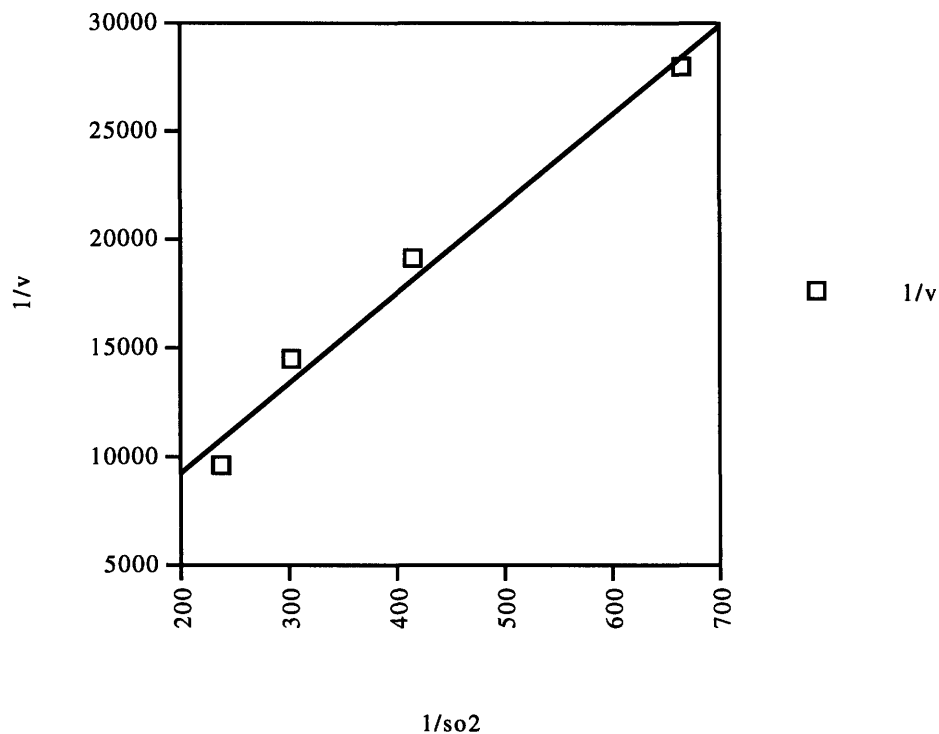


The reaction was monitored by NMR and control experiments were performed a) without the softball present, b) with the corresponding S-shaped isomer present and c) with 2-2 paracyclophane present in addition to the dimeric **42**. The S-shaped isomer bears all of the functionalities but does not assemble, whereas the paracyclophane is an excellent guest and is expected to compete with the reaction components for the encapsulation. The results are graphed in Fig. 65 which show the expected inhibition by paracyclophane and lack of catalysis by the control systems.



**Fig.65** The conversion rate to the Diels-Alder adduct **86** with compound **42-42**, without compound **42-42**, S-shaped isomer and compound **42-42** blocked with p-cyclophane.

That true catalysis takes place is shown by the fact that six turnovers are observed in the presence of the softball under the concentrations shown. In addition, reactions in which the thiphenedioxide concentration was varied showed saturation behavior, and the Lineweaver-Burk plot is shown in Fig. 66.



**Fig. 66** Lineweaver-Burk plot of the reaction rate of 79 and 85 in the presence of 42-42. The concentration of 2,5-dimethylthiopene dioxide were changed with constant concentration of p-benzoquinone.

The rate enhancements observed allow an effective molarity of approximately 2.4 to be calculated for the rate enhancement inside the softball. The observed rate enhancement is, of course, a function of conditions. For example, at 16 mM benzoquinone and the other conditions of the graph, a 8-fold increase in rate based on half life was observed. At lower concentrations, the increase in rate is enhanced accordingly. While the catalysis is still modest, the present result gives new promise for the use of molecular capsules as reaction chambers.

## 5.5 References

- 1) Hilvert, D.; Hill, K. W.; Auditor, M. T. M. *J. Am Chem Soc.* **1989**, *111*, 9261.
- 2) Grieco, P. A.; Garner, P.; He, Z.-M. *Tetrahedron Lett.* **1983**, *24*, 1897.
- 3) Breslow, R.; Maitra, U.; Rideout, D. *Tetrahedron Lett.* **1983**, *24*, 1901.
- 4) Braun, R.; Schuster, F.; Sauer, J. *Tetrahedron Lett.* **1986**, *27*, 1285.
- 5) Singh, V. K.; Raju, B. N. S.; Deota, P. T. *Syn. Comm.* **1988**, *18(6)*, 567.
- 6) Grieco, P. A.; Kaufman, M. D.; Daeuble, J. F.; Saito, N. *J. Am. Chem. Soc.* **1996**, *118*, 2095.
- 7) Breslow, R.; Guo, T. *J. Am. Chem. Soc.* **1988**, *110*, 5613.
- 8) Walter, C. J.; Anderson, H. L.; Sanders, J. K. M. *J. Chem. Soc. Chem. Comm.* **1993**, 458.
- 9) Kelly, T. R.; Meghani, P.; Ekundi, V. S. *Tetrahedron Lett.* **1990**, *31*, 3381.
- 10) Kirby, A. J. *Adv. Phys. Org. Chem.* **1980**, *17*, 183.
- 11) Meissner, R.; Garcias, X.; Mecozzi, S.; Rebek, J. Jr. *J. Am. Chem. Soc.* , in press.
- 12) Mock, W. L.; Irra, T. A.; Wepsiec, J. P.; Adhya, M. *J. Org. Chem.* **1989**, *54*, 5302.
- 13) McCurdy, A.; Jimenez, L.; Stauffer, D. A.; Dougherty, D. A. *J. Am. Chem. Soc.* **1992**, *114*, 10314.
- 14) Cram, D. J.; Tanner, M. E.; Thomas, R. *Angew. Chem. Int. Ed. Engl.* **1991**, *30*, 1024.
- 15) Torssell, K. *Acta. Chemica Scandinavica B* **1976**, *30*, 353.